8

Multiphase Reactors

Music, to create harmony,
must investigate discord

— *Plutarch*

The first part of this text was concerned with chemical reaction kinetics and reactor design-analysis procedures that showed the common features pertaining to homogeneous or pseudo-homogeneous systems. In fact, we got rather far along with the latter approach in the last chapter, extending to some rather advanced problems in reactor analysis. There comes a time[1], though, when we have to acknowledge the existence of more than one phase, and we *really* can't get around it. Some of this we have even tried to cope with in Chapter 7 regarding catalytic effectiveness, for example.

In this chapter we shall look at the analysis of multiphase reactors, typically gas-liquid-solid, that are found in diverse applications throughout the reaction engineering world. The reaction/reactor models that we have presented, at least up to Chapter 7, had some pretense of generality. As we go forward, any hope of that is gone. Our abilities in design and scale-up are not yet developed to the point where we can develop a general correlation of, for example mass transfer, that can be applied to any three-phase reactor that comes along. Thus, we will see in this chapter the development and presentation of much material that is specific to well-defined subsystems, and our basic task will be to assemble a number of these in a rational way to define the overall. This is fun, but one will quite soon see what is meant by "conservative design".

8.1 Fluidized-Bed Reactors

Fluidized-bed reactors are used in a number of applications ranging from catalytic cracking in the petroleum industry to oxidation reactions in the chemical industry. A number of advantages and disadvantages may be tabulated for this type of reactor, but we can shorten this somewhat by saying that most applications involve reactions in which catalyst decay is prominent and a continuous circuit is required for catalyst regeneration, or reactions where close control of operating conditions, particularly

[1] "... when the fat lady sings ..."—*Anonymous*

temperature, is required. We will see that the high level of mixing in most fluidized beds leads to behavior similar in some aspects to that of CSTRs. We will first describe qualitatively some simple fluid mechanics associated with fluidized beds, and then proceed to reactor applications. The treatment here is limited to some of the simpler models; much more detail is available in the work of Kunii and Levenspiel [D. Kunii and O. Levenspiel, *Fluidization Engineering,* 2 ed, Butterworth-Heinemann, Boston, MA, (1991)].

8.1.1 Simple Fluid Mechanics: Minimum Fluidization and Entrainment

Most discussions of fluidized beds begin with a discussion of some fluid mechanics, and we will follow suit. Figure 8.1 depicts what one might observe upon passing a gas upward through an initially fixed bed with increasing gas velocity. At lower velocities, in region (a), the bed of particles retains its fixed-bed configuration, and the pressure drop across the bed increases linearly with the flow velocity. At a particular point, mainly dependent upon the size and shape of the particles, there will be a slight expansion of the bed and some limited particle movement will be observed. This point is termed *incipient fluidization*, and the corresponding gas velocity is u_{mf}. Since the changes in bed configuration are still quite small at this point, it is difficult to observe visually, however, it is characteristic that above the point of incipient fluidization the pressure drop remains constant with increasing flow velocity. The configuration of the bed, though, changes considerably. Region (b) corresponds to a free bubbling behavior in which the fluidizing gas forms discrete bubbles

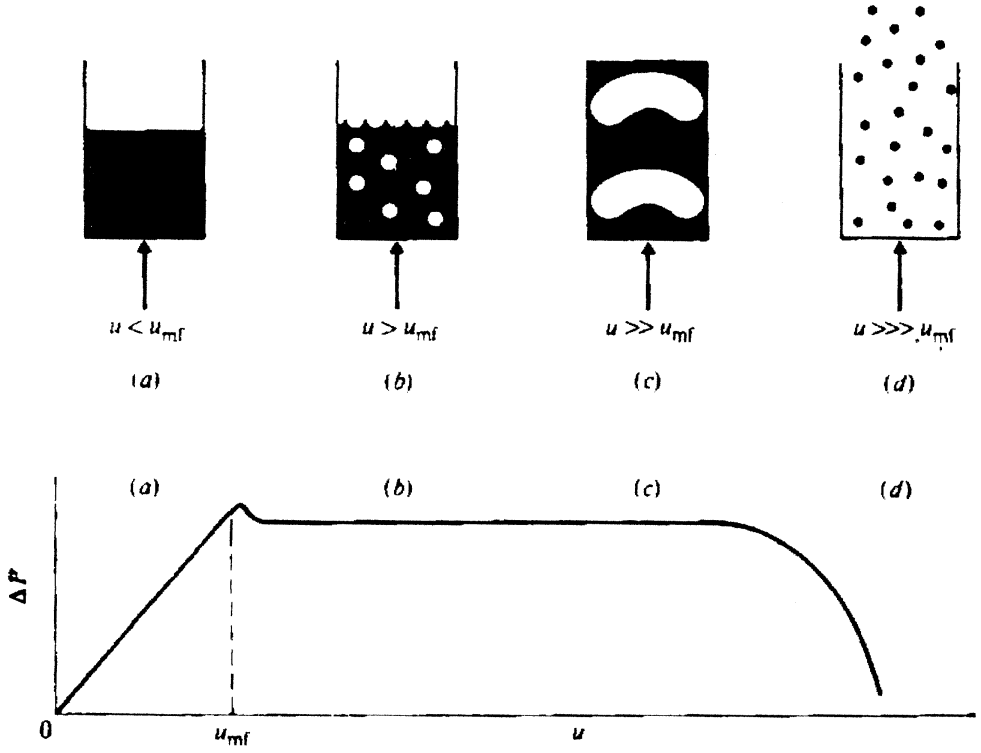

Figure 8.1 Gas transport through a bed of particulate solids regions of operation. [After J.J. Carberry, *Chemical and Catalytic Reaction Engineering*, with permission of McGraw-Hill Book Co., New York, NY, (1976).]

that pass through the now fluidized bed without interacting with each other. Region (c) is that in which bubble agglomeration is sufficient that coalescing bubbles can grow to a size on the order of the containing vessel. Finally, region (d) corresponds to fluid velocities that are sufficiently large that individual particles are entrained in the gas phase and possibly transported out of the vessel. The two quantities that we would like to know from a simple, practical point of view are this entrainment velocity, u_t, which sets a limit on the operable region of fluidization at the high end of the velocity scale, and the incipient fluidization velocity, u_{mf}, which does the same thing at the lower end of the scale. We will also see that many of the correlations used in fluid-bed design are based on u_{mf}, making knowledge of that quantity essential.

For the determination of the entrainment velocity, assuming that there is no particle-particle interaction, we may use a force balance based on Stoke's law

$$(\rho_s - \rho)gV_p = 3\pi\mu d_p u_t \tag{8-1}$$

where d_p and V_p are the particle diameter and volume, respectively, μ and ρ are gas-phase properties, and ρ_s is the density of the particles. Using spherical geometry as an example

$$V_p = \left(\frac{4}{3}\right)\pi\left(\frac{d_p^2}{2}\right) \tag{8-2}$$

and

$$u_t = \frac{(d_p)^2(\rho_S - \rho)g}{18\mu} \tag{8-3}$$

Practical operating conditions for fluidized beds must obviously be lower than this value, often about one-half of u_t. The entrainment velocity is strongly dependent upon particle diameter so that in a given operation if a range of d_p is involved and there is to be no elution of solid from the bed, then the size distribution must be taken into account.

Determination of the minimum fluidization velocity is a little more complicated, but still straightforward. The well-accepted correlation for pressure drop of a fluid flowing through a packed bed, from Ergun, we repeat here, but written in terms of the minimum fluidization velocity,

$$\frac{\Delta P}{L} = \frac{150(1-\epsilon)^2}{d_p^2\epsilon^3}\,\mu u_{mf} + \frac{1.75\rho(u_{mf})^2(1-\epsilon)}{d_p\epsilon^3} \tag{8-4}$$

We have already stated in the previous chapter reservations about the applicability of this equation to pressure drop with small particles but it seems a visible basis for much work on fluid beds—thus, if it works, don't fix it.

The ΔP is balanced by the gravitational force at the point of incipient fluidization,

$$(\rho_S - \rho)AL(1-\epsilon)g = (\Delta P)A \tag{8-5}$$

where A is the cross-sectional area, ϵ the bed void fraction, L the length of the bed, and ρ_S and ρ densities of the solid and fluid, respectively. The minimum

fluidization velocity is given implicitly by equating the pressure drops in equations (8-4) and (8-5):

$$(-\epsilon)(\rho_S - \rho)g = \frac{150(1-\epsilon)^2}{d_p^2\epsilon^3}\,\mu u_{mf} + \frac{1.75\rho(u_{mf})^2(1-\epsilon)}{d_p\epsilon^3} \tag{8-6}$$

Again, if there is a distribution of particle sizes this must be taken into account and there will be no unique u_{mf} for the bed as a whole.

8.1.2 A Two-Phase Reactor Model

If we look at the picture of fluidization given for $u > u_{mf}$ (case b of Figure 8.1), a two-phase model is suggested in which there is a dilute or bubble phase (consisting mostly of gas but perhaps some entrained particles as well) and a dense phase which is mostly particulate but with a porosity ϵ somewhat greater than that of the fixed bed (i.e., gas "entrained" in the particulate phase, if one wishes to push the analogy with the dilute phase). We can further picture that such a condition of fluidization will produce an isothermal reaction due to the mixing and agitation of the dense phase produced by bubble motion. This, indeed, is the visualization of the two-phase model proposed by Davidson and Harrison [J.F. Davidson and D. Harrison, *Fluidized Solids*, Cambridge University Press, London, England (1963)].

The two phases of the Davidson-Harrison model are a *bubble phase* of the gas passing throughout the reactor (with no catalyst entrainment), and an *emulsion phase* containing all of the catalyst particles and some gas. The bubble phase is normally-considered to pass through the reactor in plug flow, while the emulsion phase can be either well mixed or in plug flow itself. Since all of the catalyst is contained within the emulsion phase, that is where all of the reaction occurs. Communication between the bubble and emulsion phases occurs by cross-flow and diffusion across the interphase boundary. Finally, any increase in bed height upon fluidization is considered to be due to the volume of the bubbles in the bed. The emulsion phase moves at a velocity equal to the minimum fluidization velocity, u_{mf}, and the bubble phase at a kind of slip velocity, $u_0 - u_{mf}$, where u_0 is an entering gas velocity.

This description gives a formidable laundry list of requirements that are embedded in the model, and in any given system some may not be valid. We do have to start somewhere, however, and the Davidson-Harrison list of specifications is as reasonable as any at this point. Figure 8.2 presents a schematic of what is envisioned in the two-phase model. Some of the requirements can be written immediately in mathematical form. For height, we have

$$\pi R^2 L = \pi R^2 L_0 + \pi R^2 LNV$$

or

$$L = \frac{L_0}{(1 - NV)} \tag{8-7}$$

where L and L_0 are the heights of the fluid bed and the unexpanded bed, respectively, N is the number of bubbles per unit volume of bed, V the average volume per bubble, and R is the bed radius. For the mass transfer between the bubble and emulsion phases we can define a mass exchange coefficient as the sum of individual

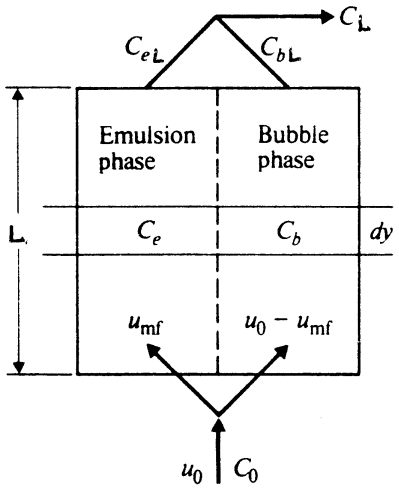

Figure 8.2 Schematic of the two-phase model of a fluidized bed according to Davidson and Harrison. [After J.J. Carberry, *Chemical and Catalytic Reaction Engineering*, with permission of McGraw-Hill Book Company, New York, NY, (1976).]

coefficients relating to diffusional transport and cross-flow

$$Q = q + k_d S \tag{8-8}$$

where Q is on overall coefficient, volume/time, q the cross-flow coefficient, k_d the normal mass-transfer coefficient (but in volumetric units), and S an interphase area. Since there is no reaction in the bubble phase, then concentration changes of position are possible only via interphase transport and the mass balance in the reactor at any point is

$$(q + k_d S)(C_e - C_b) = u_b V \left(\frac{dC_b}{dy} \right) \tag{8-9}$$

where C_e and C_b are, the concentrations of reactant in the two phases and $u_b = u_0 - u_{mf}$.

To proceed further we must make an assumption concerning the nature of the flow in the emulsion phase. Taking this to be plug flow at the velocity u_{mf}, we may now set forth an overall balance for the two phases as

$$u_{mf} \left(\frac{dC_e}{dy} \right) + (u_0 - u_{mf}) \left(\frac{dC_b}{dy} \right) + kC_e(1 - NV) = 0 \tag{8-10}$$

where the rate constant k is for Academic Reaction #1. Alternatively, if it is assumed that the emulsion phase is well mixed, we obtain

$$NVu_b(C_0 - C_e)[1 - \exp(-QL/u_b V)] + u_0(C_b - C_e) = \chi \tag{8-11}$$

with $\chi = kLC_e(1 - NV)$. The reactor model is expressed overall, then, as the combination of equations (8-9) and (8-10), or as (8-9) and (8-11). Proceeding with the

first pair, with the emulsion in plug flow, the equations (in terms of grouped coefficients) are

$$\left(\frac{dC_b}{dy}\right) + \left(\frac{\gamma}{L}\right)(C_b - C_e) = 0 \tag{8-12}$$

$$(1-\beta)\left(\frac{dC_e}{dy}\right) + \beta\left(\frac{dC_b}{dy}\right) + \left(\frac{\alpha}{L}\right)C_e = 0 \tag{8-13}$$

where

$$\alpha = \frac{kL_0}{u_0}; \qquad \beta = 1 - \frac{u_{mf}}{u_0}; \qquad \gamma = \frac{QL}{u_b V}$$

The boundary conditions for equations (8-12) and (8-13) are

$$y = 0; \qquad C_b = C_0; \qquad \left(\frac{dC_b}{dy}\right) = 0 \tag{8-14}$$

These two equations can be combined to give the following expression with C_b as the dependent variable

$$L^2(1-\beta)\left(\frac{d^2C_b}{dy^2}\right) + L(\gamma+\alpha)\left(\frac{dC_b}{dy}\right) + \alpha\gamma C_b = 0 \tag{8-15}$$

Two boundary conditions at the same point are normally to be avoided, however, the nature of what we look at here does not permit the exit derivative condition so useful in dispersion model analysis. As indicated in Figure 8.2, the overall exit concentration is determined by the combination of the expressions for C_{bL} and C_{eL}, as

$$u_0 C_L = (u_o - u_{mf})C_{bL} + u_{mf}C_{eL} \tag{8-16}$$

and, at any point, from equation (8-12)

$$C_e = C_b + \left(\frac{L}{\gamma}\right)\left(\frac{dC_b}{dy}\right) \tag{8-17}$$

The overall result for plug flow in both bubble and emulsion phases is

$$\left(\frac{C_L}{C_0}\right) = \frac{1}{(a_1 - a_2)}\left[a_1\left(1 - \frac{u_{mf}La_2}{\gamma u_0}\right)\exp(-a_2 L) - a_2\left(1 - \frac{u_{mf}La_1}{\gamma u_0}\right)\exp(-a_1 L)\right] \tag{8-18}$$

where

$$a_1, a_2 = \frac{(\gamma+\alpha) \pm [(\gamma+\alpha)^2 - 4(1-\beta)\alpha\gamma]^{1/2}}{2L(1-\beta)}$$

We will discuss the evaluation of some of these model parameters subsequently, but let us first examine a second example of modeling of fluidized beds.

8.1.3 A Three-Phase Model

In the two-phase model above it was assumed that the bubble phase contained no solids (no catalyst), and that the bubbles were spherical. In fact, both of these assumptions are wrong in most cases. We need in particular to address the question of bubble geometry. Figure 8.3 illustrates what a bubble traversing a bed of particulate solids is more likely to look like. The shape is more that of a distorted hemisphere, or the dome of a mushroom, than that of a sphere. Moreover, there is a phase immediately surrounding the bubble that contains a concentration of solids different from both the bubble and emulsion phases. This is shown in the figure as a "cloud" or "wake" phase. This view of the bubble in passage through the bed is not one made up for the sake of proposing a new model, but is based on a large amount of experimental data, much of it photographic. Obviously, such evidence would call for some restructuring of the Davidson-Harrison approach to account for actual bubble geometry and, more importantly, to account for the existence of three phases. To a considerable extent these factors depend on the types of particles that are being fluidized, which in turn determine the type of fluidization to be expected. A widely used classification is that of Geldhart [D. Geldhart, *Powder Tecnol., 7*, 285 (1973); *19*, 133 (1978)] which divides perticulates into four different types of behavior. These are

A Materials with small mean particle size and/or low particle density ($< 1.4\,g/cm^3$). These are easily fluidized and give small bubbles at higher velocities.

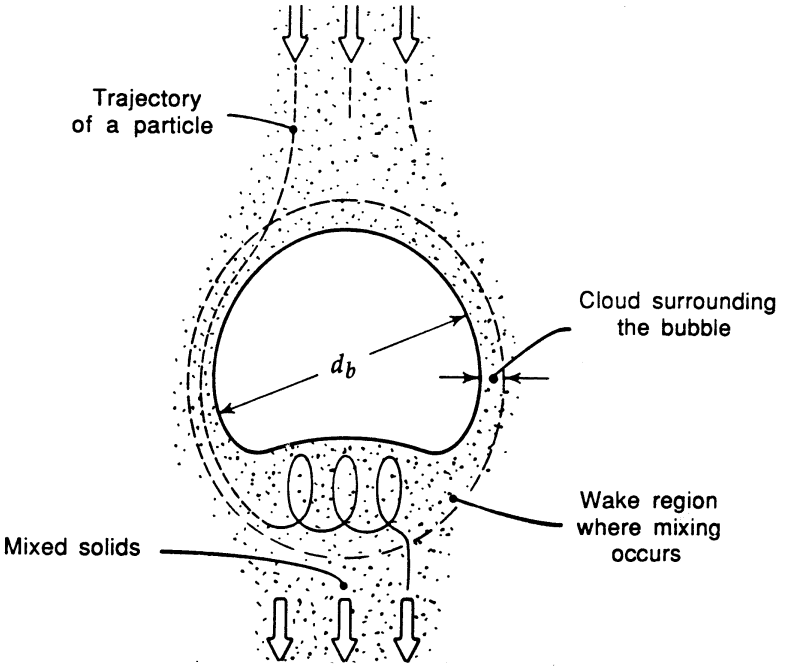

Figure 8.3 A more precise view of bubble geometry. [After D. Kunii and O. Levenspiel, *Fluidization Engineering*, with permission of Butterworth-Heinemann, Boston, MA, (1991).]

B Sand-like materials with particles 40-500 μm in diameter and density of 1.4–4.0 g/cm^3. These also fluidize well but demonstrate bubble coalescence and growth.

C Very fine powders that are cohesive due to interparticle attraction. Difficult to fluidize; flour and starch are examples.

D These are large and/or dense particles that are difficult to fluidize and give erratic fluidization patterns with channeling and spouting behavior. Drying grains, roasting coffee, and coal gusification are examples.

Each of these groups can be classified generally as to the particle size/density as a generic measure of the nature of fluidization. This is shown in Figure 8.4. As indicated in the figure, group **A** (and sub-group **A′**) are the most likely to be associated with reactor design, and the data leading to the visualization of Figure 8.3 has been obtained in large part from fluidized solids belonging to this group.

The Kunii-Levenspiel model [D. Kunii and O. Levenspiel, *Ind. Eng. Chem. Fundls., 7*, 446 (1968); *Ind. Eng. Chem. Proc. Design Devel., 7*, 481 (1968); *Fluidization Engineering,* 2 ed., Butterworth-Heinemann, Boston, MA, (1991)] envisions a solid-free bubble phase, generally corresponding to operations where $u_0 \geq 2u_{mf}$, is surrounded by the cloud-wake phase which, in turn is surrounded by the emulsion phase. In general the flow of all three phases is in the same upward direction, although in some ranges of bubble velocity the emulsion phase may flow in the opposite direction. In any event, at a given point in the reaction three rate processes occur simultaneously:

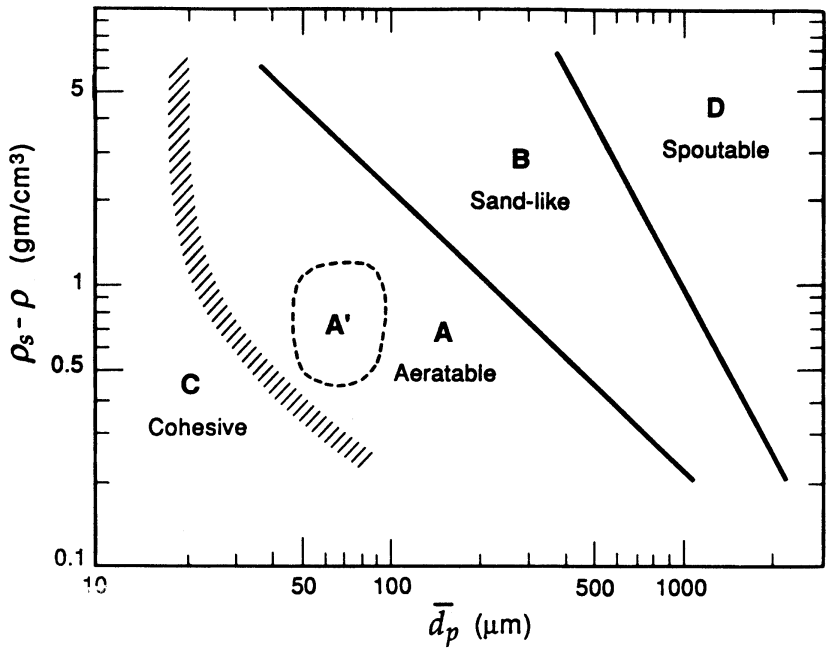

Figure 8.4 Geldhart classification of particles for fluidization by air at ambient temperature. Region A′ corresponds to the properties of well-behaved fluid cracking catalysts. [After D. Kunii and O. Levenspiel, *Fluidization Engineering*, with permission of Butterworth-Heinemann, Boston, MA, (1991).]

1. Mass transfer from the bubble to the cloud-wake phase. There is a possible chemical reaction in the bubble phase, but this will be small since the amount of catalyst in the bubble phase is also small.
2. Mass transfer of reactant into the cloud-wake phase from the bubble phase, and from there into the emulsion phase. There is chemical reaction in the cloud-wake phase.
3. Mass transfer of reactant from the cloud-wake phase into the emulsion phase. There is chemical reaction in the emulsion phase.

This sequence of events is depicted schematically in Figure 8.5, following the reactant. More precisely, we may write the balances for reactant as

Disappearance in bubble = reaction in bubble + transfer to cloud-wake
Transfer to cloud-wake = reaction in cloud-wake + transfer to emulsion
Transfer to emulsion = reaction in emulsion

Using the notation given in Figure 8.5, we have

$$-\left(\frac{dC_b}{dt}\right) = -u_b\left(\frac{dC_b}{dy}\right) = \gamma_b k_r C_b + K_{bc}(C_b - C_c) \tag{8-22}$$

$$K_{bc}(C_b - C_c) = \gamma_c k_r C_c + K_{ce}(C_c - C_e) \tag{8-23}$$

$$K_{ce}(C_c - C_e) \approx \gamma_e k_r C_e \tag{8-24}$$

If we allow ourselves the latitude to replace $\approx$ with $=$ in the above, then combination of (8-22) to (8-24) to eliminate the concentrations C_c, and C_e gives

$$-u_b \frac{dC_b}{dy} = K_f C_b \tag{8-25}$$

where $u_b = (u_0 - u_{mf})$, and K_f, the composite rate constant, is given by

$$K_f = \gamma_b k_r + \frac{1}{\beta} \tag{8-26}$$

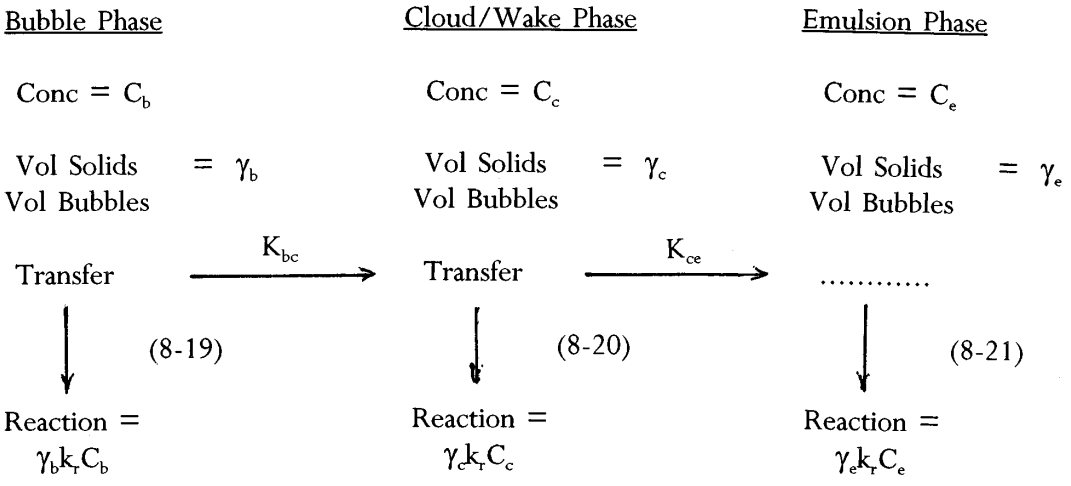

Figure 8.5 Mass transfer and reaction steps in the three-phase model.

with

$$\beta = \frac{1}{K_{bc}} + \frac{1}{\gamma_c k_r + 1/\alpha}$$

and

$$\alpha = \frac{1}{K_{ce}} + \frac{1}{\gamma_e k_r}$$

Integrating equation (8-25) gives the bubble concentration at height y as

$$\left(\frac{C_b}{C_0}\right) = \exp\left[-K_f\left(\frac{y}{u_b}\right)\right] \tag{8-27}$$

and overall

$$1 - X = \left(\frac{C_{bL}}{C_0}\right) \exp\left(-K_f L/u_b\right) \tag{8-28}$$

where X is the conversion of reactant. In beds where the bubble motion is quite vigorous, then $u_0 \gg u_{mf}$, and a good approximation of equation (8-28) is

$$1 - X = \exp\left(-\frac{k_f \gamma_b \delta L}{u_0}\right) \tag{8-29}$$

with $\delta = (u_0/u_b)$.

Some study of the structure of equation (8-26) provides support for the advice that all parameters are (can be) equal, but some are more equal than others. For a fast reaction, k_r is large and the early steps dominate. Inversely, for slow reactions k_r is small and the latter steps prevail. For a *very fast reaction* transport rates limit, and the value of K_{bc} is approached by $k_r\gamma_b$, even though γ_b is generally very small. This results in

$$K_f = (\gamma_b k_r - K_{bc}) \tag{8-30}$$

and

$$1 - X = \exp\left[-(\gamma_b k_r + K_{bc})\left(\frac{\gamma L}{u_0}\right)\right] \tag{8-31}$$

For a *very slow reaction*, $k_r \ll K_{bc}$ and K_{ce}, thus,

$$K_f = (\gamma_b + \gamma_c + \gamma_e)k_r = k_r\left(\frac{1 - \epsilon_f}{\delta}\right) \tag{8-32}$$

This will give us an expression for the overall conversion of reactant as

$$1 - X = \exp\left[\frac{-k_r(1 - \epsilon_f)L}{u_0}\right] \tag{8-33}$$

where ϵ_f is the porosity of the fluidized bed.

It is of interest to compare the efficiency of a fluidized bed in terms of the Kunii-Levenspiel model to that of a corresponding plug-flow reactor. We can do this by comparing the catalyst requirement in a PFR to that in the fluid-bed reactor (FBR) for the same conversion, which in general is the ratio of the effective

overall rate constant (first-order, remember) in the FBR to the intrinsic rate constant, so

$$E = \frac{k_e \delta}{(1-\epsilon_f)} = \frac{K_f \delta}{k_r(1-\epsilon_f)} \tag{8-34}$$

where $k_e = (K_f/k_f)$ and E is an efficiency in terms of (PFR/FBR). For a slow reaction $E \to 1$, and for a fast reaction $E \to [\gamma_b \delta/(1-\epsilon_p)]$.

An alternative development of the three-phase model, in terms of nondimensional parameters, is very good for those who like to think in terms of numbers. We define the reaction-transport parameters using the corresponding Damköhler numbers,

$$N_{Da,c} = \frac{k_r}{K_{bc}}; \qquad N_{Da,e} = \frac{k_r}{K_{ce}} \tag{8-35}$$

and phase effectiveness factors,

$$\eta_i = \frac{\gamma_i}{1+\gamma_i N_{Da,i}} \tag{8-36}$$

The fluid-bed effectiveness has the physical significance that for small $N_{Da,i}$, $\eta_i \to \gamma$ and there is total utilization of catalyst in that phase, while for large $N_{Da,i}$, $\eta_i \to 0$ and the phase is not utilized for chemical reaction. Thus, the effectiveness definitions for the three phases are

$$\begin{aligned} \eta_b &= \gamma_b \\ \eta_c &= \frac{\gamma_c}{1+\gamma_c N_{Da,c}} \end{aligned} \tag{8-37}$$

We also define the overall fluid-bed efficiency as

$$E = \left(\frac{K_f}{K_r}\right)\left(\frac{V_b}{V_s}\right) = \eta_0 \left(\frac{V_b}{V_s}\right) \tag{8-38}$$

where V_b is the volume of the bubble phase and V_s the volume of solids. For the three-phase model this is given by

$$E = \left(\frac{V_b}{V_s}\right)\left[\gamma_b + \frac{1}{N_{Da,c} + 1/(\gamma_c + \eta_e)}\right] \tag{8-39}$$

For large N_{Da} and fast reaction,

$$\eta_e = 0; \qquad \eta_c = 0; \qquad E = \left(\frac{V_b}{V_s}\right)\gamma_b \ll 1 \tag{8-40}$$

For large N_{De} and intermediate reaction,

$$\eta_e = 0; \qquad E = \left(\frac{V_b}{V_s}\right)(\gamma_b + \eta_c) < 1 \tag{8-41}$$

For small N_{Da} and slow reaction,

$$E = \left(\frac{V_b}{V_s}\right)(\gamma_b + \gamma_c + \gamma_e) \to 1 \tag{8-42}$$

8.1.4 The Parameters of Fluidized-Bed Reactors

While building up mathematical models for reactor design and performance is fun, the day of reckoning must come sooner or later when we have to determine if the model parameters are experimentally visible, or how they may be correlated to reaction conditions or properties of the reaction system.[2] An important aspect of the Kunii-Levenspiel model is that, building upon the insights provided by Davidson and Harrison, a substantial amount of information has been accumulated over the years concerning the parameters involved. We focus attention to fluid beds with discrete, noninteracting bubbles in the bed, generally corresponding to operation in region **A** (or more particularly **A**′) in the diagram of Figure 8.4. To a large extent these parameters are concerned with bubbles, bubbles, and even more bubbles.

For mass transfer from the bubble to the cloud-wake phase, we can go back to the form of equations (8-22) and (8-23), where

$$K_{bc} = (q + k_{bc}S_{bc}) \tag{8-43}$$

In this, q is the cross-flow coefficient and S_{bc} the interfacial area. From the work of Davidson and Harrison, the value of q is expressed in terms of the bubble diameter, d_b, as

$$q = (3\pi/4)u_{mf}(d_b)^2 \tag{8-44}$$

For spherical-cap bubbles and a penetration theory model, the mass-transfer coefficient is given by

$$k_{bc} = (0.975)(\mathcal{D})^{1/2}\left(\frac{g}{d_b}\right)^{1/4} \tag{8-45}$$

so that overall we have

$$K_{bc} = (4.5)\left(\frac{u_{mf}}{d_b}\right) + (5.85)\left(\frac{\mathcal{D}^{1/2}g^{1/4}}{d_b^{5/4}}\right) \tag{8-46}$$

For transport between the cloud-phase there is no net flow of gas, so that diffusion is the only mechanism of transport. This is similar to a problem worked out by Higbie [R. Higbie, *Trans. Amer. Inst. Chem. Eng., 31*, 365 (1935)] in terms of the penetration theory.

$$k_{ce} \approx \left(\frac{4\mathcal{D}\epsilon_{mf}}{\pi t}\right) \tag{8-47}$$

For bubbles with thin clouds, generally corresponding to the Geldhart region **A**′,

$$d_c \approx d_b; \qquad \frac{S_{bc}}{V_b} \approx \frac{6}{d_b} \tag{8-48}$$

[2] "Lots of models, lots of shining stars, lots of days. The models and the stars go away, but the days don't."—Ascribed to *B. Hope*

The exposure time for an element of bubble surface in contact with the emulsion phase, t, is approximated as

$$t = \left(\frac{d_b}{u_{br}}\right) \tag{8-49}$$

Now if we set the results of equations (8-48) and (8-49) into (8-47)

$$K_{ce} = \left(\frac{S_{ce}}{V_b}\right)k_{ce} = \left[\left(\frac{4\mathcal{D}\epsilon_{mf}}{\pi}\right)\left(\frac{u_{br}}{d_b}\right)\right]^{1/2}\left(\frac{S_c}{V_b}\right) \tag{8-50}$$

or

$$K_{ce} = (6.77)\left(\frac{\mathcal{D}\epsilon_{mf}u_{br}}{d_b^3}\right)^{1/2} \tag{8-51}$$

The velocity term, u_{br}, appearing in these equations is the rise velocity of the bubble with respect to the emulsion phase, and is given by

$$u_{br} = (0.711)(gd_b)^{1/2} \tag{8-52}$$

and the bubble velocity, u_b, is

$$u_b = u_o - u_{mf} + u_{br} \tag{8-53}$$

The particle distribution among the three phases of course determines the relative magnitude of chemical reaction. The γ values appearing in equations (8-22) to (8-24) are defined as (volume of solids)/(volume of bubble). If δ is the volume fraction of a bed occupied by bubbles, we have the balance,

$$\delta(\gamma_b + \gamma_e + \gamma_e) = (1 - \epsilon_f) = (1 - \epsilon_{mf})(1 - \delta) \tag{8-54}$$

and

$$\gamma_e = \frac{(1 - \epsilon_{mf})(1 - \delta)}{\delta} - \gamma_b - \gamma_c \tag{8-55}$$

For the cloud-wake phase

$$\gamma_c = \frac{(1 - \epsilon_{mf})}{(f_c + f_w)} = (1 - \epsilon_{mf})\left[\frac{3}{(u_{br}\epsilon_{mf}/u_{mf}) - 1} + f_w\right] \tag{8-56}$$

where f_c and f_w are factors for the cloud volume and wake, respectively. The value of f_c is given by

$$f_c = \frac{3}{(u_{br}\epsilon_{mf}/u_{mf}) - 1} \tag{8-57}$$

while the value of f_w is best estimated from the correlation of experimental data in terms of d_p shown in Figure 8.6. From this we go forward by combining equations (8-56) and (8-57) to obtain

$$\gamma_c = (1 - \epsilon_{mf})\left[\frac{3}{(u_{br}\epsilon_{mf})/u_{mf} - 1} + f_w\right]$$

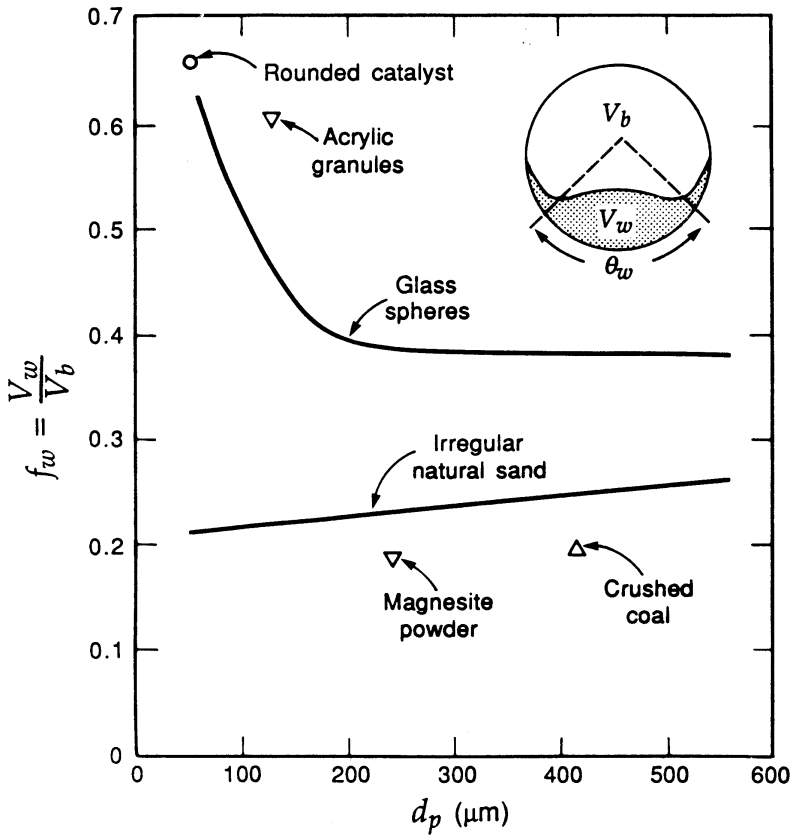

Figure 8.6 Wake fraction of three-dimensional bubbles. [After D. Kunii and O. Levenspiel, *Fluidization Engineering*, 2 ed., with permission of Butterworth-Heinemann, Boston, MA, (1991).]

and, inserting the correlations for u_{br},

$$\gamma_c = (1 - \epsilon_{mf})\left[\frac{(3u_{mf}/\epsilon_{mf})}{(0.711)(gd_b)^{1/2} - u_{mf}/\epsilon_{mf}} + f_w\right] \tag{8-58}$$

This leaves the value of γ_b, which we know to be quite small, but not necessarily zero. Kunii and Levenspiel cite values on the order of 10^{-2} to 10^{-3} based on experimental results of questionable accuracy, and suggest a rule-of-thumb value of 0.005 for γ_b.

Finally, there is the value of δ to be considered. This quantity, the fraction of the bed in bubbles, can vary significantly depending upon velocity. For *slow bubbles* $(u_b < u_e)$,

$$\delta = \frac{u_0 - u_{mf}}{u_b + 2u_{mf}} \tag{8-59}$$

where u_e is the upward superficial velocity of the gas through the emulsion phase, defined by

$$\left(\frac{\epsilon_e}{\epsilon_{mf}}\right)^3 \frac{(1 - \epsilon_{mf})}{(1 - \epsilon_e)} = \frac{u_e}{u_{mf}} \tag{8-60}$$

For *fast bubbles* ($u_b > 5u_{mf}/\epsilon_{mf}$),

$$\delta = \frac{u_0 - u_{mf}}{u_b - u_{mf}} \tag{8-61}$$

and in the limit where $u_0 \gg u_{mf}$

$$\delta = \left(\frac{u_0}{u_b}\right) \tag{8-62}$$

Equations (8-43) to (8-62) have now taken us through a full tour of the parameters of the three-phase model. Our interests here are primarily for vigorously-bubbling beds that exhibit behavior characteristic of the $\mathbf{A}'$ region of the Geldhart diagram, or at least close to it. One sees in review of these equations the very important role that d_b and u_{mf} play in determining fluid bed behavior.

Illustration 8.1[3]

Estimate the conversion for a first-order irreversible reaction with rate constant k_f of $10\,\text{m}^3\text{-gas/m}^3\text{-cat-s}$ taking place in a fluidized bed, given the following data.

Gas $\quad \mathcal{D} = 2 \times 10^{-5}\,\text{m}^2/\text{s}$

Particles $\quad (d_p) = 68\,\mu\text{m}, (\rho_s - \rho_q) = 0.8$

Bed $\quad \epsilon_m = 0.50$ (fixed bed), $\gamma_b = 0.005$

$\epsilon_{mf} = 0.55;\ u_{mf} = 0.006$ m/s; $\ d_b = 0.04\,\text{m}$

$L_0 = 7$ m; $\ u_0 = 0.1$ m/s; $\ d_{bed} = 0.26$ m

Solution

Let us first check where we are with respect to the Geldhart classification of Figure 8.4. The values of d_p and $(\rho_s - \rho_q)$ given as data land us well into the $\mathbf{A}'$ region of Geldhart **A** particles, so the parameter correlations presented above should be valid. Further $u_0 = 16u_{mf}$, and $u_b \approx 90\,u_{mf}$ (shown subsequently), so that we are dealing with a fine-particle bed, fast bubbles, and a thin cloud phase. From equation (8-52),

$$u_{br} = (0.711)(gd_b)^{1/2} = (0.711)[(9.8)(0.04)]^{1/2} = 0.445$$

from equation (8-53),

$$u_b = u_0 - u_{mf} + u_{br} = 0.1 - 0.006 + 0.445$$

$$u_b = 0.539\,\text{m/s}$$

[3] Adapted from [D. Kunii and O. Levenspiel, *Fluidization Engineering*, 2 ed., with permission of Butterworth-Heinemann, Boston, MA, (1991).]

From equation (8-54),

$$K_{bc} = \frac{(4.5)(0.006)}{0.04} + \frac{(5.85)(2 \times 10^{-5})^{1/2}(9.8)^{1/4}}{(0.04)^{5/4}}$$

$$K_{bc} = 3.26 \text{ s}^{-1}$$

From equation (8-51),

$$K_{ce} = (6.77)\left[\frac{(2 \times 10^{5})(0.55)(0.445)}{(0.04)^{3}}\right]^{1/2}$$

$$K_{ce} = 1.87 \text{ s}^{-1}$$

Since $(u_b/u_{mf}) \gg 1$, we may use equation (8-62) for δ.

$$\delta = (0.1/0.539) = 0.186$$

For the values of the various γs, we have

$$\gamma_b = 0.005$$

From equation (8-57a),

$$\gamma_c = (1 - 0.55)\left[\frac{3}{(0.445)(0.55)/(0.006) - 1} + 0.60\right]$$

where the value of f_w is obtained from the correlation of Figure 8.6 for glass spheres, $d_p = 68\,\mu\text{m}$. Thus,

$$\gamma_c = 0.304$$

From equation (8-55),

$$\gamma_e = \frac{(1 - 0.55)(1 - 0.186)}{0.186} - 0.005$$

$$\gamma_e = 1.668$$

The data give us a value for L_0, the height of the fixed (unfluidized) bed, so we must determine L for this operation. An overall mass balance for bed solids is

$$L_o(1 - \epsilon_m) = L_{mf}(1 - \epsilon_{mf}) = L(1 - \epsilon_f) \tag{i}$$

thus

$$L = \frac{L_0(1 - \epsilon_m)}{(1 - \epsilon_f)} \tag{ii}$$

The fluid bed voltage, ϵ_f, is related to the total fraction of bubbles in the bed, δ, and the voidage of the emulsion phase, ϵ_e, by

$$(1 - \epsilon_f) = (1 - \delta)(1 - \epsilon_e) \tag{iii}$$

However, we have no value for ϵ_e; a reasonable approximation in this case is that

$$\epsilon_e \approx \epsilon_{mf} \tag{iv}$$

and then

$$(1-\epsilon_f) = (1-\delta)(1-\epsilon_{mf}) \tag{v}$$

so, finally

$$(1-\epsilon_f) = (1-0.186)(1-0.55)$$

$$(1-\epsilon_f) = 0.366$$

From equation (ii),

$$L = \frac{(0.7)(1-0.50)}{0.366}$$

$$L = 0.956\,\text{m}$$

We may now consider the rate of chemical reaction. We can determine K_f from equation (8-26) using the quantities detailed above. The result is

$$K_f = 1.98\,\text{s}^{-1}$$

Then, using equation (8-28)

$$(1-X) = \exp\left(-\frac{K_f L}{u_b}\right)$$

$$(1-X) = \exp\left[-\frac{(1.98)(0.956)}{0.539}\right]$$

$$(1-X) = 0.030$$

Illustration 8.2

Develop a measure of reaction-reactor performance that can be used directly from fluid-bed operation to compare PFR and CSTR conversion limits.

Solution

This sounds formidable, but it really is not. For a feed rate v (m^3/s) of reactant gas at concentration $C_{\text{A},i}$ (mols/m^3) to a catalyst bed containing solids of volume V_s (m^3), the outlet concentration, $C_{\text{A},o}$, or the outlet fractional conversion, X_A, are given by familiar forms.

$$PFR \qquad 1 - X_\text{A} = (C_{\text{A},o}/C_{\text{A},i}) = \exp(-k_r\tau) \tag{i}$$

$$CSTR \qquad 1 - X_\text{A} = (C_{\text{A},o}/C_{\text{A},i}) = (1+k_r\tau)^{-1} \tag{ii}$$

However, rather than thinking of τ as just a contact time, let us define it as

$$\tau = \left(\frac{\textit{volume catalyst}}{\textit{volumetric flow rate}}\right) = \left(\frac{V_s}{v}\right) \tag{iii}$$

For illustration, this value of τ would be in units of (m^3 cat/m^3 feed-s). For the fluid bed, the dimensionless rate group is given by

$$k_r\tau = \frac{k_r L(1-\epsilon)}{u_0} \tag{iv}$$

for isothermal flow with no density changes.

HORATIO SAYS

We have worried previously about basing the minimum fluidization velocity on the Ergun equation. How would the results of Illustration 8.1 be affected by a ±10% uncertainty in u_{mf}?

Partially because of the backmixing behavior and partially because of the efficiency of contact between fluid- and catalyst-phases, fluidized beds are less efficient than fixed beds, at least in terms of the amount of catalyst required to attain a given conversion. Although plug flow seems reasonable for the motion of the bubbles, particularly in the Geldhart **A**–**A′** regions, bubble-emulsion interchange,

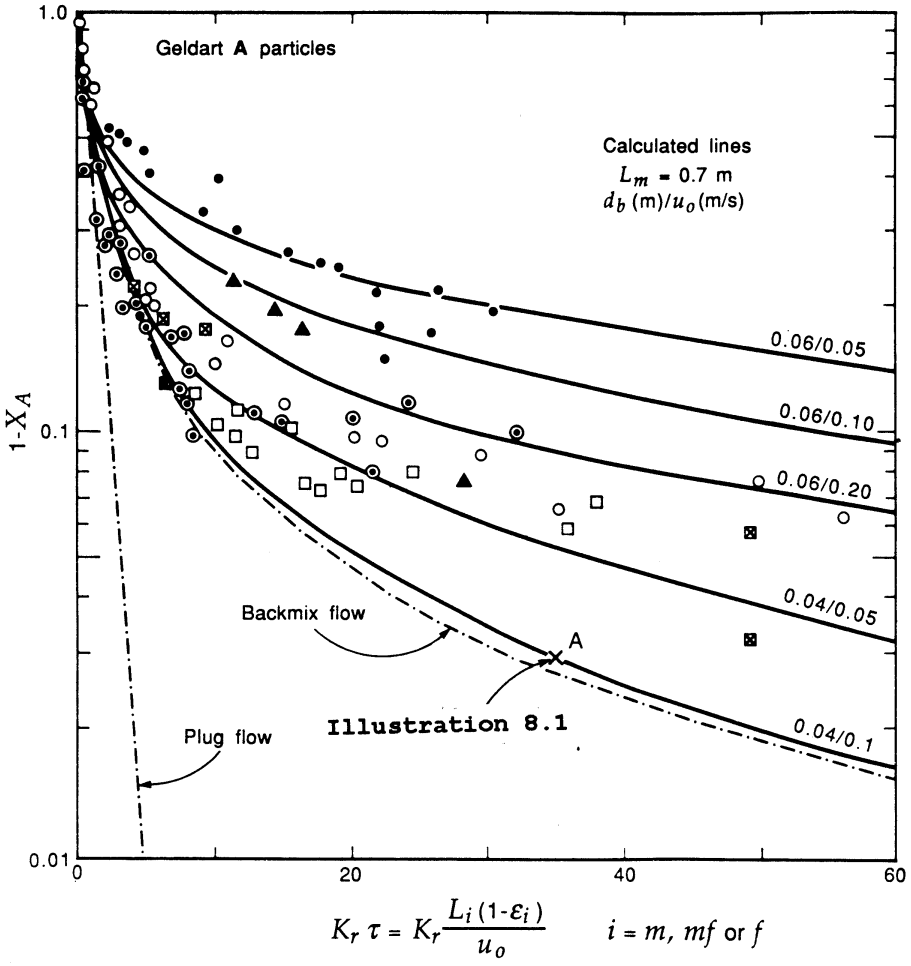

Figure 8.7 Conversion in fluid beds of very fine Geldhart A catalysts. Lines calculated with equations (8-26) and (8-27), $\mu_{mf} = 0.006$ m/s, (d_p/u_0) as the parameter; see Illustration 8.1. [After D. Kunii and O. Levenspiel, *Ind. Eng. Chem. Research*, *29*, 1226, with permission of the American Chemical Society, (1960).]

bypass flow, and other mass-transfer resistances are not accounted for and can make serious deviations from the PFR model. At the same time, though, such deviations do not approach the limits of the CSTR model. Figure 8.7 gives a summary of results for a number of experimental studies on reactions conducted on fine Geldhart **A** catalysts, together with the predictions from PFR and CSTR models. The results shown are calculated as in Illustration 8.1; the lines follow in general trend the data presented, if (d_b/u_0) is used as a parameter. We really cannot say however, that this resolves the problem of fluid-bed design, since there are still a couple of adjustable parameters lurking.

8.1.5 Selectivity Factors in Fluidized-Bed Reactors

The three-phase model is readily extended to more complex reaction systems if one is willing to endure the algebraic complications. This was worked out [O. Levenspiel, N. Baden and B.D. Kulkarni, *Ind. Eng. Chem. Process Design Devel., 17,* 478 (1978)] for the classical Denbigh reaction sequence.

$$\begin{array}{ccc} \mathrm{A} & \xrightarrow{k_{r1}} & \mathrm{R} \xrightarrow{k_{r3}} \mathrm{S} \\ {\scriptstyle k_{r2}}\downarrow & & \downarrow{\scriptstyle k_{r4}} \\ \mathrm{T} & & \mathrm{U} \end{array}$$

with $k_{r12} = k_{r1} + k_{r2}$ and $K_{r34} = k_{r3} + k_{r4}$. The key equations are the material balances for A and R. Thus, for A,

$$-u_b\left(\frac{dC_{\mathrm{Ab}}}{dy}\right) = \gamma_b k_{r12} C_{\mathrm{Ab}} + K_{bc,\mathrm{A}}(C_{\mathrm{Ab}} - C_{\mathrm{Ac}}) \tag{8-63}$$

$$K_{bc,\mathrm{A}}(C_{\mathrm{Ab}} - C_{\mathrm{Ac}}) = \gamma_c k_{r12} C_{\mathrm{Ac}} + K_{ce,\mathrm{A}}(C_{\mathrm{Ac}} - C_{\mathrm{Ae}}) \tag{8-64}$$

$$K_{ce,\mathrm{A}}(C_{\mathrm{Ac}} - C_{\mathrm{Ae}}) = \gamma_e k_{r12} C_{\mathrm{Ae}} \tag{8-65}$$

and for R,

$$-u_b\left(\frac{dC_{\mathrm{Ab}}}{dy}\right) = \gamma_b k_{r34} C_{Rb} - \gamma_b k_{r1} C_{\mathrm{Ab}} + K_{bc,R}(C_{Rb} - C_{Rc}) \tag{8-66}$$

$$K_{bc,R}(C_{Rb} - C_{Rc}) = \gamma_c k_{r34} C_{Rc} - \gamma_c k_{r1} C_{\mathrm{Ac}} + K_{ce,R}(C_{Rc} - C_{Re}) \tag{8-67}$$

$$K_{ce,R}(C_{Rc} - C_{Re}) = \gamma_e k_{r34} C_{Re} - \gamma_e k_{r1} C_{\mathrm{Ao}} \tag{8-68}$$

For no intermediate in the feed the initial conditions are

$$C_{\mathrm{Ab}} = C_{\mathrm{A}}; \qquad C_{Rb} = 0; \qquad y = 0$$

As in the case for a single reaction we eliminate the intermediate concentrations C_{Ac}, C_{Ae}, C_{Rc}, and C_{Re} in the equations above. Integration and considerable algebraic manipulation produces the following results.

$$\frac{C_{\mathrm{A}_0}}{C_{\mathrm{A}_i}} = \frac{C_{\mathrm{A}b_0}}{C_{\mathrm{A}b_i}} = \exp(-K_{f12}\tau) \tag{8-69}$$

$$\frac{C_{R_0}}{C_{\mathrm{A}_i}} = \left(\frac{K_{fAR}}{K_{f34} - K_{f12}}\right)[\exp(-K_{f12}\tau) - \exp(-K_{f34}\tau)] \tag{8-70}$$

where

$$\tau = \frac{V_s}{v} = \frac{L(1-\epsilon_f)}{u_0} = \frac{L(1-\epsilon_f)}{u_b \delta} \tag{8-71}$$

This gives a cumbersome but straightforward result for K_{f12},

$$K_{f12} = \left[\gamma_b k_{r12} + \frac{1}{(\alpha+\zeta)}\right] \frac{\delta}{(1-\epsilon_f)} \tag{8-72}$$

where

$$\alpha = 1/K_{bc,\mathrm{A}}$$
$$\zeta = [\gamma + 1/(\lambda+\omega)]$$
$$\gamma = \gamma_c k_{r12}$$

and

$$\lambda = 1/K_{ce,\mathrm{A}}; \qquad \omega = 1/(\gamma_e k_{r12})$$

Similarly, for K_{f34}

$$K_{f34} = \left[\gamma_b k_{r34} + \frac{1}{(\alpha'+\zeta')}\right] \frac{\delta}{(1-\epsilon_f)} \tag{8-73}$$

where

$$\alpha' = 1/K_{bc,R}$$
$$\zeta' = [\gamma' + 1/(\lambda'+\omega')]$$
$$\gamma' = \gamma_c k_{r34}$$

and

$$\lambda' = 1/K_{ce,R}; \qquad \omega' = 1/(\gamma_e k_{r34})$$
$$K_{f\mathrm{A}r} = \left(\frac{k_{r1}}{k_{r12}}\right) K_{f12} - K_{f\mathrm{A}} \tag{8-74}$$

Finally, $K_{f\mathrm{A}}$ is given by equation (8-75), which is sufficiently awkward to warrant its own space on the following page.

Now while those equations seem to go on and on, they essentially represent the simple combinations of reaction and mass transfer parameters that will either be known for the system (various k_r) or that can be calculated (mass-transfer coefficients). Overall there are 22 separate reaction and mass-transfer steps represented in this

$$
\begin{aligned}
K_{f\mathrm{A}} &= \frac{[A + (B)(C)](D)}{[(E)(F) + G][(H)(L) + M]} \\
A &= (K_{bc,R}K_{ce,\mathrm{A}})/\gamma_c^2 \\
B &= k_{r12} + K_{ce,\mathrm{A}}/\gamma_c + K_{ce,\mathrm{A}}/\gamma_e \\
C &= k_{r34} + K_{ce,R}/\gamma_c + K_{ce,R}/\gamma_e \\
D &= (\delta K_{bc,\mathrm{A}}k_{r1}k_{r34})/(1 - \epsilon_f) \\
E &= k_{r12} + K_{bc,\mathrm{A}}/\gamma_c \\
F &= k_{r12} + K_{ce,\mathrm{A}}/\gamma_e \\
G &= (k_{r12}K_{ce,\mathrm{A}})/\gamma_c \\
H &= k_{r34} + K_{bc,R}/\gamma_c \\
L &= k_{r34} + K_{ce,R}/\gamma_e \\
M &= (k_{r34}K_{ce,R})/\gamma_c
\end{aligned}
\tag{8-75}
$$

analysis of the Denbigh sequence as shown in Figure 8.8. The concentrations of other components involved in the reaction are obtained by a sequence of material balances as,

$$C_{S_0} = \frac{k_{r1}k_{r3}}{k_{r12}k_{r34}(C_{\mathrm{A}_i} - C_{\mathrm{A}_0})} \tag{8-76}$$

$$C_{T_0} = \frac{k_{r2}}{k_{r12}}\,(C_{\mathrm{A}_i} - C_{\mathrm{A}_0}) \tag{8-77}$$

$$C_{u_0} = \frac{k_{r1}k_{r4}}{K_{r12}k_{r34}}\,(C_{\mathrm{A}_i} - C_{\mathrm{A}_0}) \tag{8-78}$$

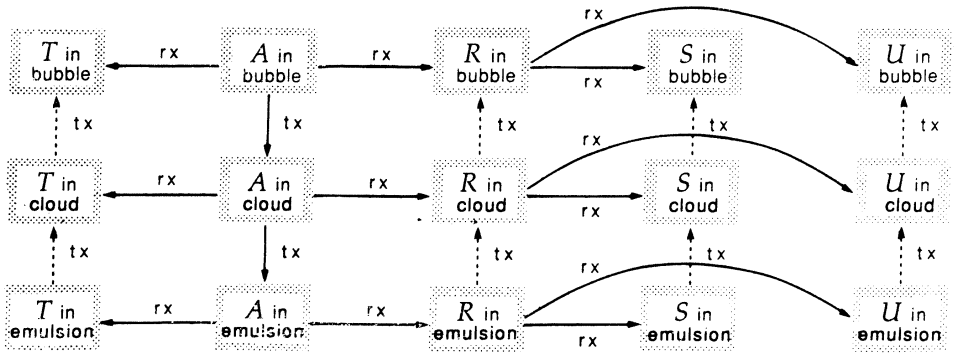

Figure 8.8 Reaction and mass transfer steps for the Denbigh reaction sequence–three-phase model. [After D. Kunii and O. Levenspiel, *Fluidization Engineering*, with permission of Butterworth-Heinemann, Boston, MA, (1991).]

As might be expected, numerous simplifications of this analysis are possible for special cases. Two of particular interest are

1. $k_{r34} \ll k_{r1}$
   In this case $k_{f\mathrm{A}}$ in equation (8–74) is small and as an approximate result

$$k_{fAR} = \left(\frac{k_{r1}}{k_{r12}}\right) K_{f12} \tag{8-79}$$

2. K_{bc} and $K_{ce} \to \infty$
   Here the balance equations can be simplified to

$$\left(\frac{C_{\mathrm{A}_0}}{C_{\mathrm{A}_i}}\right) = \exp(-k_{r12}\tau)$$
$$\left(\frac{C_{R_0}}{C_{\mathrm{A}_0}}\right) = \frac{k_{r1}}{k_{r34} - k_{r12}} \left[\exp(-k_{r12}\tau) - \exp(-k_{r34}\tau)\right] \tag{8-80}$$

   Finally, the maximum amount of intermediate is often a quantity of interest. If we consider that R is a desired product, then

$$\frac{C_R(max)}{C_{\mathrm{A}_i}} = \left(\frac{K_{f\mathrm{AR}}}{K_{f12}}\right)\left(\frac{K_{f12}}{K_{f34}}\right)^{K_{f34}/(K_{f34}-K_{f12})} \tag{8-81}$$

   with τ at $C_R(max)$ as

$$\tau(max) = \frac{V_s}{v} = \frac{\ln(K_{f34}/K_{f12})}{(K_{f34} - K_{f12})} \tag{8-82}$$

As a final word on this development of selectivity, and indeed the developments and illustrations provided throughout this discussion of fluidized beds, we must remember that good old Academic Reaction #1 was employed throughout. However, one should be able to insert any form of reaction kinetics desired with the expectation that the equations will become nonlinear. The concept of rate processes occurring in a series of steps is a core of these models, even though there is no strong *a priori* evidence to support this view.[4] A different viewpoint, picturing mass transport from a solids-lean phase to a solids-rich, cloud-emulsion phase was reported to be superior in some respects to series models such as that of Kunii and Levenspiel [see J.J. Carberry, *Trans. Inst. Chem. Eng., 59,* 15 (1981) and A.A. Shaikh, *Chem. Eng. Technol., 13,* 273 (1990)].

8.2 Slurry Reactors

As can be envisioned by the name, slurry reactors are normally three-phase reactors that involve gas and liquid phases with a catalyst solid phase. Normally the catalyst particulate phase is finely divided with motion-mixing largely governed by the motion of the liquid phase. We will also see in the following that the bubbles of the fluidized bed apply to slurries, although the correlations are somewhat different. In general, we will consider the slurry to be a continuous phase with the gas well-dispersed within the reactor.

[4] "Stick close to your desks and never go to sea."—*W.S. Gilbert*

There are many applications of slurry reactors in industrial processes, see for example, Y.T. Shah, *Gas-Liquid-Solid Reactor Design,* McGraw-Hill Book Co., New York, NY, (1979). Examples include hydrogenation of unsaturated oils, oxidation of olefins, and various polymerization reactions. Advantages over competing three-phase reactors such as trickle beds include improved catalytic effectiveness (small catalyst size), better mass transfer between phases, and better heat transfer (i.e., better temperature control). However, on the negative side it will be seen that a well-agitated slurry reactor is first cousin to a classical CSTR[5] and high conversions are best achieved by staging since the rate of chemical transformation is dictated by the exit concentration of the reactants.

In slurry systems, similar to fluidized beds, the overall rate of chemical transformation is governed by a series of reaction and mass-transfer steps that proceed simultaneously. Thus, we have mass transfer from the bubble phase to the gas-liquid interface, transport of the reactant into the bulk liquid and then to the catalyst, possible diffusion within the catalyst pore structure, adsorption and finally reaction. Then all of this goes the other way for product. Similar steps are to be considered for heat transfer, but because of small particle sizes and the heat capacity of the liquid phase, significant temperature gradients are not often encountered in slurry reactors. The most important factors in analysis and design are fluid holdups, interfacial area, bubble and catalyst particle sizes and size distribution, and the state of mixing of the liquid phase.[6]

8.2.1 An Analysis of Mass Transfer

A typical three-phase slurry reaction is

$$\mathrm{A} + \nu\mathrm{B} \rightarrow \text{Products}$$

where A and B are the reactants in the gas or liquid phases. Generally we will refer to A as a reactant in the gas phase and B as a nonvolatile reactant in the liquid phase. This is typical of hydrogenation and oxidation reactions [R.V. Chaudhari and P.A. Ramachandran, *Amer. Inst. Chem. Eng. J., 26,* 177 (1980)]. The intrinsic rate of reaction per unit weight of catalyst can be represented with a power-law kinetic model,

$$(-r) = k_{(m+n)}[A]^m[B]^n \tag{8-83}$$

or, since we are generally dealing with catalytic reactions, a Langmuir-Hinshelwood expression such as

$$(-r) = \frac{k[A][B]}{1 + K_{\mathrm{A}}[A] + K_B[B]} \tag{8-84}$$

where $(-r)$ is the local rate of reaction at a point within the catalyst where the concentrations are [A] and [B]. Often the liquid-phase reactant is present in large concentration excess. In such case, the variation in [B] in the reactor (or with time of

[5] Slurry-phase reactions are also sometimes carried out in bubble-column reactors, where mixing of the slurry phase is promoted by bubble motion in the column. We will not, however, consider this case explicitly here.

[6] After the tribulations of analyzing the Denbigh sequence in fluidized beds, a reasonable reaction might be "Worth seeing? yes; but ... worth going to see?"—*S. Johnson*

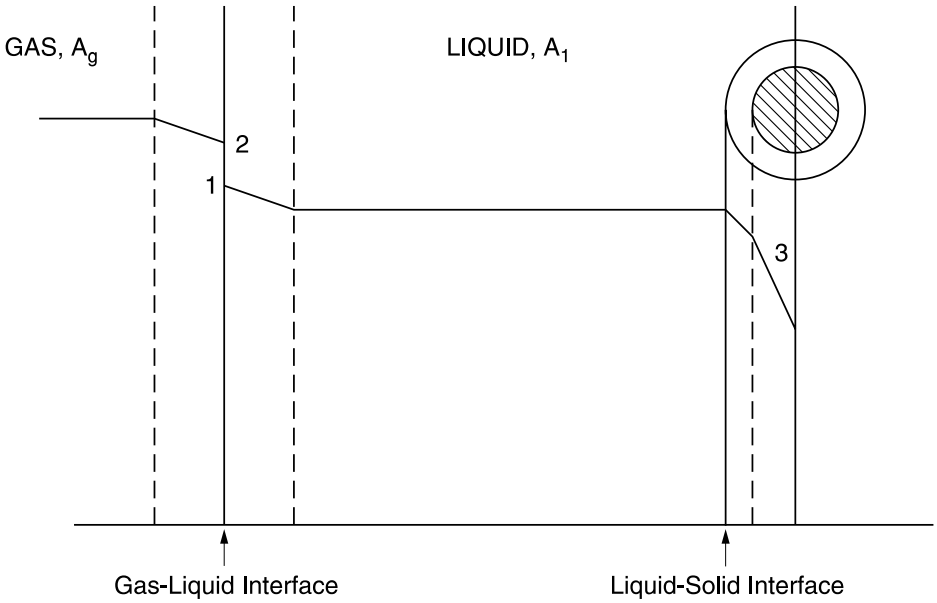

Figure 8.9 Concentration profiles for a reactant, A, in a slurry reactor. Point 1 = A_{1g}, Point 2 = A_{g1}, Point 3 = A_g.

reaction) is not significant, the intraparticle concentration of B is constant equal to that in the bulk liquid phase, and consequently the reaction is pseudo-first-order,

$$(-r_A) = k_m[A]^m \tag{8-85}$$

where $k_m = k_{(m+n)}\{[B]_1\}^n$. The overall mass transfer/reaction in a slurry reactor is illustrated in Figure 8.9 in terms of the concentration profiles characteristic of the gas-phase reactant A.

For steady-state conditions and the assumptions of plug flow in the gas phase and complete mixing in the liquid phase, one can write the mass balance for reactant at any point in the reactor as

$$-u_g\left(\frac{dA_g}{dy}\right) - (k_gS)_A(A_g - A_{gl}) = 0 \tag{8-86}$$

where y is a measure of position in the reactor (we are tacitly assuming that the bubbles will flow upwards through the reactor), u_g is bubble velocity and S is an area for mass transfer. The brackets denoting concentration have been removed for simplicity. For mass transfer we have further,

$$(k_gS)_A(A_g - A_{g1}) = (k_1S)_A(A_{lg} - A_l) \tag{8-87}$$

Now, assuming that Henry's law is valid for the gas-liquid interface,

$$A_{gl} = H_A A_{1g} \tag{8-88}$$

Combining equations (8-86) to (8-88) gives

$$-u_g\left(\frac{dA_g}{dy}\right) = (K_LS)_A\left[\left(\frac{A_g}{H_A}\right) - A_l\right] \tag{8-89}$$

where $K_L S$ is the overall mass-transfer coefficient for the transport of A from bulk-gas to bulk-liquid phase, and H_A is Henry's law constant for A. The overall mass-transfer coefficient is related to the individual coefficients by direct application of the film theory of resistances in series.

$$\frac{1}{(K_L S)_A} = \frac{1}{H_A (k_g S)_A} + \frac{1}{(k_1 S)_A} \tag{8-90}$$

which, so far, is not yet anything to get particularly excited about. Let us integrate equation (8-89) over the reactor height, y, to get

$$\frac{A_g - H_A A_l}{A_{gi} - H_A A_l} = \exp(-\alpha_A y) \tag{8-91}$$

where

$$\alpha_A = \frac{(K_L S)_A}{u_g H_A}$$

The concentration of reactant A leaving the reactor is

$$A_{g_o} = A_{g_i}[\exp(-\alpha_A L)] + H_A A_l [1 - \exp(-\alpha_A L) \tag{8-92}$$

The rate of reactant consumption per unit volume of the slurry phase is

$$R_A = \frac{H_A v}{V_L} (A_{g_o} - A_{g_i}) \tag{8-93}$$

where subscripts o and i refer to outlet and inlet conditions, respectively, v is the volumetric flow rate of gas, and V_L is the volume of the slurry. The rate of mass transfer from the liquid to the surfaces of the catalytic phase is also R_A at steady state,

$$R_A = (k_s S_p)_A (A_1 - A_s) \tag{8-94}$$

with $(k_s S_p)_A$ an appropriate mass-transfer coefficient and A_s the reactant concentration at the external surface of the catalyst particles. Combining equations (8-93) and (8-94)

$$R_A = M_A \left[\left(\frac{A_{gi}}{H_A} \right) - A_s \right] \tag{8-95}$$

with

$$M_A = \left\{ \frac{1}{(H_A v / V_L)[1 - \exp(-\alpha_A L)]} + \frac{1}{(k_s S_p)_A} \right\}^{-1} \tag{8-96}$$

Before equations (8-95) and (8-96) can be used to estimate the overall rate of mass transfer for A, we must eliminate the surface concentration, A_s. The rate of chemical reaction, written for the power-law expression of equation (8-85), is

$$(-\gamma_A) = R_A = \eta_o W k_m A_s^m \tag{8-97}$$

where W is the mass of catalyst per unit volume of slurry and k_m is the pseudo-mth-order rate constant in $(\text{cm}^3/\text{g})\ (\text{cm}^3/\text{mol})^{m-1}\text{-s}^{-1}$. The catalyst effectiveness factor, for

spherical geometry, can be approximated by

$$\eta_c = \frac{1}{\phi}\left[\coth(3\phi) - \frac{1}{3\phi}\right] \tag{8-98}$$

where ϕ is the generalized Thiele modulus as defined by Bischoff [K.B. Bischoff, *Amer. Inst. Chem. Eng. J., 11,* 351 (1965)].

$$\phi = \left(\frac{R}{3}\right)\rho_p(-r_A)_s\left[\int_0^{A_s} 2D_e\rho_p(-r_A)\,dA\right]^{-1/2} \tag{8-99}$$

where $(-r_A)$ is the local rate of reaction. For an mth-order irreversible reaction this reduces to

$$\phi = \left(\frac{R}{3}\right)\left[\frac{(m+1)\rho_p k_m A_s^{m-1}}{2D_e}\right]^{1/2} \tag{8-100}$$

with D_e, the effective diffusivity of the reactant in the catalyst pore structure and ρ_p the catalyst particle density. Since the Thiele modulus is a function of A_s, except for $m = 1$, a trial procedure is required to calculate R_A for the general power-law case.

Ramachandran and Chaudhari [P.A. Ramachandran and R.V. Chaudhari, *Can. J. Chem. Eng., 58,* 412 (1980); *Chem. Eng., J., 20,* 75 (1980)] have shown that it is advantageous to define an overall effectiveness for the reactor in such cases. This is defined as the ratio of the actual rate of chemical reaction per unit volume of the slurry to the rate that would have prevailed it the liquid phase were in equilibrium with the inlet gas phase. Following this,

$$\eta = \frac{R_A}{W[-r(A^*)]}; \qquad A^* = \left(\frac{A_{gi}}{H_A}\right) \tag{8-101}$$

For reaction of order m

$$\eta = \frac{R_A}{Wk_m(A^*)^m} \tag{8-102}$$

The effectiveness factor defined by equation (8-101) is for the entire reactor and thus, in principle, takes into account any variation of the concentration of A in the gas phase along the height of the reactor. To obtain an analytical solution for effectiveness we eliminate the surface concentration by expressing it in terms of the overall effectiveness itself. From equations (8-95) and (8-101) we get

$$a_s = \left(\frac{A_s}{A^*}\right) = 1 - \frac{\eta}{\alpha_A} \tag{8-103}$$

where

$$\sigma_A = \frac{M_A A^*}{W[-r(A^*)]}$$

Combining equations (8-103) and (8-97), the overall effectiveness factor for an mth-order reaction in a slurry reactor can be obtained as

$$\eta = \frac{1}{\phi}\left[\coth(3\phi) - \frac{1}{3\phi}\right]\left[1 - \frac{\eta}{\sigma_A}\right]^m \tag{8-104}$$

From equation (8-100) it is clear that the modulus is a function of A_s and, in turn, A_s is a function of η. Using equation (8-103), and eliminating A_s from equation (8-100), we obtain

$$\phi = \left(\frac{R}{3}\right)\left[\frac{(m+1)\rho_p k_m (A^*)^{m-1}}{2D_e}\left(1-\frac{\eta}{\sigma_A}\right)^{m-1}\right] \tag{8-105}$$

Equation (8-105) is an implicit expression for η, since η is a function of ϕ, and ϕ also a function of η, so a trial procedure is necessary to determine a final value for η. The overall rate for mth-order kinetics can be obtained from equation (8-102) once a value of η has been determined. This approach, using the overall effectiveness, incorporates all the transport resistances and thus simplifies the calculation required to obtain an overall rate of reaction.

For a first-order reaction the problem is less taxing, since

$$\phi = \left(\frac{R}{3}\right)\left[\frac{\rho_p k_1}{D_e}\right]^{1/2} \tag{8-106}$$

which is independent of A_s. Hence the rate of reaction is

$$R_A = \left(\frac{A_{gi}}{H_A}\right)\left\{\frac{1}{(H_A v/V_L)[1-\exp(-\alpha_A L)]} + \frac{1}{(k_s S_p)_A} + \frac{1}{Wk_1[\coth(3\phi)/\phi - (1/3\phi^2)]}\right\}^{-1} \tag{8-107}$$

Equations for the overall effectiveness factor and the modified Thiele modulus are shown in Table 8.1 for several types of rate equations (but all dependent upon A alone). Figure 8.10 gives some idea as to the nature of the overall effectiveness factor for the first-order case treated above.

8.2.2 Gas Mixing and Semi-Batch Operation

If the gas phase does not move in plug flow, and the gas phase is perfectly mixed for whatever reason, the mass balance for gas A is

$$v(A_{g_i} - A_{g_o}) = (K_L S)_L\left[\left(\frac{A_{g_o}}{H_A}\right) - A_l\right] \tag{8-108}$$

Solving for A_{g_o}, the concentration of A leaving the reactor, gives

$$A_{g_o} = \frac{A_{g_i}}{(1+\alpha_A L)} + H_A A_l\left(1 - \frac{1}{(1+\alpha_A L)}\right) \tag{8-109}$$

If we compare equation (8-109) with the corresponding balance for plug flow, equation (8-92), it can be seen that the only difference is that the term $\exp(-\alpha_A L)$ in (8-92) is replaced by $[1/(1+\alpha_A L)]$ in (8-109).

Slurry reactors are also sometimes used in the semi-batch or batch-filling mode, and we should look at an analysis of this type of operation. These are most often used in situations where a gas phase is passed through an agitated slurry phase with

Table 8.1a Equations for Overall Effectiveness for a Slurry Reactor with Various Rate Equations

Kinetic model mole/gm/sec	Overall effectiveness factor, η^2	Generalized Thiele modulus definition, ϕ
$k_m A^m$	$\eta_c\left(1-\frac{\eta}{\sigma_A}\right)^m$	$\frac{R}{3}\left[\frac{(m+1)}{2}\frac{\rho_p k_m A^{*m-1}}{D_{eA}}\left(1-\frac{\eta}{\sigma_A}\right)^{m-1}\right]^{1/2}$
$k_1 A$	See equation (8-107)	$\frac{R}{3}\left(\frac{k_1\rho_p}{D_{eA}}\right)^{1/2}$
k_0	$\sigma_A\left[1-\frac{\phi^2}{6}\{1-3(1-\eta)^{2/3}+2(1-\eta)\}\right]$	$R\left[\frac{\rho_p k_0}{D_{eA}A_0}\right]^{1/2}$
$\frac{k_1 A}{1+K_A A}$	$\eta_c\left[\frac{(1+K_A A_0)(1-\eta/\sigma_A)}{[1+K_A A_0(1-\eta/\sigma_A)]}\right]$	$\frac{R}{3}\left[\frac{\rho_p k_1}{D_{eA}}\right]^{1/2}\cdot\frac{K_A A_0(1-\eta/\sigma_A)}{\{1+K_A A_0(1-\eta/\sigma_A)\}\sqrt{2[K_A A_0(1-\eta/\sigma_A)-\ln\{1+K_A A_0(1-\eta/\sigma_A)\}}}$
$\frac{k_1 A}{(1+K_A A)^2}$	$\eta_0\left[\frac{(1+K_A A_0)^2(1-\eta/\sigma_A)}{[1+K_A A_0(1-\eta/\sigma_A)]^2}\right]$	$\frac{R}{3}\left[\frac{\rho_p k_1}{D_{eA}}\right]^{1./2}\cdot\frac{K_A A_0(1-\eta/\sigma_A)}{\{1+K_A A_0(1-\eta/\sigma_A)\}^2\sqrt{2\ln\left[\{1+K_A A_0(1-\eta/\sigma_A)\}-\frac{K_A A_0(1-\eta/\sigma_A)}{1+K_A A_0(1-\eta/\sigma_A)}\right]}}$

Table 8.1b Overall Rate of Reaction in a Slurry Reactor without Intraparticle Diffusional Effects

Reaction type	Kinetic model (mols/gm/s)	Rate of reaction (R_A mols/cm^3/s)
First-order	$k_1 A$	$A_0\left[\frac{1}{M_A}+\frac{1}{wk_1}\right]^{-1}$
Second-order	$k_2 A^2$	$\frac{M_A^2}{2k_2 w}\left[\left(1+\frac{2wk_2A_0}{M_A}\right)-\left(1+\frac{4wk_2A_0}{M_A}\right)^{1/2}\right]$
Half-order	$k_{1/2}\sqrt{A}$	$\frac{(wk_{1/2})^2}{2M_A}\left[\left(1+\frac{4A_0M_A^2}{(wk_{1/2})^2}\right)^{1/2}-1\right]$
Langmuir-Hinselwood [single site]	$\frac{k_1 A}{(1+K_A A)}$	$\frac{M_A}{2K_A}\left\{\left(1+K_AA_0+\frac{wk_1}{M_A}\right)-\left[\left(1+K_AA_0+\frac{wk_1}{M_A}\right)^2-\frac{4wkK_AA_0}{M_A}\right]^{1/2}\right\}$

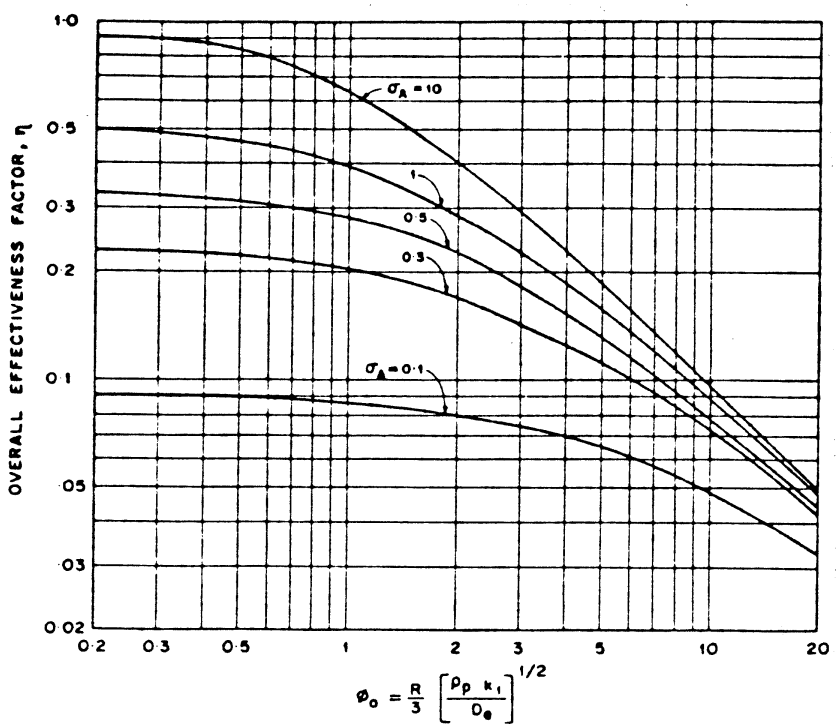

Figure 8.10 Overall effectiveness factor for a first-order reaction in a slurry reactor. [After R.V. Chaudari and P.A. Ramachandran, *Amer. Inst. Chem. Eng., Jl.*, *26*, 177, with permission of the American Institute of Chemical Engineers, (1980).]

no net flow of the slurry. Normally, then, we wish to determine the conversion of liquid-phase reactant B as a function of time. The previous analysis is modified, because [B] $\gg$ [A] does not apply here. In the semibatch operation the concentration of B is changing continuously, just as in any batch reactor (sort of) and simplifying assumptions about kinetics are not likely to be good.

Consider a reaction that is first-order in A, and zero-order in B. The batch time, t_B, required for a given conversion, x, of the liquid phase reactant B is

$$t_B = \frac{B_{l_0} x}{\nu A^*} \left(\frac{1}{M_A} + \frac{1}{\eta_c W K_1} \right) \tag{8-110}$$

where the effectiveness factor η_c is given by equation (8-98) and ϕ is defined by equation (8-106).

In a more realistic case we may have the reaction first-order in both A and B, where the analysis is complicated by the fact that the Thiele modulus becomes a function of B_1, which is changing with time. This complication is tractable, however, and the final time-conversion relationship is

$$t_B = \frac{B_{l_o} x}{\nu A^* M_A} + \frac{B_{l_o} R^2 \rho_p I}{3 \nu A^* W D_e} \tag{8-111}$$

where I is an integral function defined as

$$I + \int_{1-x}^{1} \frac{dx}{\phi_0 x^{1/2} \coth(\phi_0 x^{1/2}) - 1} \tag{8-112}$$

In equation (8-111) B_{l_0} is the initial concentration of B, and t_B is the batch time required to reach a conversion of x. The quantity ϕ_0 is the Thiele modulus at $t = 0$, that based on the initial concentration of B

$$\phi_0 = R \left(\frac{\rho_p k_2 B_{l_o}}{D_e} \right)^{1/2} \tag{8-113}$$

A plot of I versus $(1 - x)$ convenient for calculation is given in Figure 8.11. For $\phi_0 < 0.2$, the effectiveness factor η_c approaches unity and equation (8-111) simplifies to

$$t_B = \frac{B_{l_o} x}{\nu A^* M_A} - \frac{\ln(1 - x)}{\nu A^* W K_2} \tag{8-114}$$

For a general m, nth order reaction (power-law form) the rate of reaction of B per unit volume of slurry is obtained from the expression

$$\frac{dB_1}{dt} = \nu R_A = \nu W K_2 \eta \left(\frac{A_{g_i}}{H_A} \right)^m (B_1)^n \tag{8-115}$$

The effectiveness factor is a function of B_1, thus numerical solution will be required to obtain the B_1 versus t relationship.

8.2.3 Another Approach

The slurry reactor analysis given above employed the concept of an overall effectiveness factor. It is informative to break down the problem into analysis of individual phase effectiveness factors assembled together as was done for the three-phase fluid-bed model. Equating the rates of the individual steps in a manner similar to

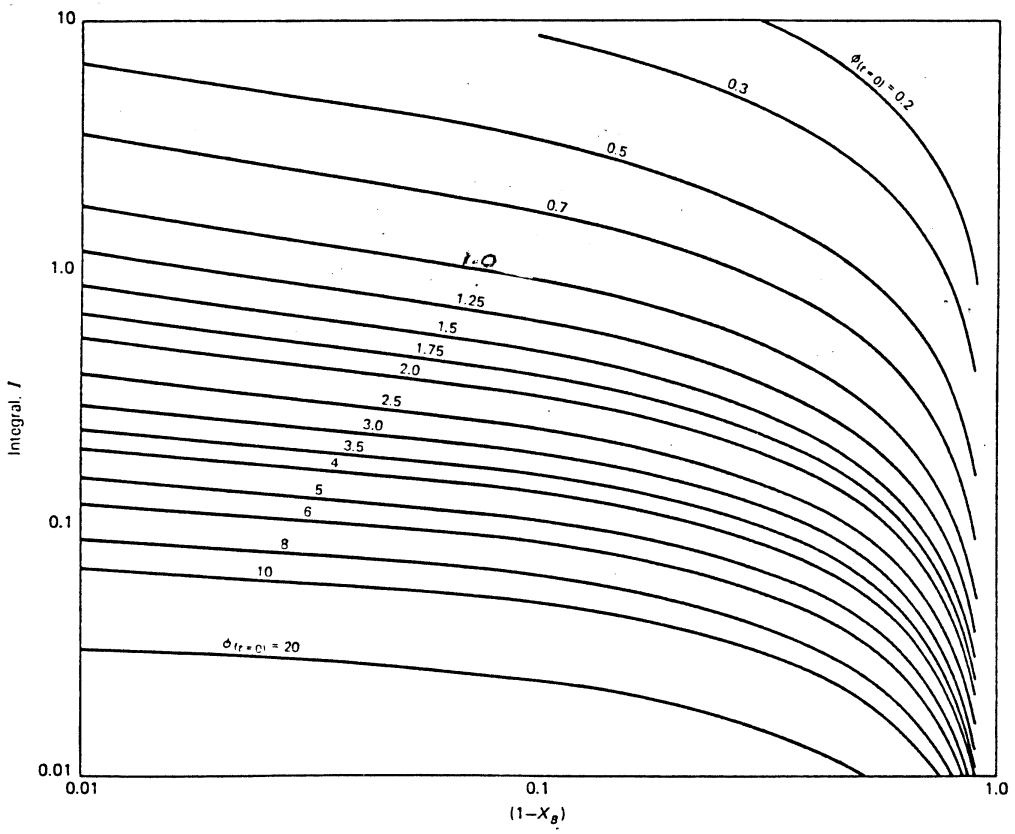

Figure 8.11 Design chart for equation (8-112). Semi-batch slurry reactor with reaction first-order in both A and B. Parameter is ϕ at $r = 0$.

equation (8-87) gives,

$$\begin{aligned} R_A &= (k_g S_b)(A_g - A_{g1}) \\ &= (k_1 S_b)(A_{1g} - A_1) \\ &= (k_s S_p)(A_1 - A_s) \\ &= \eta k S_p A_s \end{aligned} \tag{8-116}$$

for our example first-order reaction. We wish to combine all these factors into an over-all expression that will allow a determining rate via the measurable quantity, A_g, i.e.,

$$(-\gamma_A) = R_A = K_0 A_g \tag{8-117}$$

Eliminating intermediate concentrations in equation (8-116),

$$\frac{A_g}{R_A} = \frac{1}{K_0} = \left(\frac{1}{\eta k} + \frac{1}{k_s}\right)\left(\frac{1}{S_p}\right) + \left(\frac{1}{k_1} + \frac{1}{k_g H_A}\right)\left(\frac{1}{S_b}\right) \tag{8-118}$$

where H_A is the Henry's law constant. Now, let us define phase effectiveness as

$$\eta_b = \frac{1}{1 + (N_{Da})_b} \tag{8-119}$$

$$\eta_1 = \frac{1}{1 + (N_{Da})_1} \tag{8-120}$$

where

$$(N_{Da})_b = \frac{k_1}{K_g H_A}; \qquad (N_{Da})_1 = \frac{\eta k}{k_s}$$

Substitution in equation (8-118) and rearrangement gives

$$K_0 = \frac{\eta_1 \eta k S_p}{1 + (\eta_1 \eta k S_p / \eta_b k_1 S_b)} = \frac{\eta_1 \eta k S_p}{1 + (N_{Da})_0} \tag{8-121}$$

where

$$(N_{Da})_0 = \frac{\eta_1 \eta k S_p}{\eta_b k_1 S_b}$$

Now η_0 can be defined as an overall effectiveness

$$\eta_0 = \frac{1}{1 + (N_{Da})_0} \tag{8-122}$$

Then, $\eta_0 = 1 - \eta_0 (N_{Da})_0$, and dividing by $\eta_0 k_1 S_b$,

$$\frac{(N_{Da})_0}{1 + (N_{Da})_0} = \eta_0 (N_{Da})_0 = \frac{K_0}{\eta_b k_1 S_b} \tag{8-123}$$
$$\tag{8-124}$$

This is about as far as we can go with the individual phase effectiveness; however, it should suffice if η_0 is available from observation and correlations are available for the mass-transfer and area parameters. This brings us to exactly the same point addressed in Section 8.14 for fluidized beds. How can we estimate the parameters involved?

8.2.4 The Parameters of Slurry Reactor Design

At issue here are the determination of values for the mass-transfer coefficients k_g, k_1, and k_s, and the interfacial areas S_b and S_p.

Mass transfer between spheres and surrounding fluids has been a topic of extensive study through the years. The most comprehensive situation is when the relative velocity between the solid and liquid phases is small, which is approximately the case in slurries of small particles. The general results are represented by the curve in Figure 8.12, showing the relationship between the Sherwood number, $(k_s d_p / Đ)$, and a Peclet number $(g d_p^3 \Delta\rho / 18 \mu Đ)$. The solid curve is given by [P.L.T. Brian and H.B. Hales, *Amer. Inst. Chem. Eng. Jl., 15*, 419 (1969)]

$$\left(\frac{k_s d_p}{Đ}\right)^2 = 4 + 1.2 \left(\frac{g d_p^3 \Delta\rho}{18 \mu Đ}\right)^{2/3} \tag{8-125}$$

and the dotted line is that of an asymptotic solution obtained by Levich [V.G. Levich, *Physicochemical Hydrodynamics,* Prentice-Hall, Englewood Cliffs, NJ, (1962)].[7] This gives us the relationship

$$N_{Sh} = \left(\frac{k_s d_p}{Đ}\right) = 0.997 (N_{Pe})^{1/3} \tag{8-126}$$

[7] In practice, working values of k_s appear to be about twice the value that would be computed from this correlation. "A miss is as good as a mile."—*Anonymous*

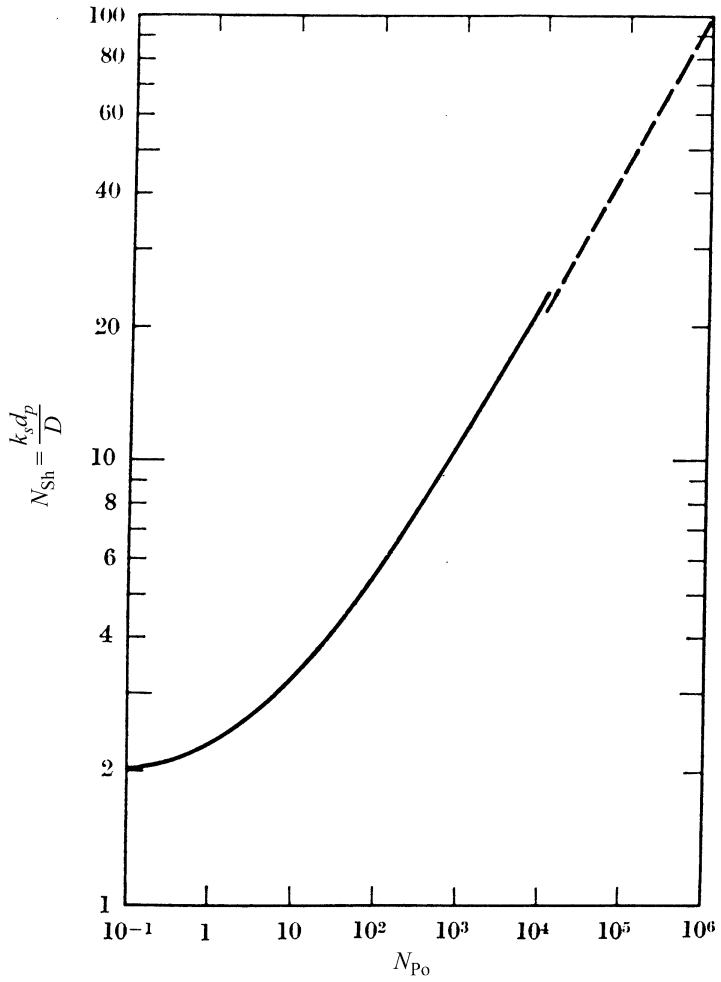

Figure 8.12 Correlation of mass transfer to a single sphere in a liquid for low relative velocities. [After C.N. Satterfield, *Mass Transfer in Heterogeneous Catalysis*, with permission of MIT Press, Cambridge, MA, (1970).]

where N_{Pe} (Figure 8.12, x-axis) is

$$N_{Pe} = \left(\frac{g d_p^3 \Delta\rho}{18 \mu \mathcal{D}} \right)$$

Considerable work has been reported also for the case of bubble-liquid mass transfer and its associated coefficient k_1. A general review of much of this was given by Calderbank [P.H. Calderbank in *Mixing, Vol. II* (V.W. Uhl and J.B. Gray, eds.), Academic Press, New York, NY, (1967)], and a correlation reported there has passed the test of time rather well,

$$k_1 (N_{Sc})^{1/2} = 0.42 \left(\frac{g \mu \Delta\rho}{\rho_1^2} \right) \tag{8-127}$$

where N_{Sc} is for the liquid phase. Equations (8-125) and (8-127), then, provide at least a good initial estimate for the transport coefficients k_s and k_1. Further detail on these correlations is given by Satterfield [C.N. Satterfield, *Mass Transfer in Heterogeneous Catalysis,* MIT Press, Cambridge, MA, (1970)].

The quantity k_q is sort of the "odd-man-out" in most work on slurry reactors (and even also for fluid-bed and gas-liquid reactors). If the bubble (gas) phase consists of pure reactant only, then a mass-transfer resistance in a film inside the bubble loses its meaning and k_q drops out of the problem. Even in the case of mixed gas-phase components, gas phase mass-transfer coefficients are so much larger than their liquid-phase counterparts that the gas-phase transport rate would seldom be of importance in determining the overall rate of chemical reaction.

The interfacial areas do not appear explicitly in the correlations of equations (8-125) and (8-127), but they present another correlation problem in themselves. One is easy; one is more difficult. The easy one is a_p, the interfacial area between the catalyst particles and the liquid making up the slurry phase. Here, if the particle size (or average particle size) is known and the weight loading of catalyst is known,

$$S_p = \left(\frac{6m}{\rho_p d_p}\right) \tag{8-128}$$

where m is the loading (in g cat/volume expanded slurry). The estimate of S_b is a little more tricky. The expression

$$S_b = \left(\frac{6h}{d_p}\right) \tag{8-129}$$

where h is the gas holdup and d_p the bubble diameter, was suggested by both Carberry [J.J. Carberry, *Chemical and Catalytic Reaction Engineering,* McGraw-Hill Book Company, New York, NY, (1976)] and Fan [L-S. Fan, *Gas-Liquid-Solid Fluidization Engineering*, Butterworths, Boston, MA, (1989)]. However, this would appear to change one estimation problem into another, since the holdup (or the bubble diameter for that matter) may not be known *a priori.* If the number of bubbles per volume, N, and the volume per bubble, V, are known, then holdup can be calculated as shown previously for gas-solid fluidized beds, and d_b also comes from the estimate. Slurry reactors, however, seem to be reluctant to yield to correlations of S_b that have any generality. In Figure 8.13a is a generalized diagram of interfacial area versus holdup resulting from a correlation of data for both bubble- and slurry-bubble columns [M. Fukuma, K. Muroyama and A. Yasunishi, *J. Chem. Eng. Japan, 20,* 321 (1987)]. These results seem to arrange themselves along a diagonal, as they are plotted, but with a very generous $\pm$ range. Note particularly in this regard that the correlation is given on a log-log plot. Attempts at correlation of S_b versus gas bubble velocity are of about the same dubious quality (as per Figure 8.13b).

The high and low ranges of results shown in Figure 8.13b are the result of special circumstances and can be ignored in non-foaming systems that do not have high catalyst loadings. Then, once again, we have a diagonal portion of the figure reporting S_b with a generous $\pm$ variation. Aside from the graphical correlation, Chang et al. [S.K. Chang, Y. Kang and S.D. Kim, *J. Chem. Eng. Japan, 19,* 524 (1986)] reported more quantitative results.

$$S_b = (2.08 \times 10^6)(u_g)^{0.35}(u_1)^{0.85}(d_p)^{0.85} \tag{8-130}$$

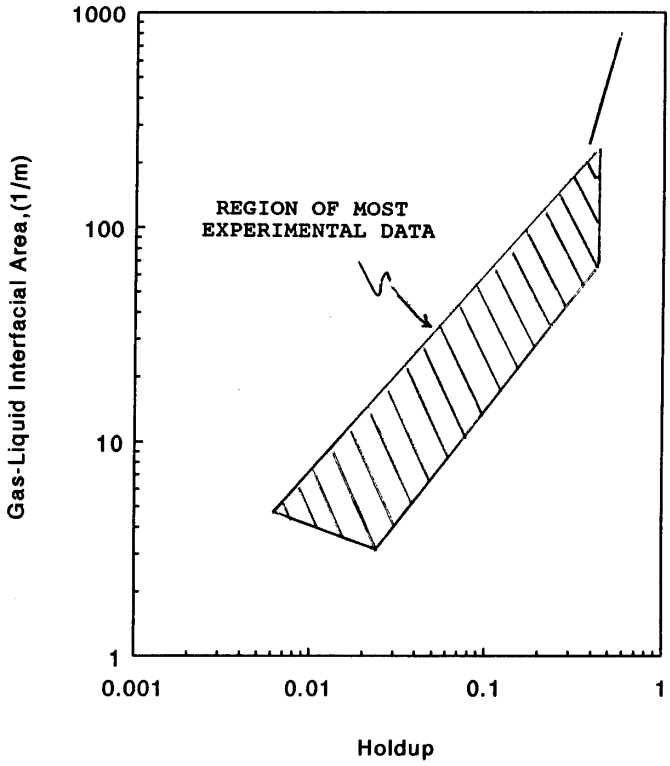

Figure 8.13 (a) Correlation of interfacial area (gas-liquid) with holdup in slurry bubble columns. [After M. Fukuma, K. Muroyama and A. Yashnishi, *J. Chem. Eng. Japan*, *20*, 321, with permission of the Japanese Society of Chemical Engineers, (1987).]

and

$$k_1 S_b = (1597)(u_g)^{0.68}(u_1)^{0.63}(d_p)^{1.12} \tag{8-131}$$

where the numerical values given are consistent with SI units, m, (m^2/m^3), and (mol/s).

If we substitute the parameter correlations of equations (8-125), (8-127), (8-128), and (8-129) into the expression for the overall rate constant, K_0, given by equation (8-118), then

$$\frac{1}{K_0} = \left(\frac{\rho_p d_p}{6\eta_1 \eta k}\right)\left(\frac{1}{m}\right) + \frac{d_b}{6\eta_b k_1 h} \tag{8-132}$$

Recalling that K_0^{-1} (as defined) is equal to the ratio of the observed global rate of reaction to the exit concentration of reactant in the gas phase, then a series of experiments in which rate is measured as a function of catalyst loading, m, can yield information on the magnitude of various parameters (or groups of parameters). Then plots of $(1/R_A)$ versus $(1/m)$ should be straight lines (always a fervent hope), with a slope of $(\rho_p d_p/6\eta_1 \eta k)$ and intercept $(d_b/6\eta_b k_1 h)$. We must keep in mind that the graphical correlation of equations (8-130) and (8-131) are based on data from slurry bubble-columns and should be used gingerly for reactors of other geometry.[8]

[8] "We know to tell many fictions like to truths."—*Hesiod*

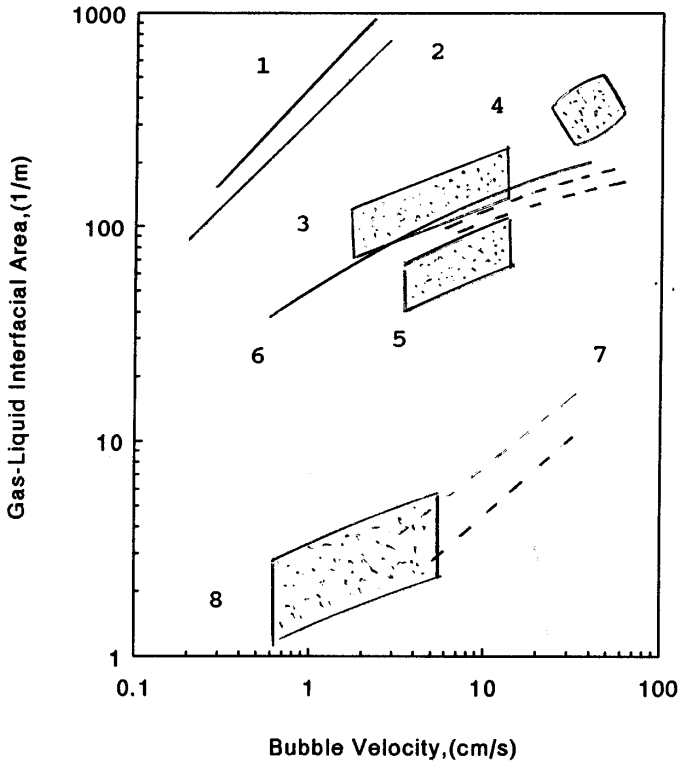

Figure 8.13 (b) Correlation of interfacial area (gas-liquid) with bubble velocity in slurry bubble columns. 1. Deckwer et al. (1980); CO-paraffin-alumina slurry. 2. Sakai and Ohi (1977); Hydrogen-methylstyrene-Pd black slurry. 3. Quicker et al., (1984); Air-sulfite-activated carbon slurry. 4. Sada et al., (1987); Sulfite-alumina slurry. 5. Capuder and Koloni (1984); CO_2-calcium hydroxide slurry. 6. Sada et al. (1987); water. 7. Godbole et al. (1983); Air-sulfite-polystyrene slurry. 8. Fukuma et al. (1987); Air-water-glass beads slurry. Citations from [L-S. Fan, *Gas-Liquid-Solid Fluidization Engineering*, Butterworths, Boston, MA (1989).]

Illustration 8.3[9]

An unsaturated hydrocarbon oil is to be hydrogenated at 316 °C and 54.5 atm using a slurry reactor with a catalyst loading of 8 g-cat per liter of oil. Assuming that the oil can be maintained at hydrogen saturation what space velocity would be required if the reaction consumes 89 m^3 (15 °C, 1 atm) per m^3 liquid feed? We may assume that the catalyst is very active and that the overall rate of hydrogenation is controlled by the rate of mass transfer of hydrogen from the liquid phase to the catalyst particle surfaces. Data:

Mol. wt. Oil = 170
Specific gravity = 0.51 at 316 °C
Viscosity = 0.07 cP
H = Henry's law coefficient = 5.0 (mol fraction in gas/mol fraction in liquid)
$\mathcal{D}$ = Hydrogen in oil at 316 °C = 5×10^{-4} cm^2/s
d_p (spherical) = 0.001 cm
$\rho_p = 3.0$ g/cm^3

[9] [After C.N. Satterfield, *Mass Transfer in Heterogeneous Catalysis*, with permission of MIT Press, Cambridge, MA, (1970).]

Solution
We will consider, as an estimate from the given data, that the catalyst particles can be considered as small spheres in the limit of Stoke's settling law, where

$$N_{Pe} = \frac{d_q^3 g \Delta\rho}{18\mu\mathcal{D}} = \frac{(0.001)^3(981)(3.0 - 0.51)}{(18)(0.0007)(5 \times 10^{-4})} = 0.39$$

The corresponding N_{Sh} from Figure 8.12 is about 2.0. Now, since this is a value based on the terminal settling velocity of small spheres in liquids, it has been shown to give values that are low compared to practical situations where turbulence arising from various factors may exist. Harriott [P. Harriott, *Amer. Inst. Chem. Eng. J., 8,* 93 (1962)] suggested that actual k_s values might range from 2 to 4 times those estimated from the figure [or from equation (8-125)]. Thus, we estimate k_s for this case as

$$k_s = \frac{(2)(2)(5 \times 10^{-4})}{0.001} = 2 \text{ cm/s}$$

The particle surface area is estimated from equation (8-125) as

$$S_p = \frac{6m}{\rho_p d_d} = \frac{(6)(8.0 \times 10^{-3})}{(3)(0.001)} = 16 \text{ cm}^2/\text{cm}^3 \textit{ slurry}$$

The hydrogen concentration in the oil (pure hydrogen in the gas phase) is $(1.0/5.0) = 0.2$ mol fraction, and for this concentration the average molecular weight of the liquid phase is 136. Assuming that the specific gravity of the saturated oil is somewhat lower than that of the pure material, say 0.15, then the hydrogen concentration in the liquid phase is about 0.00066 gmol/cm^3. Then

$$\textit{Hydrogen transfer} = (2)(16)(1000)(0.00066) = 21.2 \text{ gm}$$

This gives a (LHSV) liquid hourly space velocity requirement for the feed as

$$LHSV = \frac{(21.2)(22.4)(288)(3600))}{(89)(273)}$$

or

$$LHSV = 20{,}200 \text{ m}^3/\text{h-m}^3$$

What happens if some things were changed around, such as hydrogen consumption, or if the rate constant (poor catalyst), was much lower?

HORATIO SAYS

Let's try to develop a profile on the case above. What happens, in addition to the problem statement, if

a) The reaction consumes 40 m^3/m^3 of feed?
b) The reaction consumes 120 m^3/m^2 feed?

All the other assumptions used in the Illustration are valid.

8.3 Gas-Liquid Reactors

At first glance gas-liquid reactors might appear to be easier to analyze than slurry reactors since they both involve gas and liquid phases, but the solid phase is not present in the former. On the other hand, the fluid mechanics and transport behavior have been investigated in more detail in gas-liquid systems than in gas-liquid-solid systems, so it is possible to include a little more detail in analysis if desired. The analysis and design equations can also be applied to liquid-liquid systems, as described below.

In Chapter 7 we discussed the basics of the theory concerned with the influence of diffusion on gas-liquid reactions via the Hatta theory for first-order irreversible reactions, the case for rapid second-order reactions, and the generalization of the second-order theory by Van Krevelen and Hofitjzer. Those results were presented in terms of classical two-film theory, employing an "enhancement factor" to account for reaction effects on diffusion via a simple multiple of the mass-transfer coefficient in the absence of reaction. By and large this approach will be continued here however, alternative and more descriptive mass transfer theories such as the penetration model of Higbie and the surface-renewal theory of Danckwerts merit some attention as was done in Chapter 7.

Gas-liquid reactions are most often conducted in stirred-tank systems with flow of both gas and liquid through the reactors, or in bubble columns, or in packed columns—with countercurrent flow typical in the last two. For the most part the analysis given is independent of the specific configuration of the reactor (bubbles are still with us and still important in design), but correlations for transport coefficients may vary with the individual reactor and type of operation.

8.3.1 Diffusion and Reaction Considerations

If we return to the Hatta picture of reaction and diffusion, recall that reaction and diffusion occur *only* in the film. Reaction also occurs in the bulk liquid phase, of course, but there the concentration of reactants as a function of position is determined by the nature of mixing in that phase. Let us reformulate the problem so that the fraction of liquid phase occupied by the film, α, is defined explicitly. If L is film thickness and S_L interfacial area, then

$$\alpha = (V/S_L L) \tag{8-133}$$

where V is the total liquid volume per volume of reactor. For diffusion and reaction in the film we have

$$\frac{d^2 f}{dy^2} = \phi^2 f \tag{8-134}$$

where the boundary conditions are

$$y = 0; \qquad f = 1$$

$$y = 1; \qquad -\frac{df}{dy} = \phi^2(\alpha - 1) \tag{8-135}$$

and

$$f = \left(\frac{A}{A_0}\right); \qquad y = \left(\frac{1}{L}\right); \qquad B = constant$$

$$\phi = K\sqrt{\frac{kB}{D}} = \frac{\sqrt{kBD}}{k_{1_o}}$$

with k_{1_o} the mass-transfer coefficient in the absence of reaction. The diffusional modulus, ϕ is a first cousin of the a_0 defined in Chapter 7, but the boundary condition at $y = 1$ differs. The solution of equation (8-134) with the boundary conditions of (8-135) is

$$f = \frac{\cosh[\phi(1-y)] + \phi(\alpha-1)\sinh[(\phi(1-y)]}{\cosh\phi + \phi(\alpha-1)\sinh\phi} \tag{8-136}$$

For the flux, mols/area-time,

$$(-R_A) = -\left(\frac{DA_0}{L}\right)\left(\frac{df}{dy}\right)_{y=0} = \left(\frac{DA_0}{L}\right)\frac{\phi[\phi(\alpha-1)+\tanh\phi]}{(\alpha-1)\phi\tanh\phi+1} \tag{8-137}$$

$$(-R_A) = k_1 A_0 \tag{8-138}$$

where k_1 is the mass-transfer coefficient in the presence of reaction. The enhancement factor, λ, defined by this result is

$$\lambda = \frac{k_1}{k_{1_o}} = \phi\left[\frac{\phi(\alpha-1)+\tanh\phi}{(\alpha-1)\phi\tanh\phi+1}\right] \tag{8-139}$$

We may also define a *phase utilization factor* as the ratio of observed rate to the intrinsic rate (kBA_0V/S_L)

$$\eta = \frac{\phi(\alpha-1)+\tanh\phi}{\alpha\phi[(\alpha-1)\phi\tanh\phi+1]} \tag{8-140}$$

Limiting cases of this analysis turn out similarly to those identified in Chapter 7, so that

1. *kB is large*

$$\tanh\phi \to 1; \qquad (k_1/k_{1_o}) = \phi; \qquad \eta \to \left(\frac{1}{\phi}\right)$$

$$k_1 = \sqrt{kBD}: \qquad \textit{reaction within the film}$$

2. *kB is small*

$$\left(\frac{k_1}{k_{1_o}}\right) = \frac{\alpha\phi^2}{\alpha\phi^2 - \phi^2 + 1} \tag{8-141}$$

$$\eta = \frac{1}{\alpha\phi^2 - \phi^2 + 1} \tag{8-142}$$

The analysis for kB small may further be divided into two situations.

(a) *ϕ is small and $\alpha\phi^2$ large*

$$\left(\frac{k_1}{k_{1_o}}\right) \to 1; \qquad k_1 \to k_{1_o}$$

$$\eta \to \frac{1}{\alpha\phi^2}$$

(b) *ϕ is small and $\alpha\phi^2$ small*

$$\left(\frac{k_1}{k_{1_o}}\right) < 1$$

$$\eta \to 1$$

Note that in this case the reaction occurs throughout the liquid phase and the rate is determined by the intrinsic kinetics of the chemical reaction.

The results obtained in equations (8-136) to (8-142) assume constant B, i.e., the reaction is pseudo-first-order in A. Another limiting case that yields to analytical solution is that in which the rate of reaction is very rapid and the reaction occurs wholly within the film. Here we consider the reaction $A + \nu B \to P$ to occur very rapidly compared to mass-transfer/diffusion rates. The profiles look as in Figure 7.17b, and the overall flux and enhancement factor are given by

$$(-R_A) = k_1 A_g H_A \tag{8-143}$$

where H_A is Henry's law constant and A_g is the concentration of reactant in the gas phase. The enhancement factor is

$$\lambda = \left(\frac{D_B}{D_A}\right)\left(\frac{B}{A_g}\right) + 1$$

For the intermediate region encompassed by a finite reaction rate, in between equations (8-139) and (7-82) we have the solution of Van Krevelen and Hoftijzer [D.W. Van Krevelen and P.J. Hoftijzer, *Rec. Trav. Chim., 67*, 563 (1984)] given in Chapter 7 by equation (7-83) and Figure 7.18.

We can summarize the major results of this section in terms of the three enhancement factor equations—(8-139), (7-82) and (7-83) for the pseudo-first-order reaction, the infinitely rapid second-order reaction, and the true second-order reaction, respectively. Via λ all mass-transfer coefficients under reaction conditions can be expressed in terms of their pure mass-transfer relatives, so correlations developed for the mass-transfer coefficient k_{1o} can be used for estimation of k_1. These three cases probably constitute the large majority of gas-liquid reactions one is likely to encounter. Some additional cases are discussed by Fromont and Bischoff [G.F. Froment and K.B. Bischoff, *Chemical Reactor Analysis and Design, 2 ed.,* John Wiley and Sons, New York, NY (1990)].

8.3.2 Overall Analysis for Batch or Counter-Current Contactors

Here we consider a batch case with a reaction, first-order irreversible once again, with the reaction $A \to B$ occurring in the liquid phase. The components of the liquid

phase are considered to be nonvolatile.[10] For the mass-transfer rate we have the normal film theory expression overall

$$N_{\mathrm{A}} = k_1 S_1 (A^* - A_1) \tag{8-144}$$

with $A^* = H_{\mathrm{A}} A_g$. Individual balances in gas and liquid phases are

$$-V_g \left(\frac{dA_g}{dt} \right) = k_1 S_1 (H_A A_g - A_1) V \tag{8-145}$$

$$-V_1 \left(\frac{dA_1}{dt} \right) = k A_1 V_1 - k_1 S_1 (H_{\mathrm{A}} A_g - A_1) V \tag{8-146}$$

where V is the reactor total volume. Combination of the two individual mass balance gives,

$$\left(\frac{V_g}{V k_1 S_1} \right) \frac{d^2 A_g}{dt^2} + \left(H_{\mathrm{A}} + \frac{k V_g}{V k_1 S_1} + \frac{V_g}{V_1} \right) \frac{dA_g}{dt} + k H_{\mathrm{A}} A_g = 0 \tag{8-147}$$

with solution of the general form

$$A_g = G_1 e^{\rho_1 t} + G_2 e^{\rho_2 t} \tag{8-148}$$

and

$$A_1 = G_1 \left(H_{\mathrm{A}} + \frac{V_g \rho_1}{V k_1 S_1} \right) e^{\rho_1 t} + G_2 \left(H_{\mathrm{A}} + \frac{V_g \rho_2}{V k_1 S_1} \right) e^{\rho_2 t} \tag{8-149}$$

From the initial conditions of the system,

$$G_1 + G_2 = A_{g_0} \tag{8-150}$$

and

$$G_1 \left(H_{\mathrm{A}} + \frac{V_g}{V k_1 S_1} \rho_1 \right) + G_2 \left(H_{\mathrm{A}} + \frac{V_g}{V k_1 S_1} \rho_2 \right) = A_{1_0} \tag{8-151}$$

For B, assuming equimolal reaction with A, we have from stoichiometry

$$B_1 = (A_{g_0} - A_g) \left(\frac{V_g}{V_1} \right) + (A_{1_0} - A_1) \tag{8-152}$$

Now, for nonvolatile reactant B, $B_g = 0$. If we are dealing with a liquid-liquid system, however, another balance can be written for B (assuming here and above that $B_{1_0} = 0$).

$$\left[\frac{V_1}{V (k_1 S_1)_B} \right] \frac{d^2 B_1}{dt^2} + \left(\frac{V_1}{V_2} + H_B \right) \frac{dB_1}{dt} = k A_2 \tag{8-153}$$

where 1 and 2 refer to the two liquid phases involved. Thus,

$$B_1 = H_0 + H_1 e^{\sigma t} + A_1 e^{\rho_1 t} + A_2 e^{\rho_2 t} \tag{8-154}$$

[10] The analysis here is sufficiently general that it can be applied to liquid-liquid reactions as well, with only minor modifications [See P. Trambouze, M.T. Trambouze and E.L. Piret, *Am. Soc. Chem. Eng. Jl.*, *7*, 138 (1961).]

where

$$A_1 = \frac{kG_1[H_A + \rho_1 V_1/(k_1 S_1)_A V]}{\rho_1[\rho_1 V_1/(k_1 S_1)_B V + (V_1/V_2) + H_B]}$$

$$A_2 = \frac{kG_2[H_A + \rho_1 V_1/(k_1 S_1)_A V]}{\rho_1[\rho_1 V_1/(k_1 S_1)_B V + (V_1/V_2) + H_B]}$$

and

$$B_2 = H_B H_0 + H_1\left[\frac{V_1\sigma}{V(K_1S_1)_B} + H_B\right]e^{\sigma t} + A_1\left[\frac{V_1\rho_1}{V(k_1S_1)_B + H_B}\right]e^{\rho_1 t} + A_2\left[\frac{V_1\rho_2}{V(k_1S_1)_B + H_B}\right]e^{\rho_2 t} \tag{8-155}$$

The constants H_0 and H_1 are also determined from initial conditions. For ρ_1 and ρ_2 we start with (8-147) again, now in operator notation

$$(AD^2 + ND + R)A_1 = 0$$

Then,

$$D = \frac{-N \pm \sqrt{N^2 - 4AR}}{2A}$$

where A, N and R are identified with the corresponding coefficient terms in equation (8-147). Thus, $A = V_1/V(k_1S_1)_A$, and so on. The result is,

$$\rho_1, \rho_2 = \frac{-[H_A + kV_1/Vk_1S_1)_A + (V_1/V_2)}{2V_1/V(k_1S_1)_A} \pm \frac{\{[H_A + kV_1/V(k_1S_1)_A + (V_1/V_2)]^2 - 4H_A(k_1S_1)_A V_1/V(k_1S_1)_B\}^{1/2}}{2V_1/V(k_1S_1)_A}$$

This analysis gives the general result for a batch reaction (both phases) for either gas-liquid or liquid-liquid reactions—in the latter case for reactant B distributed between both phases (but reaction in phase 2 only). Determination of the constants (G and H) is left as an algebraic exercise for those with sufficient patience.

For the case of a *countercurrent contactor,* we envision the arrangement as shown in Figure 8.14. We will consider that both phases are in plug flow, and again we have the irreversible reaction that occurs in phase 2. Since we have the possibility of either gas-liquid or liquid-liquid reaction, we will just number the phases 1 and 2. Now, over dy, we can write the mass balances as

$$d(F_1A_1) - K_A(A_2^* - A_2)S_c dy = 0 \tag{8-156}$$

$$d(F_2A_2) - K_A(A_2^* - A_2)S_c dy = kA_2S_c\epsilon dy \tag{8-157}$$

where S_c is a contact area defined such that $\epsilon S_c dy = dV_2$. The equilibrium will be

$$A_2^* = \alpha_A A_1 + \beta_A$$

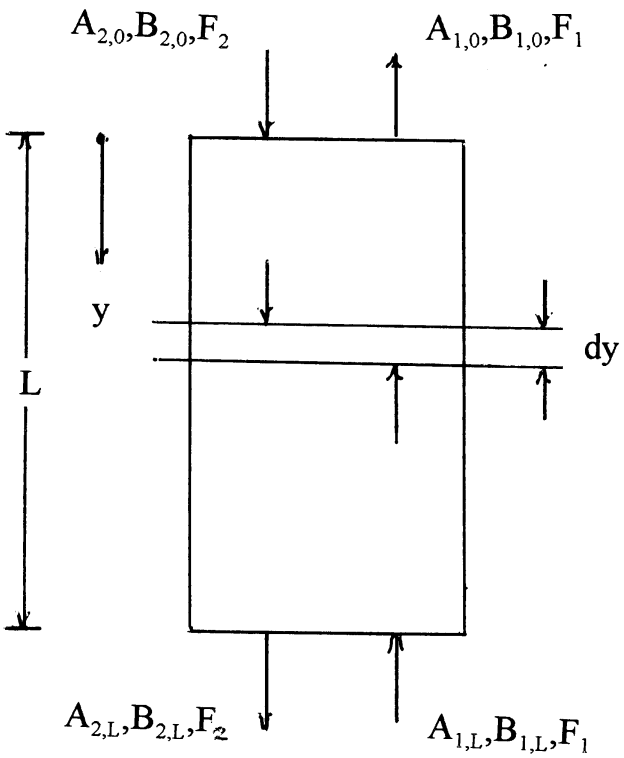

Figure 8.14 A countercurrent reactor; gas-liquid or liquid-liquid.

This is a linear relationship, but more complex than Henry's law, so

$$\frac{F_1}{S_c}\left(\frac{dA_1}{dy}\right) - K_A\beta_A + K_A A_2 - K_A\alpha_A A_1 = 0 \tag{8-158}$$

and

$$-\frac{F_2}{S_c}\left(\frac{dA_2}{dy}\right) + K_A\beta_A - K_A\alpha_A A_1 - k\epsilon A_2 = 0 \tag{8-159}$$

where k is the rate constant for the first-order reaction, here assuming pseudo-first order in the transferred component A. Combining by eliminating A_1

$$\left(\frac{F_1F_2}{K_A S_c^2\alpha_A}\right)\frac{d^2A_2}{dy^2} + \frac{1}{S_c}\left[\frac{F_1}{\alpha_A}\left(1+\frac{k\epsilon}{K_A}\right) - F_2\right]\frac{dA_2}{dy} - k\epsilon A_2 = 0 \tag{8-160}$$

so

$$A_2 = G_1 e^{\rho_1 y} + G_2 G e^{\rho_2 y}$$

This really gets a lot worse, but since an analytical solution in terms of the reactor/reaction parameters is available, one can't dodge it. For the exponential constants

ρ_1, and ρ_2 we have

$$\rho_1, \rho_2 = -\left\{ \frac{F_1}{\alpha_A} \left[1 + \left(\frac{k\epsilon}{K_A} \right) \right] - F_2 \left(\frac{1}{2F_1F_2/K_A S_c \alpha_A} \right) \right. \\ \left. \pm \frac{\left\{ \left[\frac{F_1}{\alpha_A} \left(1 + \frac{k\epsilon}{K_A} \right) - F_2 \right]^2 + \frac{4k\epsilon F_1 F_2}{K_A \alpha_A} \right\}^{1/2}}{(2F_1F_2/K_A S_c \alpha_A)}$$

The concentration A_1 may be evaluated from equation (8-156), similarly indigestible but unavoidable,

$$\beta_A + \alpha_1 A_1 = G_1 \left(\frac{F_2}{K_A S_c} \rho_1 + \frac{K_A + k\epsilon}{K_A} \right) e^{\rho_1 y} + G_2 \left(\frac{F_2}{K_A S_c} \rho_2 + \frac{K_A + k\epsilon}{K_A} \right) e^{\rho_2 y} \tag{8-161}$$

Similarly for B_1 and B_2

$$B_2 = H_0 + H_1 e^{\sigma y} + A_1 e^{\rho_2 y} + A_2 e^{\rho_2 y} \tag{8-162}$$

where

$$\sigma = \frac{S_c K_B \alpha_B}{F_1 F_2} \left(F_2 - \frac{F_1}{\alpha_B} \right)$$

$$D_1 = \frac{2k\epsilon G_1}{\rho_1} + \frac{F_1\rho_1 - S_c K_B \alpha_B}{(F_1F_2\rho_1/S_c) + F_1 K_B - F_2 K_B \alpha_B}$$

$$D_2 = \frac{2k\epsilon G_2}{\rho_2} + \frac{F_1\rho_2 - S_c K_B \alpha_B}{(F_1F_2\rho_2/S_c) + F_1 K_B - F_2 K_B \alpha_B}$$

and

$$B_1 = \frac{1}{\alpha_B} \left[H_0 - \beta_B + H_1 \left(\frac{F_2\sigma}{S_c K_B} + 1 \right) e^{\sigma y} + D_1 \left(\frac{F_2\rho_1}{S_c K_B} + 1 \right) e^{\rho_1 y} \right. \\ \left. + D_2 \left(\frac{F_2\rho_2}{S_c K_B} + 1 \right) e^{\rho_2 y} - \frac{2k\epsilon}{K_B} (G_1 e^{\rho_1 y} + G_2 e^{\rho_2 y}) \right] \tag{8-163}$$

As for the batch case, H_0 and H_1 are determined from the feed compositions. In these analyses, whenever we can write two mass balances with only the first derivative of concentration, they may be combined into a single second-order equation for one concentration.

8.3.3 Another Approach

The basic equations for these gas-liquid reactors are, to start with, not terribly complicated or difficult to understand conceptually, but the analysis of the section above shows that we are left with cumbersome solutions with many terms—enough so that one might reasonably feel somewhat uncomfortable working with them.

Another way to approach the topic of gas-liquid reactor design is just to state the basic phase balances in very general form, and then simplify according to the particular situation. A possible drawback is that there is a seemingly endless number of these individual situations, e.g., is there plug flow or CSTR behavior (in one or both phases), is bubble size constant, is the equilibrium according to Henry's law,

and so on. We seek some reasonable classification scheme to order these various possibilities. One such scheme is to divide the treatment into analysis of systems either involving gas-liquid "tank-type" reactors or systems involving "tubular" reactors (normally vertical, but not always), and then proceed with subdivisions in the pertinent area. This approach was established by Russell et al. [R.W. Schaftlein and T.W.F. Russell, *Ind. Eng. Chem., 60,* 12 (1968); P.T. Cichy, J.S. Ultman and T.W.F Russell, *Ind. Eng. Chem., 61,* 6 (1969)] and will be followed.

Tank-type reactors

These are generally classified as either CSTRs, semiflow batch reactors (SFBR), or plain batch reactors, which we treated in the previous section. If the reactor is well-mixed, the liquid-phase mass balance is the same general form for all. For component j,

$$vC_{oj} - vC_j + K_G a' P V_b N V_L \left(y_j - C_j \frac{H}{P} \right) - r_j V_L = \frac{d}{dt} (V_L C_j) \tag{8-164}$$

where a' is the ratio of surface area to single bubble volume (λ), V_b the volume of a single bubble (λ^3), N the number of bubbles per unit volume of liquid, r_j the rate of reaction for component j, V_L volume of the liquid phase, and v is the volumetric flow rate of the liquid phase.

One can see immediately that this approach will be a little more detailed than the previous section, since the bubble mechanics are contained in the basic material balance. Various simplifications of equation (8-164) are possible according to the reactor type by deleting terms; for a steady-state CSTR the time derivative is zero, for a batch reactor the flow rate terms are zero, etc. For the gas phase the situation is complicated by the fact that the configuration (and concentration) of bubbles can be a function of both time and position; that is, the total mass of j in a given bubble, $(PV_b y_j / RT)$, can depend on both position z and time t.

If the bubbles are passed through the liquid phase in the absence of mechanical agitation it is possible to approach plug flow behavior, and the gas (bubble) mass balance is

$$-K_G a' P V_b \left(y_j - C_j \frac{H}{P} \right) - v_b \frac{\partial}{\partial z} \left(\frac{P V_b}{RT} y_j \right) = \frac{\partial}{\partial t} \left(\frac{P V_b}{RT} y_j \right) \tag{8-165}$$

where H is Henry's law constant and v_b is the bubble velocity. If there is mechanical agitation, or other factors that promote mixing in the liquid phase, then the well-mixed bubble mass balance is

$$G_1 y_{oj} - G_2 y_j - K_G a V_L P \left(y_j - C_j \frac{H}{P} \right) = \frac{d}{dt} \left[(N V_L V_b) \left(\frac{P y_j}{RT} \right) \right] \tag{8-166}$$

with G_1, G_2 the molar gas flow into and out of the reactor, aV_L the total area for mass transfer, $NV_L V_b$ the total gas volume, and a the mass-transfer area per unit volume of continuous phase. From the above we can also define the average liquid residence time,

$$t_L = V_L / v$$

and the total surface area per volume of liquid

$$a = a' V_L N$$

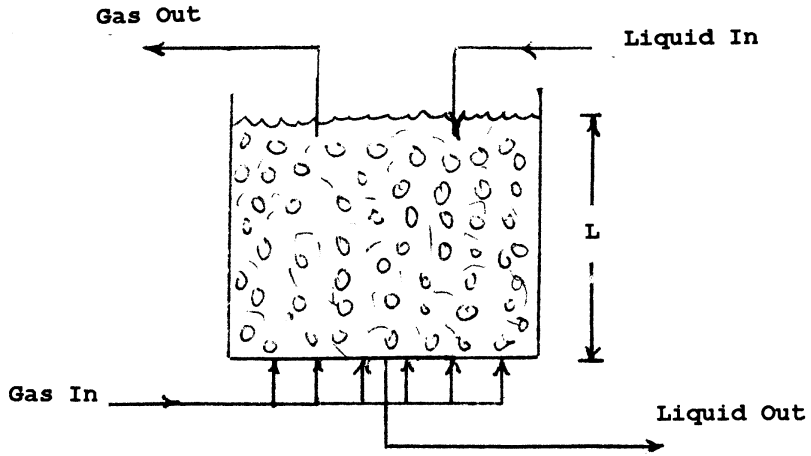

Figure 8.15 A CFTR with plug-flow gas and well-mixed liquid phases.

Now, on the basis of equations (8-164) to (8-166) we can break down the analysis into simplified forms that apply to very specific situations. The most obvious place to start is with the continuous flow case with both gas and liquid passing through the reactor [termed *continuous flow tank reactors* (CFTR) by Russell et al.], as shown in Figure 8.15. Let us look at some of the specific situations.

Plug-flow gas and well-mixed liquid CFTR. From the general balance of equations (8-164) and (8-165), for the gas phase in steady state

$$-K_G a' P V_b \left(y_j - C_j \frac{H}{P} \right) - v_b \frac{d}{dz} \left(\frac{P V_b}{RT} y_j \right) = 0 \tag{8-167}$$

and for the liquid phase

$$v C_{oj} - v C_j + K_G \bar{a}' P \bar{V}_b N V_L \left(\bar{y}_j - C_j \frac{H}{P} \right) - r_j V_L = 0 \tag{8-168}$$

where the overlined quantities represent suitable average values for the liquid phase. The gas-phase concentration is a function of position if the gas feed is not composed of pure reactant, so averages such as

$$\bar{y}_j = \left(\frac{1}{L} \right) \int_0^L y_j(z)\, dz \tag{8-169}$$

must be computed in the most general case.

Now we have written the balance in some detail as to the properties and behavior of the gas (bubble) phase, so we must establish further subclassifications according to this. Consider V_b constant, which will be true if y_j is small or mass transfer is slow. In this case a' and V_b are both constant, and equation (8-167) can be integrated directly as

$$y_j = C_j \left(\frac{H}{P} \right) + \left(y_{oj} - C_j \frac{H}{P} \right) \exp(-K_G a' RTL / v_b) \tag{8-170}$$

and from equation (8-169)

$$\bar{y}_j = C_j\left(1 - \frac{1 - e^{-n}}{n}\right)\left(\frac{H}{P}\right) + y_{oj}\left(\frac{1 - e^{-n}}{n}\right) \tag{8-171}$$

with $n = (K_G a' RTL/v_b)$. For the liquid-phase concentration, the best we can do is an implicit equation for C_j obtained by substituting y_j in equation (8-168),

$$C_j = C_{oj} + \left[y_{oj} - C_j\left(\frac{H}{P}\right)\right]\left(\frac{PV_b NV_L v_b}{RTvL}\right) \cdot \left[1 - \exp\left(-\frac{K_G a' RTL}{v_b}\right)\right] - r_j\left(\frac{V_L}{v}\right) \tag{8-172}$$

Another important case is that for $V_b =$ constant but $y_j = 1$ (pure gas phase). Here the bubble volume changes because of the transfer of reactant into the liquid (reaction) phase, and both a' and V_b are functions of position. We have to have some detail on the bubbles. If it is assumed that all bubbles are spherical, then

$$\begin{aligned} S &= (6)^{2/3}\pi^{1/3} = 4.84 \\ a' &= SV_b^{-1/3} \end{aligned} \tag{8-173}$$

where S is a bubble shape factor. An expression for the bubble rise velocity, borrowed from Davidson and Harrison, is

$$v_b = WV_b^{1/6} \tag{8-174}$$

with

$$W = (0.711)g^{1/2}(6/\pi)^{1/6}$$

The gas-phase balance can now be integrated to give us V_b as a function of z

$$V_b(z) = \left\{V_{0_b}^{1/2} - \frac{K_G RTS}{2W}\left[1 - C_j\left(\frac{H}{P}\right)\right]z\right\}^2 \tag{8-175}$$

and

$$\bar{V}_b = V_{0_b} + \left(\frac{L^2F^2}{3} - V_{0_b}^{1/2}LF\right) \tag{8-176}$$

$$F = \frac{K_G RTS}{2W}\left[1 - C_j\left(\frac{H}{P}\right)\right] \tag{8-177}$$

and from equation (8-173)

$$\bar{a}' = S\bar{V}_b^{1/3} \tag{8-178}$$

Again we obtain an implicit equation for C_j, this time in terms of a' and V_b,

$$C_j = C_{oj} + K_G\bar{a}'\bar{V}_b NP\left(\frac{V_L}{v}\right)\left[1 - C_j\left(\frac{H}{P}\right)\right] - r_j\left(\frac{V_L}{v}\right) \tag{8-179}$$

Keep in mind for later calculation via equations (8-172) and (8-179) that all the odds and ends are still not tidied up, because we still need numbers for quantities such as V_{0_b} and N.

The most general case is for CFTRs in which $V_b \neq$ constant and $y_j \neq 1$. The overall gas-phase balance is now

$$-K_G a' P V_b \left[y_j - C_j \left(\frac{H}{P} \right) \right] - v_b \frac{d}{dz} \left(\frac{P V_b}{RT} \right) = 0$$

which we can rewrite as

$$K_G a' RT \left[y_j - C_j \left(\frac{H}{P} \right) \right] + \frac{v_b}{(1 - y_j)} \left(\frac{dy_j}{dz} \right) = 0 \tag{8-180}$$

This equation requires expressions for a' and v_b as related to y_j in order to be solved. The path to solution is sort of convoluted: a' and v_b are functions of V_b, as shown in equations (8-173) and (8-174). Then we can obtain a' and v_b via

$$\int_{a'_o}^{a'} da' = \int_{y_{oj}}^{y_j} \left(\frac{da'}{dV_b} \right) \frac{v_b}{(1 - y_j)} \, dy_j$$

and V_b is related to y_j via

$$V_b = V_{0_b} \left(\frac{1 - y_{oj}}{1 - y_j} \right)$$

Step by step, then, with a' and v_b as functions of y_j, equation (8-180b) can be integrated and $\bar{y}_j$ determined. The value of V_b is then obtained from the overall mass balance using y_j as obtained from (8-180b). With $\bar{V}_b$ known, then $\bar{a}'$ can be determined.

Well-mixed gas and liquid phases in the CFTR. In this case, under steady-state conditions, there is no variation of concentration with position. Although it is possible to obtain some degree of mixing in the gas phase through bubble motion alone, normally tank-type reactors fitting this description are agitated via externally powered impellers of various designs. The following were obtained directly from equations (8-164) and (8-166). For the gas,

$$G_1 y_{oj} - G_2 y_j - K_G a V_L P \left[y_j - C_j \left(\frac{H}{P} \right) \right] = 0 \tag{8-181}$$

and for the liquid,

$$\left(\frac{v}{V_L} \right) (C_{oj} - C_j) + K_G a P \left[y_j - C_j \left(\frac{H}{P} \right) \right] - r_j = 0 \tag{8-182}$$

These form an algebraic pair, and the overall two-phase model is obtained by determining y_j from equation (8-181) and substituting it into (8-182).

The second important configuration is that of the *semiflow batch reactor (SFBR)*, in which the liquid phase is contained and only the gas flows through. This is also envisioned in Figure 8.15, but with no liquid flow. Again, we will take the liquid phase to be well-mixed, with limiting gas-phase behavior either plug flow or well mixed.

Plug-flow gas, well-mixed liquid SFBR. Here, from the general phase balance, for the gas

$$K_G a' P V_b \left[y_j - C_j \left(\frac{H}{P} \right) \right] + v_b \frac{d}{dz} \left(\frac{P V_b}{RT} y_j \right) = 0 \tag{8-183}$$

and for the liquid,

$$K_G a' P V_b N V_L \left[\bar{y}_j - C_j\left(\frac{H}{P}\right)\right] - r_j V_L = \frac{d}{dt}\,(V_L C_j) \tag{8-184}$$

An important point in analysis is that even though the batch liquid-phase concentration is time dependent, this is not important if changes (within one bubble rise-time in the reactor) are small compared to changes with respect to position. For $V_b =$ constant and first-order reaction in the liquid phase, we first obtain y_j as in equation (8-169) to (8-171). For the liquid phase the balance is

$$\frac{dC_j}{dt} = -C_j(HK_G a' V_b N + k) + K_G a' P V_b N \bar{y}_j \tag{8-185}$$

Substituting for y_j and simplifying gives

$$\frac{dC_j}{dt} + k_1 C_j = k_2 \tag{8-186}$$

$$C_j = \left(\frac{k_2}{k_1}\right) + (C_{oj} - k_2/k_1)e^{-k_1 t} \tag{8-187}$$

where

$$k_1 = k + (1 - e^{-n})HV_b N v_b / RTL$$

$$k_2 = y_{oj}(1 - e^{-n})V_b N v_b P / RTL$$

and k is the reaction rate constant.

For $V_b \neq$ constant but $y_j = 1$, the general equations yield, for the gas phase, equation (8-183) again, and for variable bubble volume equations (8-176) to (8-178) again. Substituting into the liquid-phase model, (8-184), gives

$$\frac{dC_j}{dt} = -C_j(HK_G \bar{a}' \bar{V}_b N + k) + K_G \bar{a}' \bar{V}_b N P \tag{8-188}$$

Solution of this set of equations is best accomplished numerically. Horatio may ask a question about this later.

Well-mixed gas, well-mixed liquid SFBR. In this case the concentrations are spatially invariant, but do depend on time because of the batch liquid phase. For the gas

$$G_1 y_{oj} - K_G a V_L P\left[y_j - C_j\left(\frac{H}{P}\right)\right] = 0 \tag{8-189}$$

and for the liquid,

$$K_G a P\left[y_j - C_j\left(\frac{H}{P}\right)\right] - kC_j = \frac{dC_j}{dt} \tag{8-190}$$

Here the gas-phase equation may be solved for y_j; this is substituted into the liquid-phase equation which can then be integrated to obtain $C_j(t)$. The results are of the same form as equations (8-187a) end (8-187b).

Tubular or Column Reactors

The approach to analysis of reactors of this type depends to a large extent on the nature of the flow patterns. (Is this news?) In bubble-column reactors, which are of

primary interest, such patterns can be described in a way similar to those used for fluidized beds. A general description would include the following:

1. Dispersed flow. Liquid flows as individual droplets in a high-velocity turbulent gas stream.
2. Annular-flow. Liquid flows as a thin film around the inner surface of the column. The film thickness is not usually a function of position within the column, but the gas-liquid interface is not smooth.
3. Slug flow. Here we have alternating flows of gas and liquid slugs that are of the same size as the column diameter.
4. Bubble flow. The gas travels in discrete volumes with a distribution of sizes and shapes, ranging from single bubbles moving separately to bubble swarms or clouds.

An analysis of flow patterns in vertical countercurrent contactors was reported by Govier et al. [G. Govier, B.A. Rodford, and J.S.C. Dunn, *Can. J. Chem. Eng., 38*, 58 (1957)] and a generalized flow regime chart based on their findings is given in Figure 8.16.

In fact, the flow patterns are even more complex than appear in the figure. Russell and co-workers identified no less than 26 regions of flow behavior, including both horizontal and vertical configurations [P.T Cichy, J.B. Ultman, and T.W.F. Russell, *Ind. Eng. Chem., 61,* 6 (1968)]. The most basic divisions, as far as reactor modeling is concerned, are those systems in which both gas and liquid phases are continuous versus those in which the two phases are discrete. Those are treated accordingly below.

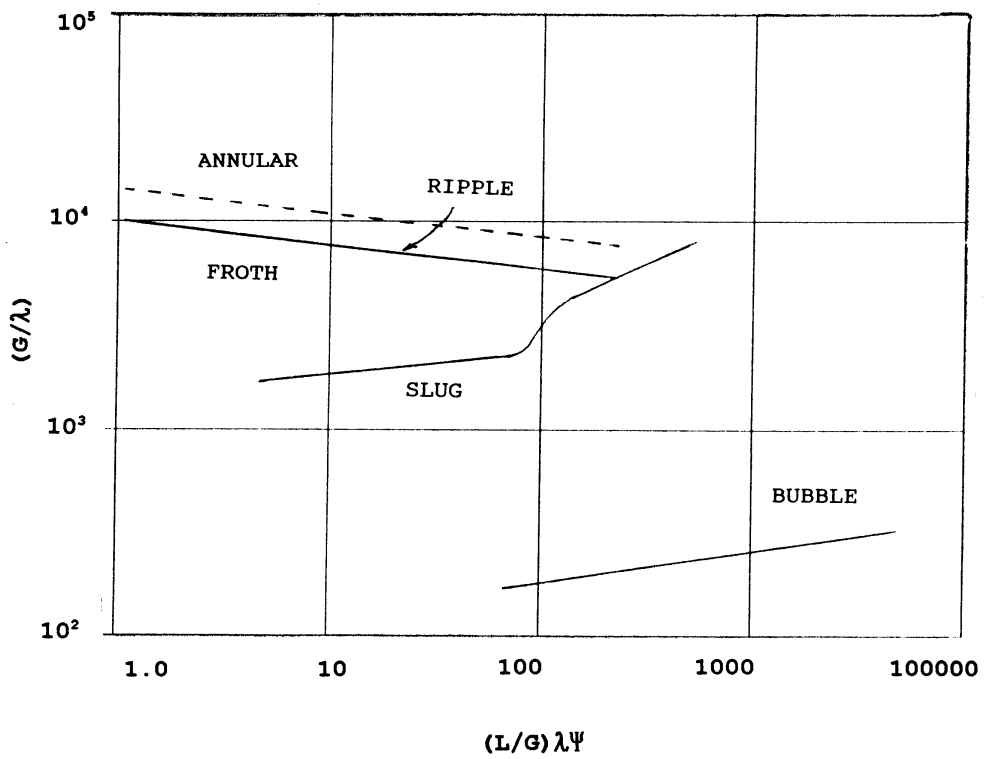

Figure 8.16 Govier chart for bubble-liquid flow in vertical columns. $\lambda = (\rho_G/0.075)(\rho_L/62.3)^{1/2}$; $\psi = (73/\gamma_L)[\mu_L(63.2/\rho_L)^2]^{1/3}$. [O. Baker, *Oil Gas Jl., 56*, 256 (1958).]

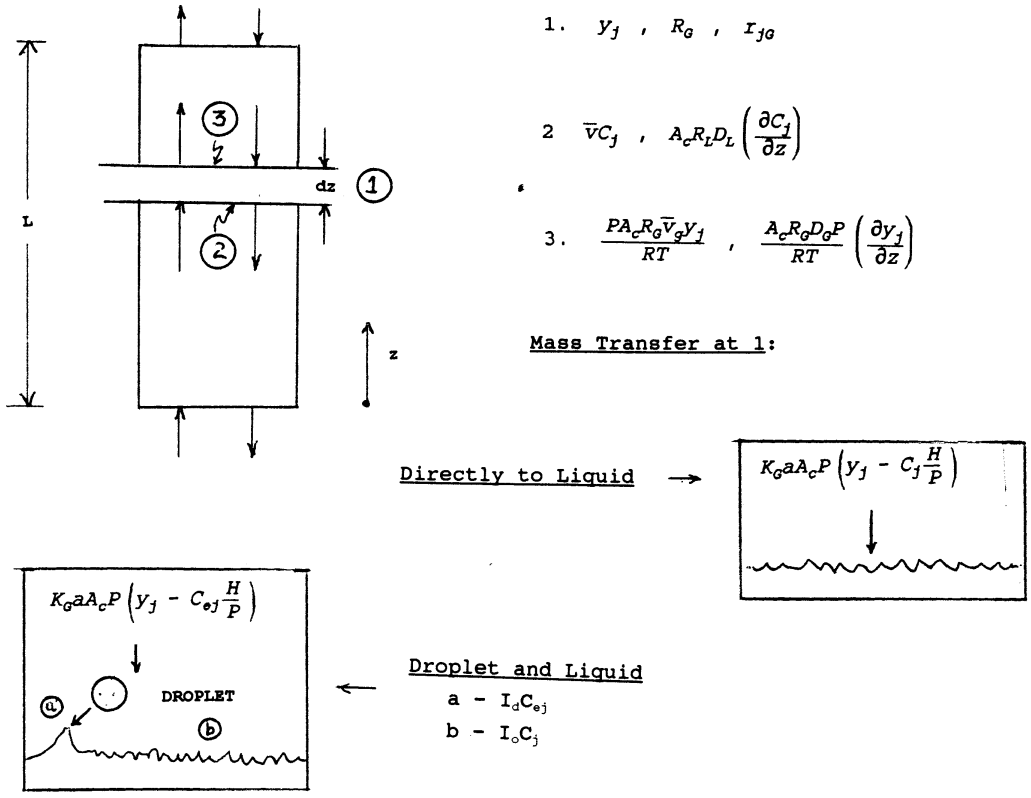

Figure 8.17 A two-phase mass transfer model for gas-liquid reactors.

When the two phases may be considered as continuous, we can envision the transport and reaction process as shown in Figure 8.17. This two-phase model, as written for a length, dz, and a column cross sectional area, A_c, comprises both the familiar term for interphase transfer plus the addition of mass transfer from the gas phase to entrained liquid droplets, given by $(I_0 C_j/\rho_0)$ and $(I_d \bar{C}_{ej}/\rho_d)$ to account for convective transport to and from the droplets. The quantity I_d is the rate of deposition of the dispersed droplet phase on the liquid film (m/tz) and I_0 is a corresponding rate of entrainment from the liquid phase into droplets. The very general mass balances below will consider both types of mass transfer, will also consider the possibility of reaction in both gas and liquid phases, and will include a dispersion factor to model deviations from actual plug flow if necessary. Now this is a little like diving off the 10 meter board, but here we go with the continuous gas-phase balance.

$$\frac{\partial}{\partial t}\left(\frac{Py_j R_G A_c}{RT}\right) = -\frac{\partial}{\partial z}\left(\frac{\bar{v}_b P y_j R_G A_c}{RT}\right) - K_G a A_c P\left[y_j - C_j\left(\frac{H}{P}\right)\right]$$
$$-\frac{\partial}{\partial z}\left(\frac{PR_G A_c D_G}{RT}\frac{\partial y_j}{\partial z}\right) - r_G R_G A_c$$
$$-(K_G a)' A_c P\left[y_j - \left(\frac{\bar{C}_{oj} H}{P}\right)\right] \qquad (8\text{-}191)$$

where R_L is the liquid-phase holdup and $R_G = (1 - R_L)$, r_G is the gas-phase rate of reaction in mols/time-volume, and $\bar{C}_{oj}$ is the average concentration of species j in the

entrained liquid phase. The two mass-transfer coefficients $(K_G a)'$ and $K_G a$ are included to account for differences between direct transfer from the gas phase and transfer via dispersed droplets. Now, continuing with the liquid-phase balance,

$$\frac{\partial}{\partial t}(R_L A_c C_j) = -\frac{\partial}{\partial z}(\bar{v} R_L A_c C_j) + K_G a A_c P\left[y_j - C_j\left(\frac{H}{P}\right)\right] - \frac{\partial}{\partial z}\left(A_c R_L D_L \frac{\partial C_j}{\partial z}\right) - r_L R_L A_c - \frac{I_0 C_j}{\rho_0} + \frac{I_d \bar{C}_{oj}}{\rho_d} \tag{8-192}$$

The dispersion coefficients D_G and D_L are included to account for deviations from plug flow in both gas and liquid phases, as mentioned above. Equations (8-191) and (8-192) include all possibilities (or at least as many as we are willing to consider at this point), so we can now look at individual cases of interest by chipping away the particular parts that do not apply.

Continuous fluid phases with a well-defined interface. This case, not particularly the most important, is nonetheless convenient to start with since the interface between phases formed by vertical annular flow without droplets gives us an area for mass transport that is easy to determine.[11]

Other important assumptions for this example consist of operation in the steady state, liquid holdup constant (or represented by an appropriate average value), reaction in the liquid phase only, first-order irreversible kinetics (yet again), constant temperature and total pressure, and H independent of concentration. These assumptions allow some considerable simplifications to the general balance equations given above. First, we will define gas and liquid flow rates as

$$G = \frac{P R_G A_c \bar{v}_b}{RT}; \qquad q = R_L A_c \bar{v}$$

For the gas phase,

$$\frac{d}{dz}(G y_j) = -K_G a A_c P\left[y_j - C_j\left(\frac{H}{P}\right)\right] - \frac{R_G A_c D_G P}{RT}\left(\frac{d^2 y_j}{dz^2}\right) \tag{8-193}$$

and for the liquid phase,

$$q\left(\frac{dC_j}{dz}\right) = K_G a A_c P\left[y_j - C_j\left(\frac{H}{P}\right)\right] - A_c R_L D_L\left(\frac{d^2 C_j}{dz^2}\right) - k R_L A_c C_j \tag{8-194}$$

In addition, we can write an overall gas-phase balance

$$\left(\frac{dG}{dz}\right) = -K_G a A_c P\left[y_j - C_j\left(\frac{H}{P}\right)\right] \tag{8-195}$$

in the event that there are significant changes in the gas flow rate through the contactor.

This model bears a familial resemblance to some that were discussed earlier in this chapter. When the dispersion terms are discarded and appropriate changes in the names and significance of some of the parameters are recognized, then we end up basically at the Davidson-Harrison model for fluidized beds.

[11] We deviate from the wise advice to "do the most important thing first ..." to "do the easiest thing first ..."

The first consideration is the very general one where both the gas-phase flow rate, G, and the solute concentration, C_j, are functions of axial position, but plug flow prevails. This is roughly the situation when the solute is transferred from a concentrated gas stream. The following governing equations can be written.

Gas phase

$$\frac{G(z)}{(1-y_j)}\left(\frac{dy_j}{dz}\right) = -K_G a A_c P\left[y_j - C_j\left(\frac{H}{P}\right)\right] \tag{8-196}$$

Liquid phase

$$q\left(\frac{dC_j}{dz}\right) = K_G a A_c P\left[y_j - C_j\left(\frac{H}{P}\right)\right] - kR_L A_c C_j \tag{8-197}$$

where

$$G(z) = G_0 - \int_0^z K_G a A_c P\left[y_j - C_j\left(\frac{H}{P}\right)\right] dz$$

After evaluation of $G(z)$, the concentration profile can be obtained using a procedure similar to that suggested for equations (8-180a) md (8-180b).

When dispersion is not important and G is constant, we have a much simpler situation.

$$\left(\frac{dy_j}{dz}\right) = -\frac{K_G a A_c P}{G}\left[y_j - C_j\left(\frac{H}{P}\right)\right] \tag{8-198}$$

$$\left(\frac{dC_j}{dz}\right) = \frac{K_G a A_c P}{G}\left(\frac{G}{q}\right)\left[y_j - C_j\left(\frac{H}{P}\right)\right] - \frac{kR_L A_c C_j}{q} \tag{8-199}$$

This can be solved directly for the liquid concentration profile,

$$\begin{aligned} C_j(z) = C_0\Bigg[&\frac{(1-r_1)}{(r_2-r_1)}\exp\left(-\frac{K_G a A_c P}{G} r_1 z\right) - \frac{(1-r_1)}{(r_2-r_1)}\exp\left(-\frac{K_G a A_c P}{G} r_2 z\right)\Bigg] \\ &+ \frac{y_0 G}{q}\left[\left(\frac{1}{(r_2-r_1)}\right)\exp\left(-\frac{K_G a A_c P}{G} r_1 z\right)\right] \\ &- \left(\frac{1}{(r_2-r_1)}\right)\exp\left(-\frac{K_G a A_c P}{G} r_2 z\right)\Bigg] \end{aligned} \tag{8-200}$$

where

$$-r_1 = \left(\frac{1}{2\alpha}\right)[-(1+\beta+\alpha) + (1+2\beta+\beta^2+2\alpha-2\alpha\beta+\alpha^2)^{1/2}]$$

$$-r_2 = \left(\frac{1}{2\alpha}\right)[-(1+\beta+\alpha) - (1+2\beta+\beta^2+2\alpha-2\alpha\beta+\alpha^2)^{1/2}]$$

where

$$\alpha = \frac{Pq}{(1+G)}; \qquad \beta = \frac{kR_L}{K_G a H}$$

When dispersion is not important and there is a pure gas phase, then

$$y_j = 1$$

$$C_j = C_0 \exp\left[-\left(\frac{A_c}{q}\right)(HK_G a + kR_L)z\right] + \frac{K_G aP}{HK_G a + kR_L}\left\{1 - \exp\left[-\left(\frac{A_c}{q}\right)(HK_G a + kR_L)z\right]\right\} \tag{8-201}$$

One continuous and one discrete fluid phase. Most often this will be a discrete (bubble) phase and a continuous liquid phase. The simplifying assumptions made above will be retained for this case as well. For the general model equations (8-191) and (8-192), with negligible dispersion and constant bubble size and velocity in the gas phase,

$$\left(\frac{dy_j}{dz}\right) = -\frac{K_G a' RT}{\bar{v}_b}\left[y_j - C_j\left(\frac{H}{P}\right)\right] \tag{8-202}$$

where $\bar{v}_b$ is the average velocity of bubble phase rise. For the liquid phase,

$$\left(\frac{dC_j}{dz}\right) = \frac{N_B V_{DG} K_G a' A_c P}{q}\left[y_j - C_j\left(\frac{H}{P}\right)\right] - \frac{kR_L A_c}{q} C_j \tag{8-203}$$

with N_B the number of bubbles per reactor volume, V_{DG} the volume of bubble, and $K_G a'$ the mass-transfer coefficient based upon the area per unit volume (a') of discrete phase.

Finally, assuming no dispersion and pure gas phase,

$$\left(\frac{dC_j}{dz}\right) = \frac{N_B A_c K_G a' P}{q}\left[y_j - C_j\left(\frac{H}{P}\right)\right] - \frac{kR_L A_c}{q} C_j \tag{8-204}$$

with initial conditions for both (8-203) and (8-204) of C_0 at $z = 0$.

Well, the idea was to try to simplify some of the equations we started with, but the temptation was too much, and we included all the bubble interactions. The equations become large; so much for that good intention.[12]

Now, our quest for knowledge concerning gas-liquid reactors, if we look at it, began with equation (8-164); so we should feel nearly saturated at this point. In fact, though, there are many other cases considered in the work of Russell et al., that may be of use in certain applications. We have taken what might be considered the most important, or most frequently encountered for presentation. As in the case for fluid-bed or slurry reactors, we must now determine where the many parameters appearing in the reactor equations for gas-liquid systems originated. But first, an example.

Illustration 8.4

Consider the batch liquid-liquid contractor illustrated below, in which the two largely nonmiscible phases are agitated sufficiently to be homogeneous in concentration, but not sufficiently to disperse one of the phases into the other. (We note that this is a liquid-liquid reactor, not gas-liquid, but the flexibility of the gas-liquid theory will be seen here. Some of the correlations may be different.)

[12] "The road to Hell is paved with good intentions."—*W. J. Butt*

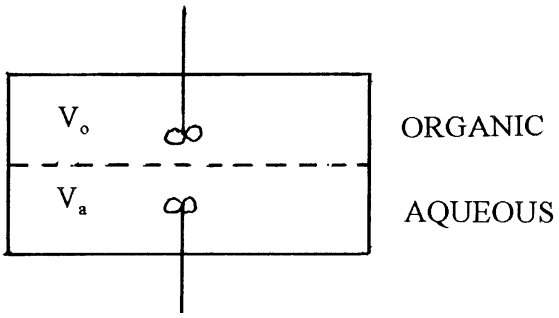

An example of this type of reactor/reaction would be

$$\mathrm{R{-}\overset{\overset{\mathrm{O}}{\|}}{\mathrm{C}}{-}R} + \mathrm{NaOH} \rightarrow \mathrm{Salt} + \mathrm{R}$$

that is,

$$\mathrm{B} + \mathrm{C} \rightarrow \mathrm{D} + \mathrm{E} \text{ (in the aqueous phase)}$$

The mass transfer occurs from the organic to the aqueous phase only, and it may be assumed that V_0 and V_a, do not change as the reaction progresses. We define the concentration the organic of reactant as A in the organic phase and B in the aqueous (reaction) phase.

Determine the concentrations $B(t)$ and $D(t)$ in the aqueous phase. The interfacial equilibrium is given by a distribution coefficient K, where $A_i = KB_i$. The overall mass-transfer coefficient is K_DS, and the reaction rate constant is k.

Solution

It is reasonable to assume that the concentration of B in the reaction phase is $\ll$ than that of C, hence k is a pseudo-first-order rate constant. We may also assume that C, D and E are not transferred into the organic phase to any extent. The pertinent balance equations are then,

$$-V_0\left(\frac{dA}{dt}\right) = K_DS(A - KB) \tag{i}$$

and

$$V_a\left(\frac{dB}{dt}\right) = K_DS(A - KB) - kV_aB \tag{ii}$$

Now, if we look at the second derivative of B,

$$\frac{d^2B}{dt^2} = \left(\frac{K_DS}{V_a}\right)\left[\left(\frac{dA}{dt}\right) - K\left(\frac{dB}{dt}\right)\right] - k\left(\frac{dB}{dt}\right) \tag{iii}$$

Substitution of (dA/dt) from equation (i) into (iii) and rearranging gives

$$\frac{d^2B}{dt^2} = M\left(\frac{dB}{dt}\right) + NB = 0 \tag{iv}$$

with

$$M = \left(\frac{K_DS}{V_0} + k + \frac{K_DSK}{V_a}\right); \qquad N = \frac{K_DSk}{V_0}$$

The solution comes fairly directly as

$$B = C_1 \exp\left(\frac{-M + \sqrt{M^2 - 4N}}{2}\, t\right) + C_2 \exp\left(\frac{-M - \sqrt{M^2 - 4N}}{2}\, t\right) \tag{v}$$

When,

$$t = 0; \qquad B = 0$$

and

$$C_1 + C_2 = 0$$

Then,

$$B = 2C_1 \exp\left(-\frac{Mt}{2}\right) \sinh\left(\frac{\sqrt{M^2 - 4N}}{2}\, t\right) \tag{vi}$$

For the constant C_1,

$$\frac{dB}{dt} = \left(\frac{K_D S}{V_a}\right) A_0$$

at $t = 0$. Then,

$$B(t) = \frac{2K_D S A_0}{V_0 \sqrt{M^2 - 4N}} \exp\left(-\frac{Mt}{2}\right) \sinh\left(\frac{\sqrt{M^2 - 4N}}{2}\, t\right) \tag{vii}$$

For the product D,

$$D - D_0 = \int_0^t kB(t)\, dt$$

Let

$$\alpha = \frac{\sqrt{M^2 - 4N}}{2}; \qquad \beta = \frac{K_D S A_0}{V_a}$$

then,

$$D(t) = D_0 + \left(\frac{k\beta}{2\alpha}\right)\left[\frac{e^{(-M/2+\alpha)t} - 1}{\alpha - (M/2)} + \frac{e^{(-M/2-\alpha)t} - 1}{\alpha + (M/2)}\right] \tag{viii}$$

HORATIO SAYS

All this seems tiresome but not very difficult. I worry about mass-transfer correlations for liquid-liquid phases. Go through the literature and see how many experimental studies you can find that report mass-transfer data (or any correlation) for liquid-liquid phases. Do you think that it is possible to use $K_D S$, from gas-liquid to liquid-liquid, only by making density corrections?

Our chief interest is concerned with the quantities required for analysis of an existing reactor or one that, for design purposes, is to be compared with other

possibilities. Certain parameters are either known or are variables that may be adjusted to obtain the design objectives; these are normally the liquid volume, V_L, the liquid flow rate, q, the pressure, P, temperature, T, initial concentrations, C_{oj} (liquid phase) and y_{oj} (gas phase), the gas phase flow rate, G, and the required conversion. We would also assume that if one is serious enough to contemplate the design of a reactor, separate information concerning phase equilibria (treated here in terms of Henry's law constant, H), and reaction kinetics r_j is available as well.

In reviewing this list it becomes clear that the remaining parameters have to do with *bubbles*.[13] This second list would include the mass-transfer coefficient K_G, and the individual bubble parameters a', V_b, v_b, and N. There is some difference in the correlations pertaining to tank-type and columnar reactors, so we consider them separately below.

8.3.4 The Parameters of Tank-Type Reactors

The overall coefficient K_G employed in the design equations is related to individual coefficients for liquid and gas phases by the inverse addition law for systems that follow Henry's law.

$$\frac{1}{K_G} = \frac{H}{k_L} + \frac{1}{k_G} \tag{8-205}$$

In most of the cases involved in design for gas-liquid systems, the gas-phase resistance to mass transfer, $1/k_G$, is small compared to the liquid-phase term, (H/k_L), unless there is a very fast liquid-phase reaction. Thus, correlations for k_L are the ones we seek for design purposes. We have seen in Section 8.3.1 the analysis of the effect of reaction on the mass-transfer coefficient for several types of reactions. These were reported via the values of an enhancement factor applied to the magnitude of the liquid-phase mass-transfer coefficient in the absence of reaction, which we will term here k_L°. There are numerous correlations available for k_L^o in bubbling systems, summarized in the work of Russell et al. A reasonable and typical correlation is that of Hughmark [G.A. Hughmark, *Ind. Eng. Chem. Proc. Design Devel., 6*, 218 (1967)], claimed to fit experimental data to about ±15%.

$$N_{Sh} = \frac{k_L^o d_b}{D} = 2 \pm \left[N_{Re}^{0.48} N_{Sc}^{0.34} \left(\frac{d_b g^{1/3}}{D^{2/3}} \right)^{0.072} \right]^b (a) \tag{8-206}$$

where

$$N_{Re} = \frac{u d_b}{\mu}; \qquad N_{Sc} = \frac{\nu}{D}$$

For single bubbles u is the bubble velocity, for bubble swarms u is the bubble/(slip velocity), ν is the kinematic viscosity $(\text{length})^2/t$, and D the molecular diffusivity $(\text{length})^2/t$.

For single bubbles $a = 0.061$ and $b = 1.61$; for bubble swarms $a = 0.019$ and $b = 1.61$. When N_{Rs}, N_{Sc} and $(d_b g^{1/3}/D^{2/3})$ are all $\ll 2$ then there is an apparent

[13] "A harbor, even if it is a little harbor, is a good thing."—*S.O. Jewett*

relationship between single bubbles and bubble swarms given by

$$\frac{(k_L^\circ)_{BS}}{(k_L^\circ)_{SB}} \approx 0.31$$

which signals the interesting fact that the mass-transfer coefficient for single bubbles is greater than that for bubble swarms. In the event of mechanical agitation of the liquid phase, the reported correlations become highly specific as to power input and configuration, as discussed by Hughmark.

In order to convert these values of k_L° into useful mass-transfer coefficients it is convenient to use the classification of Astarita (G. Astarita, *Mass Transfer with Chemical Reaction,* Elsevier, Amsterdam, (1967)]. Let us define two characteristic times,

$$t_D = \frac{D}{(k_L^\circ)^2} \tag{8-207}$$

$$t_R = \frac{C_{ej} - C_{\epsilon j}}{r_j} \tag{8-208}$$

where C_{ej} is the interfacial (equilibrium) concentration determined by Henry's law and $C_{\epsilon j}$ is an equilibrium value for j in cases of reversible reaction (and thus zero for irreversible reaction). The physical interpretation of these times is: t_D is a diffusion time characteristic of the life of a surface fluid element exposed to the gas phase and t_R is a reaction time representative of the time required for the chemical reaction in the liquid phase to go to an appreciable extent of conversion. This would be taken, for example, for a first-order irreversible reaction, as $t_R = 1/k$. For bubbling systems the situation is a little more complicated, and

$$0.005 < t_D < 0.04\,\text{s}$$

and for typical values of D in the liquid phase this translates to

$$0.015 < k_L^\circ < 0.04\,\text{cm/s}$$

If the liquid-phase reaction is slow ($t_D \ll t_R$), then we can identify three differing situations as follows:

1. Diffusion subregime The overall driving force is dominated by diffusional transport. Here

$$\frac{D}{k_L} \ll \frac{1}{a}$$

and

$$(1/a)(r_j)(C_{ej} - C_{\epsilon j}) > k_L^\circ(C_{ej} - C_{\epsilon j})$$

For typical values of D and k_L° this gives an a range as

$$(1/a) \gg 2.5 \times 10^{-4}\,\text{cm}$$

Further, K_G is just (H/k_L°) in this subregime, and since the entire rate process is diffusion-driven, $k_L = k_L^\circ$.

2. Kinetic subregime The chemical reaction in the liquid phase is very slow and diffusional transport effects are not important. Then

$$(1/a)(r_j)(C_{ej} - C_{\epsilon j}) \ll k_L^\circ(C_{ej} - C_{\epsilon j})$$

In this case mass-transfer terms in the reactor model equations may be neglected.

3. Intermediate subregime As expected, this is intermediate between the limits of (1) and (2). Here

$$(1/a)(r_j)(C_{ej} - C_{\epsilon j}) = k_L^\circ(C_{ej} - C_{\epsilon j})$$

and for a first-order irreversible reaction

$$k_L = \left(\frac{1}{k_L^\circ} + \frac{a}{k}\right)^{-1}$$

One must remember that all three of the subregimes above are subject to $t_D \ll t_R$.

If the liquid-phase reaction is fast ($t_D \gg t_R$), for a first-order example once again,

$$k_L = (Dk)^{1/2}$$

Finally, if the liquid phase reaction is very, very fast, corresponding to the physical picture envisioned in the derivation of equation (7-82),

$$\frac{t_D}{t_R} \gg \frac{C_{ol}}{\alpha C_{ej}}$$

where C_{ol} is the initial bulk concentration of liquid-phase reactant, C_{ej} the interfacial concentration of gaseous reactant in the liquid phase, and α is a stoichiometric coefficient, mols liquid-phase reactant/mol absorbed reactant. This regime is typical of acid-base reactions in the liquid phase. Further details concerning the analysis of this regime are given in the text by Astarita.

Gas phase properties As stated before, all the model equations involve parameters that are determined by the behavior of bubbles, either alone or in groupings, and the analysis becomes more of an exercise in bubble fluid mechanics than in reactor design. For *plug-flow* gas phase reactors there are a number of correlations that relate in-reactor bubble properties as a function of the inlet conditions. These are available for the bubble volume V_b, the bubble rise velocity v_b, the surface to volume ratio a', and the number of bubbles per unit volume N. In addition, if bubbles are spherical (or approximately so), information on d_b allows determination of a' and V_b. However, these correlations are subdivided by the gross characteristics of bubble formation, namely whether there is a gas phase consisting of discrete bubbles, or whether there is interaction among bubbles with some coalescence, commonly termed a swarm bubble phase.

For a *discrete bubble phase* we borrow heavily from work done with single bubbles for correlations. Many of those are posed in terms of the initial bubble diameter as the gas is introduced into the liquid phase via an orifice or other type of dispersion device. For low flow rates, where single bubbles are emitted at some fixed frequency, f, a force balance yields

$$(d_{ob})^3 = \frac{6D_0\sigma}{g(\rho_L - \rho_G)} \tag{8-209}$$

where D_0 is the orifice diameter and σ the interfacial tension of the gas-liquid interface. For spherical bubbles the frequency f is also easily calculated as

$$f = \frac{Qg(\rho_L - \rho_G)}{\pi D_o \sigma} \tag{8-210}$$

where Q is the gas volumetric flow rate. For somewhat higher flow rates (orifice N_{Re} to 2000) an, empirical correlation was proposed,

$$d_{ob} = (0.18) D_o^{0.5} N_{Re}^{0.33} \tag{8-211}$$

There are not much data available for the region of "jet flow" (higher velocities still), but some assistance can be found in handbook correlations. For bubble velocity we have used the expression presented by Davidson and Harrison,

$$v_b = (0.711)(g d_b)^{1/2} \tag{8-212}$$

where d_b is some equivalent spherical bubble diameter if the bubbles are not spherical. If we have a value for the bubble rise velocity we can calculate the number of bubbles per unit volume as

$$N = \frac{QL}{V_{ob} v_b V_L} \tag{8-213}$$

where V_{ob} is the initial bubble volume and V_L the volume of the liquid phase. Remember that the indicated relationship of N to $(v_b)^{-1}$ means that the number of bubbles may vary with position in the liquid phase, depending upon the value of d_b in equation (8-212).

The correlations for the *swarm bubble phase,* still for the gas in plug flow, are rather equipment-specific. For example, for bubble swarms issuing from porous plates, the bubble diameter may be estimated from the correlation of Koide et al., [K. Koide, T. Hirahara and H. Kubata, *Chem. Eng. (Japan), 30*, 712 (1966)],

$$d_{ob} = 1.35 (N_{Fr} / N_{We}^{1/2})^{0.28} (g\rho / \sigma\delta) \tag{8-214}$$

where N_{Fr} (Froude number) is $(u^2/g\delta)$, N_{We} (Weber number) is $(\delta u^2 \rho/\sigma)$, δ is the orifice diameter in the gas-phase distributor, σ is the liquid surface tension, and ρ is liquid density. From this point on there are a number of different procedures suggested in the literature to obtain bubble velocity, the number per unit volume, and the gas holdup for the swarm. Approaches are suggested in the review of Cichy et al., who also give a number of references to some of the basic work on parameters of the swarm bubble phase. As mentioned above, these tend to be very specific to particular operating situations, and it is probably more fruitful to consider the original work rather than report the litany here.

8.3.5 The Parameters of Column Reactors

Our primary interests here are directed toward vertical-flow contacting devices, generally referred to as bubble-column reactors. These can be empty, with stagewise placing of porous plates for bubble redispersion, or filled with a commercial packing such as Raschig rings. These two types have received full attention in work directed toward mass-transfer/separation processes, and will not be considered further here. What we will examine now is the case in which there are discrete

gas-phase bubbles passing through a continuous liquid phase. This puts us generally in the southeast corner of the Govier chart of Figure 8.16.

As in the situation for tank-type reactors, we need first to define the characteristic time quantities associated with the reactor design. The characteristic diffusion time, t_D, is given in equation (8-207), and the extent-of-reaction time, t_R, is given in equation (8-208). The third time here is t_p, the length of time an element of fluid remains in the reactor. This is reminiscent of the exit-age distribution function developed for homogeneous tubular-flow reactors, but the development of the theory for multiphase reactors has been different.[14]

We may estimate t_p from a knowledge of the liquid holdup in the reactor, R_L, via

$$(t_p)_L = \frac{R_L A_c L}{q} \tag{8-215}$$

$$(t_p)_G = \frac{(1 - R_L)(A_c LP)}{GRT} \tag{8-216}$$

where R_L is the liquid-phase holdup (ratio of cross sectional area of column occupied by liquid to the total cross sectional area), q is the volumetric flow rate of liquid, A_c the total cross sectional area, and G is a molar gas flow rate. A number of correlations for holdup are available, some with a semi-theoretical basis and others more or less completely empirical. Two that have passed the test of time rather well are those of Hughmark [G.A. Hughmark, *Chem. Eng. Prog., 58*, 62 (1964)] and Lockhart and Martinelli [R.W. Lockhart and R.C. Martinelli, *Chem. Eng. Prog., 45*, 39 (1949)].

The interfacial area, based on a unit volume of reactor, is given by the general relation

$$a = Na' V_{DG} \tag{8-217}$$

where V_{DG} is the average bubble volume. If the bubbles are spherical V_{DG} is easily estimated if there is some information concerning the size distribution. The value of N can also be estimated from inlet conditions,

$$N = \frac{(1 - R_L)}{(V_{DG})_0} \tag{8-218}$$

This value would not be expected to change much with position for the discrete bubble regime that we are considering. The initial bubble volume, $(V_{DG})_0$, is estimated from

$$(V_{DG})_0 = \frac{G_0 RT}{P\nu} \tag{8-219}$$

where ν is a bubble formation frequency that must be known from other data, or may be roughly estimated from the average bubble volume and the gas volumetric flow rate.

The bubble rise velocity, important in determining gas-phase residence time, is estimated by a correlation reminiscent of fluidized beds.

$$\bar{v}_B = \bar{v}_L + 0.711 g^{1/2} \left(\frac{6}{\pi}\right)^{1/8} (V_{DG})^{1/6} \tag{8-220}$$

[14] "That great dust-heap called 'history'."—*A. Birrell*

where $\bar{v}_L$ is the average velocity of the liquid phase. All of these expressions offer ways of approximating interfacial areas, most often through the assumption of spherical geometry, determination of V_{DG}, and then area from equation (8-217). A direct correlation for a was reported by Scott and Hayduk [D.S. Scott and W. Hayduk, *Can. J. Chem. Eng., 44*, 130 (1966)],

$$a = \left(\frac{A}{LA_c}\right)\left(\frac{\alpha}{LA_c}\right)\left[\frac{G_0}{G_0 + (qRT/P)}\right]^m \tag{8-221}$$

where $\alpha = (qP/HG)$, A is the total surface area in the reactor, and q and G_0 are as defined before. The exponent m is a value obtained from curve-fit that can vary from 0.66 to 1.0. One wonders how useful this correlation may be, since the estimate of A required would seem no less of a task than simply estimating a value for a based on intuition or experience. The whole business seems fairly insecure, if we remember the fluid-bed studies that have shown that bubbles in multiphase reactors are anything but spherical. There isn't much else to go on, however.

Estimation of the mass-transfer coefficients associated with columnar operation, at least for the discrete bubble phase we are considering, is the same in practice as for tank-type reactors. Thus, one determines the value of the diffusion time by equation (8-207) and goes on to the calculation of k_L for the appropriate conditions as defined in the classification of Astarita.

Two final comments are appropriate here. First is reminder that if one gets "stuck" among the intricacies of all the correlations and sub-classifications described, an unhurried perusal of the procedure given in Perry's Handbook is always a good place to start.[15] The second comment has to do with some straw men that have been set up in the general derivations, then not mentioned again (aside from spherical bubbles). In particular these include the droplet-liquid model of Figure 8.17, and the possible use of axial dispersion models to describe deviations from ideal plug flow or completely mixed phase behavior. These approaches may be appropriate in specific instances, but are beyond what we need here. So, we depart from the topic of gas-liquid reactors secure with the knowledge that such insecure methods exist.[16]

Illustration 8.5[17]

The reaction of ethylene oxide with water to produce monoethylene glycol can be represented by

$$A + B \rightarrow R$$

where the aqueous liquid phase is A, the pure gas of ethylene oxide is B, and the monoglycol product is R. Experimental data on this reaction were obtained under isothermal conditions at 90°C in a semi-flow reactor with a volume of 445 cm^3, with cylindrical geometry, 1-inch i.d. and length 32.4 in. A summary of experimental conditions is given below. What reactor subregime would apply here?

---

[15] Maybe some more Debussy will help. Definitely not Wagner.

[16] "The most difficult of all musical instruments to learn to play is second fiddle."—*Anonymous*

[17] After R.W. Schaftlein and T.W.F. Russell, *Ind. Eng. Chem., 60*, 12, with permission of the American Chemical Society, (1968).

$C_{eB} = 0.01838\,\text{lb mol/ft}^3$

$D_0 = 0.0825\,\text{in}$

$d_{ob} = 0.4\,\text{cm}$ (observed experimentally)

$H = 0.0498\,\text{lb mol/ft}^3\text{-atm}$

$k = 0.789\,\text{h}^{-1}$

$L = 2.7\,\text{ft}$

$P = 1\,\text{atm}$

$Q_1 = 40\,\text{cm}^3/\text{min}$

$T = 90^\circ\text{C}$

$V_L = 445\,\text{cm}^3$

Solution

The experimental measurements produced concentration-time plots of ethylene oxide and ethylene glycol in the liquid phase, as shown in Figure 8.18. The physical picture of this reaction/reactor system is most closely approximated by the plug-flow gas phase, well-mixed batch liquid phase. The appropriate relationships to model this system are given in equations (8-176) to (8-178), (8-183), and (8-188). The bubble volume is variable, and the nature of the variation changes with the extent of conversion (i.e., concentration of glycol in the liquid phase), however, the pure oxide gas phase allows $y_B = 1$. The modified equations specific to this reactor are then

$$\frac{dC_\text{B}}{dt} = (\bar{a}'\bar{V}_b N)k_L C_{eB} - [(\bar{a}'\bar{V}_b N)k_L + k]C_\text{B} \tag{i}$$

$$a = \bar{a}'\bar{V}_b N = NS[V_{ob} + (L^2F^2/3 - V_{ob}^{1/2}LF)^{2/3}] \tag{ii}$$

and

$$F = \frac{k_L RTS}{2PW} \tag{iii}$$

$$C_R(t) = k\int_0^t C_\text{B}(t)\,dt \tag{iv}$$

The boundary conditions for equations (i) and (iv) are,

$$\begin{aligned} &t = 0, \qquad C_\text{A} = 0; \qquad C_\text{B} = 0 \\ &t = t; \qquad C_\text{B} = C_\text{B}; \qquad C_R = C_R \end{aligned} \tag{v}$$

We now need to determine the reaction regime (classification of Astarita) for this operation. From equation (8-208) for an irreversible reaction, together with

$r_j = kC_{ej}$

$k = (2.2 \times 10^{-4})\,\text{s}^{-1}$

then

$$t_R = (1/k) = (4.55 \times 10^4)\,\text{s} \tag{vi}$$

The typical range of t_D for bubbling systems is from 0.005 to 0.04 s, thus $t_R \gg t_D$ and

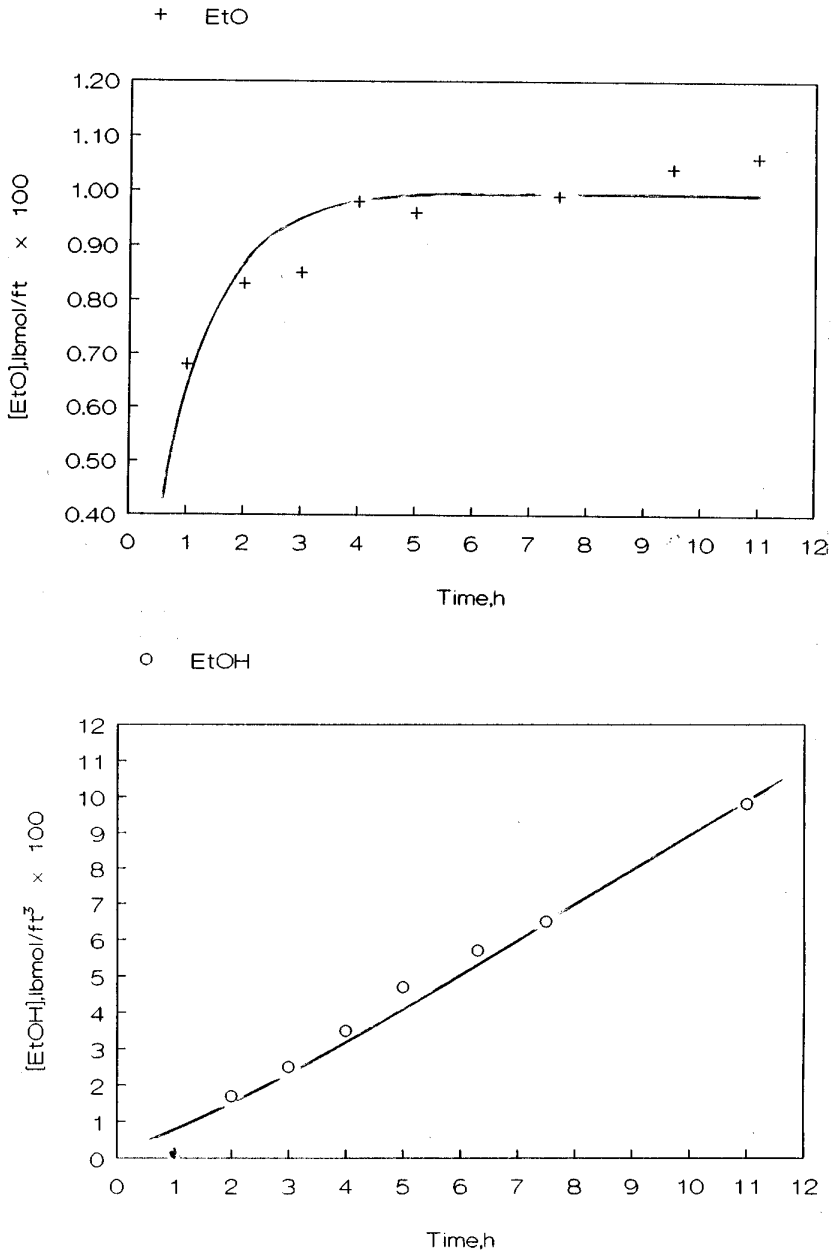

Figure 8.18 Concentration-time profiles for the reaction of ethylene oxide with water. Solid lines are model predictions.

the reaction belongs to the "slow reaction" regime, and we have to determine which of the reaction subregimes (diffusion, kinetic, or intermediate) is applicable. For the conditions given, this ends up in terms of the following criteria.

$$\left(\frac{k}{a}\right) >; \qquad =; \qquad < k_L^\circ ? \tag{vii}$$

The value of k_L° is determined from equation (8-206) to be 8.21 ft/h. From equation (8-209) we estimate d_{ob} as 0.43 cm. Thus, from equation (ii), using

$$\bar{a}' \approx \frac{6}{d_{ob}}; \qquad \bar{V}_b = \frac{\pi (d_{ob})^3}{6}$$

N from equation (8-213), and v_b from equation (8-212), we obtain

$$k_L^\circ = 8.21\,\text{ft/h}; \qquad N = 5940\,\text{ft}^{-3}; \qquad a \approx 3.64\,\text{ft}^{-1}$$

Using these values one obtains numbers for the comparison of equation (vii) as

$$(k/a) = 0.22$$

$$k_L^\circ = 8.21$$

which puts us into the "intermediate" subregime, where kinetic and diffusion rates are of the same order of magnitude, and

$$k_L = \left(\frac{1}{k_L^\circ} + \frac{a}{k}\right)^{-1} \tag{viii}$$

Equations (i) to (viii) comprise the reactor model.

A test of this model is reported by Schaftlein and Russell, in which best-fit values for k_L and N were determined from the data in Figure 8.18, using an observed value of 0.4 cm for d_{ob}. These calculations are represented by the solid lines in Figure 8.18, with best-fit parameter values of

$$k_1 = 0.56\,\text{ft/h}; \qquad N = 5900\,\text{ft}^{-3}; \qquad a = 1.40\,\text{ft}^{-1}$$

This should be considered a reasonable agreement between correlation and best-fit values, as such things go.

HORATIO SAYS

Here I go again with my favorite question. Suppose there is a doubt of ±20% in such estimation used above. Where would this put us as far as the answer is concerned? We must *always* remember that correlations do not descend from Higher Powers. Unpleasant results can, and do happen from time to time.

8.4 Trickle-Bed Reactors

The name "trickle-bed reactor" is usually applied in reference to a fixed bed in which a liquid phase and a gas phase flow concurrently throughout a bed of catalyst. By far the most important application, and hence much of the work, on these reactors has been in the hydrotreating of heavy feedstocks in the petroleum industry (hydrocracking, hydrodesulfurization, hydrodenitrogenation). However, this seems a very versatile processing method, and has not been exploited nearly to its potential in other areas such as waste water treatment—at least as the scientific literature would indicate.

The hydrodynamics of trickle beds are complex, to say the least, and although an enormous amount of time and effort has been expended on research in this area, it is probably true to say that design and scale-up procedures are somewhat more tenuous than for fixed- or even fluid-bed reactors. Fortunately, there are relevant reviews that give some insight [C.N. Satterfield, *Amer. Inst. Chem. Eng. Jl., 21,* 209

(1975); H. Hofmann, *Catal. Rev. Sci. Engr., 17,* 71 (1978); A. Gianetto, G. Baldi, V. Speccina, and S. Sicardi, *Amer. Inst. Chem. Eng. Jl., 24*, 1087 (1978)], as well as a book devoted to the topic [Y.T Shah, *Gas-Liquid-Solid Reactor Deeign*, McGraw-Hill Book Co., New York, NY, (1979)].

As in the case of other multiphase reactors discussed in this chapter, topical material divides itself rather naturally into three major aspects: hydrodynamics, transport, and reaction processes. We will stay with fairly simple approaches, particularly in the area of hydrodynamics and correlations. An extensive amount of research continues to this day on trickle beds, so we cannot attempt to present the latest word.

8.4.1 Hydrodynamics in Trickle Beds

The areas concerned with hydrodynamics in trickle beds include flow regimes, liquid distribution on the solid (catalyst) packing, pressure drop, liquid holdup, and, more generally, the effect of the physical properties of the liquid and gas phases on all hydrodynamic properties.

The basic "trickle-flow regime" is most often associated with low liquid and gas flow rates (often termed "gas-continuous regime"), in which the liquid flows over the packing in the form of films, and rivulets or drops that essentially can be considered to be in laminar flow and not affected much by the gas phase flow, be it either laminar or turbulent. As the gas rate is increased a larger liquid phase velocity is induced via increased drag on the liquid, and eventually turbulence will result, with some liquid even becoming separated from the liquid film as slugs or droplets, eventually to reform over the packing.[18] This is commonly called "ripple" or "pulsating" flow and is probably most characteristic of the hydrodynamics encountered in commercial operation. At high liquid rates and low gas rates, however, the liquid phase can become the continuous phase and the gas passes through the reactor in a bubble (dispersed bubble) flow. Various flow maps—somewhat reminiscent of the Geldhart correlation for fluid beds—have been reported. One of the most easily visualized is that of Satterfield given in Figure 8.19. This is presented together with a tabulation of limiting flow conditions encountered in typical petroleum processing applications in Table 8.2. Large differences in behavior are seen between foaming and nonfoaming systems. Our discussion is limited to the former.

A somewhat more quantitative approach to the designation of flow regimes was attempted by Gianetto et al. in correlation of the results of several investigations. In particular the correlation recognizes that a large portion of flow research on trickle-beds, at least that which had been published, had employed the air-water system and required an act of deep faith to be extended to non-aqueous systems. In order to cope with this, one can devise some system-scaling parameters, of which the most useful are

$$\lambda = [(\rho_o/\rho_{air})(\rho_L/\rho_{H_2O})]^{1/2} \tag{8-222}$$

[18] For more on this and other aspects, the reader is referred to J.M. deSantos, T.R. Mell, and L. E. Scriven, *An. Rev. Fluid Mach., 23*, 233 (1991).

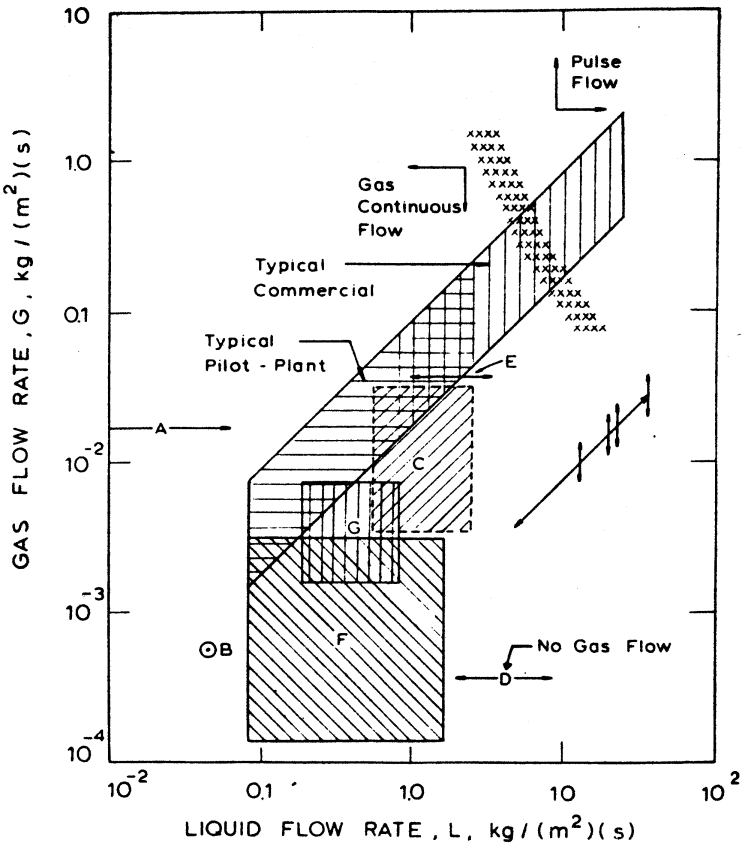

Figure 8.19 Ranges of gas and liquid flow rates utilized in laboratory, pilot plant, and commercial trickle-bed reactors. [After C.N. Satterfield, *Amer. Inst. Chem. Eng. J1., 21*, 209, with permission of the American Institute of Chemical Engineers, (1975).]

Table 8.2 Representative Limiting Conditions for Trickle-Bed Applications in Petroleum Processing

	Superficial liquid velocity			Superficial gas velocity[a]		
	ft/hr		kg/m^2 s	ft/hr (STP)	cm/s (STP)	kg/m^2 s
Commercial reactor	10		0.83	1,780	14.8	0.0132
				8,900	74.2	0.066
	to					
	300		25.0	53,500	444	0.395
				266,000	2,200	1.97
Pilot plant[b]	1		0.083	178	1.48	0.0013
				890	7.42	0.0066
	to					
	30		2.5	5,350	44.4	0.0395
				26,600	222	0.197

[a] Values of G calculated for 1000 and 5000 std. cu. ft. of H_2/bbl, respectively, and assume all hydrocarbon is in the liquid phase. Although expressed at S.T.P. conditions, operating pressures are usually in the range of 500 to 1500 lb./sq.in., and occasionally higher.

[b] Length of pilot plant reactor assumed to be 1/10 that of a commercial reactor.

[c] 1 lb./(hr.)(ft^2) = 1.36×10^{-3} kg/m^2 s.

Source. After C.N. Satterfield, *Amer. Inst. Chem. Eng. J., 21*, 209, with permission of the American Institute of Chemical Engineers, (1975).

and

$$\psi = (\sigma_{H_2O}/\sigma_L)(\mu_L/\mu_{H_2O})^{1/3}(\rho_{H_2O}/\rho_L)^{2/3} \tag{8-223}$$

Use of these in a flow-rate correlation provides a somewhat clearer picture of the transition between flow regimes, as shown in Figure 8.20. While there are undoubtedly some exceptions to the generalized correlation here, it can be considered fairly reliable for the majority of systems. Our specific interests in this section are limited for the most part to the region of "gas-continuous trickling flow". For a more recent attempt at defining the shaded transition region in Figure 8.20, the reader is referred to the paper of Dimenstein and Ng [D.M. Dimenstein and K.M. Ng, *Chem. Eng. Commun., 41,* 215 (1986)].

Pressure drop is a factor that we have not considered in this chapter, for it is only of secondary importance in the design or analysis of fluidized beds, slurry reactors, or gas-liquid contactors. However, for trickle beds the situation is more complex end there is no generally accepted correlation such as the Ergun equation for fixed beds. A summary of a number of these can be found in the review of Gianetto et al. [A. Gianetto, G. Baldi, V. Speccia and S. Sicardi, *Amer. Inst. Chem. Eng. Jl., 24,* 1087 (1978)]. One possibility in the absence of any other information is to use the single-phase pressure drop correlation with the void fraction reduced to account for liquid holdup in the bed, treating the liquid phase as an extension of the solid phase, which is very conservative. There is no lack of ideas in between for determining trickle-bed pressure drop, however. Many of these propose what are basically combining rules for liquid-phase and gas-phase pressure drops determined individually. One well-known correlation is that of Larkins et al. [R.P. Larkins, A.R. White and D.W. Jeffrey, *Amer. Inst. Chem. Eng. Jl., 7,* 231 (1961)],

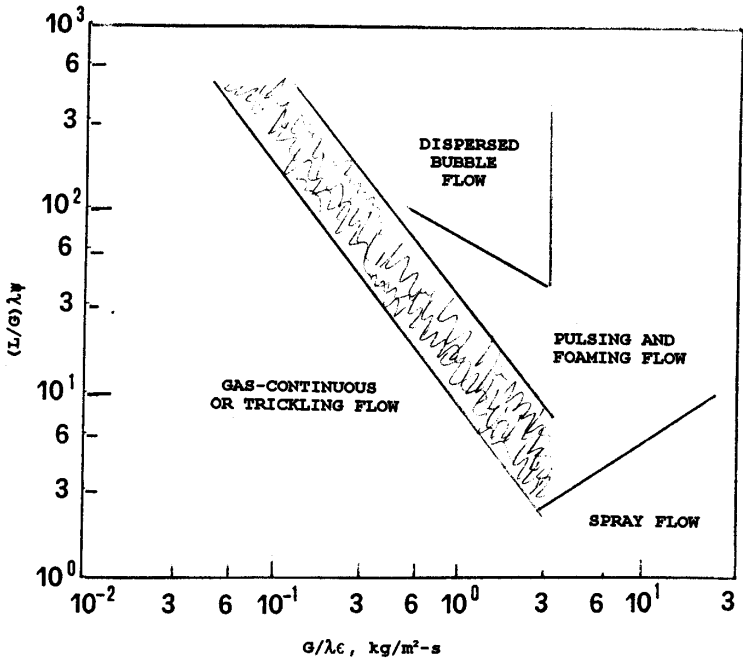

Figure 8.20 Generalized flow map for trickle-bed reactors. The shaded area is the transition region from gas-continuous to gas-dispersed glow.

which proposes

$$\log\left(\frac{\Delta P_{LG}}{\Delta P_L + \Delta P_G}\right) = \frac{0.42}{\log(\chi)^2 + 0.67} \tag{8-224}$$

where $\chi = (\Delta P_L/\Delta P_G)^{1/2}$ is in the range 0.05 to 30. Equation (8-224) was derived from results with various packing materials, with dimensions on the order of 10 mm, for all of the flow regimes shown in Figure 8.20. Later modifications of this approach, offering perhaps better correlation (at the expense of additional complexity), were offered by Sato and Hashiguchi [Y. Sato and Y. Hashaguchi, *J. Chem. Eng. Japan, 6,* 315 (1973)] and Midoux et al. [N. Midoux, M. Favier and J.C. Charpentier, *J. Chem. Eng. Japan, 9,* 350 (1976)]. In terms of simplicity, the latter is particularly attractive.

$$\left(\frac{\Delta P_{LG}}{\Delta P_L}\right)^{0.5} = 1 + \left(\frac{\Delta P_L}{\Delta P_G}\right)^{-0.5} + (1.14)\left(\frac{\Delta P_L}{\Delta P_G}\right)^{-0.27} \tag{8-225}$$

One caution that applies to the use of these pressure-drop correlations has to do with the possible buildup of deposits in the trickle bed with increasing time-on-stream, particularly in the case of hydrotreating. Here the buildup of carbonaceous or metallic deposits on the catalyst may possibly block a portion of the bed void present initially, and ΔP_{LG} will be much greater than expected on the basis of equation (8-224) or (8-225).

Liquid holdup is another factor that is important in the design and analysis of trickle beds that we have not been concerned with in any detail in earlier sections of this chapter. The effect of liquid holdup on performance depends upon the nature of the reaction occurring. In some hydrotreating reactions such as hydrosulfurization or demetallaton, the liquid holdups encountered are sufficiently high that all the solid phase surfaces are wetted. In other reactions requiring less demanding conditions, this may or may not be so. In the latter case the effective reaction rate will then decrease with an increase in liquid holdup, since the mass-transfer resistance is greater in the liquid phase than in the gas phase.

The liquid-phase holdup is expressed as a fraction of bed volume, i.e., volume of liquid present per volume of empty reactor. This is then subdivided into *external holdup*, liquid contained in the void fraction of the bed outside of the catalyst particles, and *internal holdup*, liquid within the pore volume of the catalyst. There is an even further subdivision of the external holdup into a "*static holdup*"—the amount of liquid in the bed that remains after the bed has been allowed to drain freely—and "*dynamic* holdup" which depends on a number of factors but is most simply defined as the difference between total holdup and static holdup.[19]

The maximum internal holdup is determined primarily by the pore structure/volume of the catalyst, and can range from about 0.1 to 0.4 for typical materials. Static holdups in the range of 0.02 to 0.05 are characteristic of most packed beds of porous catalyst. Summaries of such correlations for work done up to about 1980 are found in the reviews of Gianetto et al., and Satterfield, as cited. These seem fairly

[19] Related measures may have external holdup divided into "free-draining" and "residual" fractions. The latter is related to the static holdup, but be careful. The names sound the same but result in entirely different numbers. "...and a cast of thousands."—*Anonymous*

well established figures, and not much work directly on this point has been done in recent years.

The static holdup, β_r, depends primarily on the physical properties of the liquid phase, and particle size, shape and wetting. This is often correlated in terms of yet another nondimensional parameter, the Eötos number,

$$N_{Eo} = \left(\frac{\rho_L g d_p^2}{\sigma_L} \right) \tag{8-226}$$

which expresses the ratio of gravity to surface forces. Smaller particle diameters and fluid density, and larger surface tension, thus give larger static liquid holdups. As indicated by its name, static holdup is not particularly sensitive to operating conditions and, as stated above, we can select some number on the order of 0.05 as representative ($N_{Eo} < 4$ for $\epsilon\beta_r \sim 0.05$, decreasing with increasing N_{Eo}). Workable correlations for dynamic holdup, β_f, and total holdup, β_t, have been proposed in a number of studies. From Larkin et al.,

$$\log(\beta_f) = (0.525) \log\ \chi - (0.11)(\log\ \chi)^2 - 0.774 \tag{8-227}$$

for $0.05 < \chi < 30$ [see equation (8-224)]. Midoux et al. give one correlation for all hydrodynamic regimes for nonfoaming systems

$$\beta_t = \frac{0.66(\chi)^{0.81}}{1 + 0.66(\chi)^{0.81}} \tag{8-228}$$

for $0.1 < \chi < 80$. Speccia et al. [V. Speccia, G. Baldi and A. Gianetto, *Chem. Eng. Sci., 32,* 515 (1977)] propose, for the low interaction regime

$$\beta_f = 3.86(N_{Re})_L^{0.545}(N_{Ga})_L^{-0.42}\left(\frac{a_v d_p}{\epsilon} \right) \tag{8-229}$$

where

$$(N_{Ga})_L = \frac{d_p^3 \rho_L (\rho_L g + \Delta P_{LG})}{\mu_L^2}$$

and $3 < (N_{Re})_L < 470$. Shah has recommended the use of equation (8-229) for the low interaction range for trickle-flow conditions in calculation of dynamic liquid holdup, and the correlation of Midoux et al. for calculation of total liquid holdup in all flow regimes. In the above equations ϵ is the void fraction of the bed and a_v, the area per unit volume of the catalyst external surface.

It is hard to find out much about internal holdup. Presumably this will be determined by the internal void fraction of the catalyst, which one may assume is totally filled with liquid phase—at least for reactions in which no phase change to vapor occurs.

In the above we have seen only a few of the many correlations that exist for hydrodynamic factors in trickle-bed flow reactors, and more specifically those dealing with aqueous- or hydrocarbon-based reactions. Once again we are faced with the question of how to select the particular correlation to be used from a rich menu available. Again, also, there is no fixed procedure, but the most important general rule is never to extrapolate a correlation beyond reasonable limits corresponding to

its database. Unfortunately, this may not always be possible and one is left to pick the most conservative value among several possibilities.

8.4.2 Mass-Transfer Correlations

As one might expect, these are conveniently subdivided into correlations for gas-liquid coefficients and for liquid-solid coefficients. The overall structure of these correlations is not much different from those we have seen for other multiphase reactors, but the correlation coefficients, of course, are very-specific to the application.

Gas-liquid. Charpentier [J.C. Charpentier, *Chem. Eng. Jl., 11,* 161 (1976)] presented a thorough summary of literature on gas-liquid mass transfer in trickle beds some time ago. The liquid phase mass-transfer coefficient is affected by both gas and liquid flow rates. At very high gas- and liquid-flow rates values of $k_L a_L$ may exceed 1 s^{-1}, a value normally not achieved in any other type of gas-liquid conductor. In the trickle-flow regime, however, $k_L a_L$ values are more consistent with those expected on the basis of experience with other contactors. Trends in the gas-phase coefficient, $k_G a_L$, also follow in general order expectations based on experience with gas-liquid slurry reactors. For $k_L a_L$ a modified correlation following the earlier suggestions of Reiss [L.P. Reiss *Ind. Eng. Chem. Proc. Design Devel., 6*, 486 (1967)] is recommended by both Satterfield and Charpentier.

$$(k_L)_1 a_L = (0.0011)(E_L)\left(\frac{D_{AL}}{2.4 \times 10^{-9}}\right) s^{-1} \tag{8-230}$$

where D_{AL} is the diffusivity of reactant A in the liquid phase, and E_L is an energy dissipation factor for liquid-phase flow, given by

$$E_L = \left(\frac{\Delta P_{LG}}{\Delta z}\right) u_{SL} \tag{8-231}$$

where u_{SL} is the superficial liquid-phase velocity and E_L is in W/m^3. This is shown in Figure 8.21a. Goto et al. [S. Goto, J. Levec and J.M. Smith, *Catal. Rev. Sci. Eng., 15*, 187 (1977)] gave a summary of results on $k_L a_L$ in both cocurrent and countercurrent contractors as a function of liquid velocity, shown in Figure 8.21b. The results of Gianetto et al. are much lower than those of other reports, however, they establish a norm for conservative design.

The gas phase mass-transfer coefficient can also be correlated with an equation in the form of equation (8-230). In this case,

$$k_G a_L = 2.0 + C_1 (E_G)^{0.66} \tag{8-232}$$

where the energy dissipation term is

$$E_G \left(\frac{\Delta P_{LG}}{\Delta z}\right) u_{SG}$$

and $C_1 = 0.10$ for E_G in W/m^3. Alternative correlations to be considered are given in the papers of Gianetto et al. (Figure 8.21c) or Shende and Sharma [B.W. Shende and M.M. Sharma, *Chem. Eng. Sci., 29*, 1763 (1974)]. As was shown previously for fluidized bed and slurry reactors, the gas phase mass-transfer resistance is most often smaller than that of the liquid phase in the overall transport process, and disappears altogether in the case of a pure component gas feed.

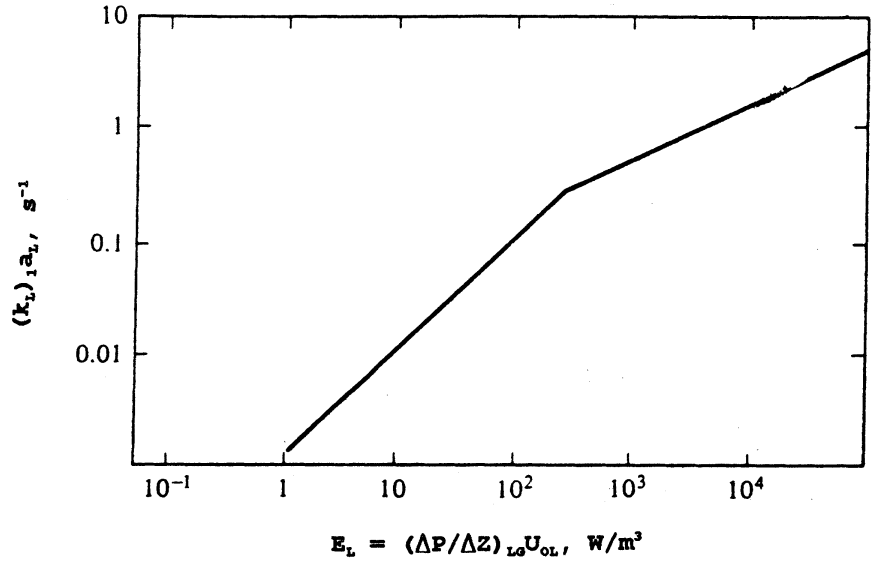

(a)

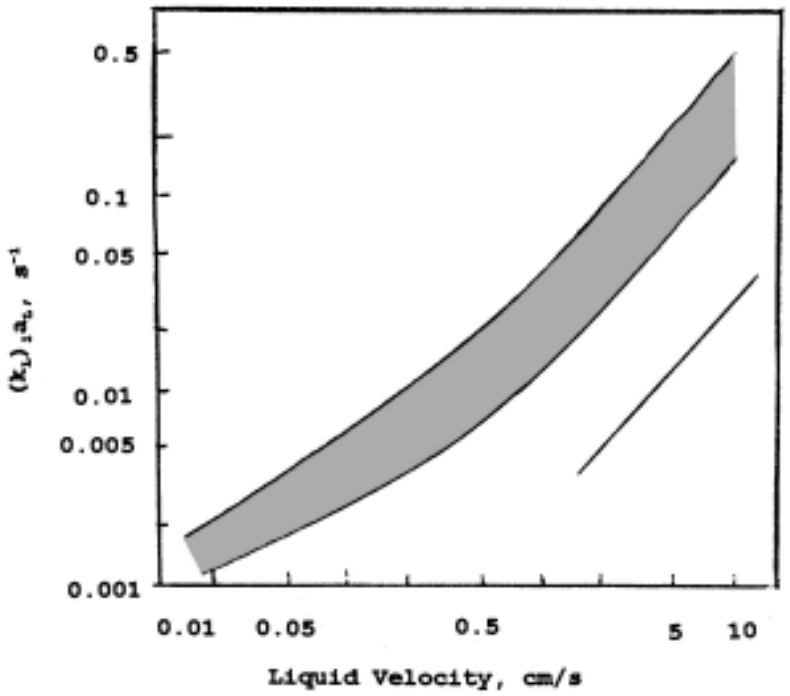

(b)

Figure 8.21 (a) Energy dissipation correlation for $k_L a_L$ in cocurrent downflow trickle beds. (b) Correlation of $k_L a_L$ with liquid velocity in cocurrent and countercurrent contactors. Line: countercurrent, $0.001 < k_L a_L < 0.03\,s^{-1}$; shaded, cocurrent, $0.003 < k_L a_L < 0.5\,s^{-1}$. [After A. Gianetto, G. Baldi and V. Specchia, *Quad. Eng. Chim. Ital., 6*, 125 (1970); *Amer. Inst. Chem. Eng. Jl., 19*, 916, with permission of the American Institute of Chemical Engineers, (1973).] (c) Energy dissipation correlation for K_G in cocurrent downflow trickle beds.

Packing	Ψ, m^{-1}
6 mm glass spheres	24.5
6 mm Berl saddles	18.4
6 mm ceramic rings	36.5
6 mm glass rings	17.1

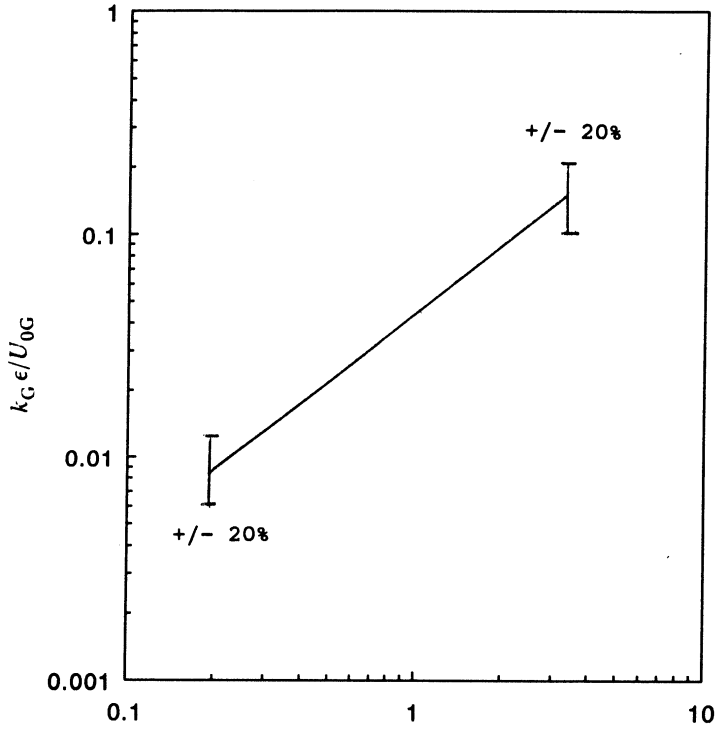

(c)

Liquid-solid. Transport between the liquid and solid (catalyst) phases in trickle-bed reactors is at least a first cousin to transport in more conventional fixed beds, and our understanding of the liquid phase mass-transfer coefficient here benefits from the decades of research devoted to that topic. A good correlation was reported as far back as 1948 by Van Krevelen and Krekels [D.W. Van Krevelen and J.T.C. Krekels, *Rec. Trav. Chim. Pays-Bas, 67*, 512 (1948)], who proposed

$$N_{Sh} = 1.8(N_{Re})_L^{0.5}(N_{Sc})^{0.33} \tag{8-233}$$

with

$$N_{Sh} = \left(\frac{k_{L_2}}{a_S D_{AL}}\right); \qquad N_{Re} = \left(\frac{\rho_L L}{A_c a_s \mu_L}\right)$$

where a_S is the liquid-solid interfacial area per unit volume, A_c the column cross-sectional area, and L the volumetric liquid flow rate. The data on which equation (8-233) is based indicated that the liquid-solid mass-transfer coefficient is greater in the trickle bed than in a comparable bed with a continuous liquid phase for large catalyst particle size (presumably via turbulence induced by gas-phase flow), although for smaller particles ($d_p < 2\,\text{mm}$) Goto and Smith [S. Goto and J.M. Smith, *Amer. Inst. Chem. Eng. Jl., 21,* 706 (1975)] reported a reverse effect, which is a reasonable result.

Other correlations reported for k_L generally follow the same form. Reasonable alternatives to equation (8-233) are the correlations reported by Dharwadkar and Sylvester [A. Dharwadkar and N.D. Sylvester, *Amer. Inst. Chem. Eng., Jl., 23,* 376

(1977)] and by Ruether et al. [J.A. Ruether, C.S. Yang and W. Hayduk, *Ind. Eng. Chem. Proc. Design Devel., 19,* 103 (1980)]. From the former,

$$j_D = \left(\frac{k_{L_2}}{a_S D_{AL}}\right)(N_{Sc})^{0.67} = 1.64(N_{Re})_L^{0.33} \tag{8-234}$$

for $0.2 < (N_{Re})_L < 2400$. From Ruether et al.,

$$\theta\epsilon\left(\frac{k_{L_2}}{a_S D_{AL}}\right) = s[(N'_{Re})_L]^q (N_{Sc})^{0.33} \tag{8-235}$$

where θ is the catalyst porosity and ϵ is the bed void fraction. The correlation constants s and q depend upon the flow regime defined in terms of the modified Reynolds number $(N'_{Re})_L$

$s = 0.842; \quad q = 0.78 \quad$ for $(N'_{Re})_L < 55$ (trickle flow)

$s = 0.044; \quad q = 1.52 \quad$ for $55 < (N'_{Re})_L < 100$

$s = 0.680; \quad q = 0.42 \quad$ for $(N'_{Re})_L > 100$ (pulse flow)

where $(N'_{Re})_L = (\rho_L u_L / a_s \mu_L \beta_t)$, and the total β_t can be determined from equation (8-228).

Finally, some experimental results from the work of Hirose et al. [T. Hirose, M. Toda and Y. Sato, *J. Chem. Eng. Japan, 7*, 187 (1974)] are shown in Figure 8.21d.

Intraparticle diffusion. Contrary to fluid beds or slurry reactors, which normally employ finely divided catalyst particles, trickle beds normally are employed with catalyst particles of similar dimension to those of conventional fixed beds, and intraparticle diffusion can become an important factor in the overall rate of reaction and/or selectivity to various products in complex reactions. Indeed, both Satterfield [C.N. Satterfield, *Amer. Inst. Chem. Eng. Jl., 21*, 209 (1975)] and Speccia et al., [V. Speccia, G. Baldi and A. Gianetto, *Chem. Eng. Sci., 32*, 515 (1977)] pointed

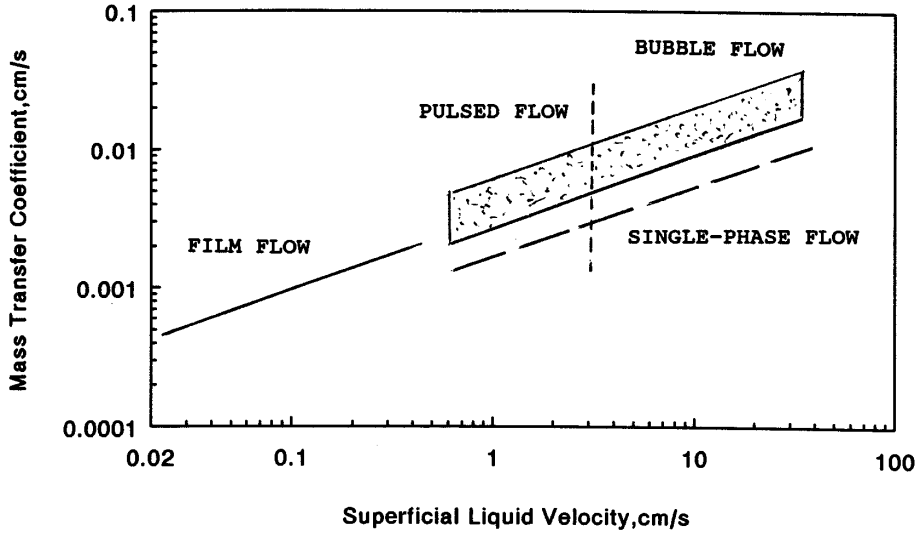

Figure 8.21 (d) Experimental results for the liquid-solid mass-transfer coefficient in a downflow trickle bed; liquid velocity range from 1 to 100 cm^3/s. For film flow $d_p = 9 - 12$ mm; for other regimes $d_p = 12$ mm.

out that gas-liquid and liquid-solid mass transfer resistances can be neglected if the diffusional (Thiele) modulus for the catalytic reaction is > 1.

Normal procedures for estimation of the effectiveness factor, η, in reaction with single-phase flow were discussed in Chapter 7, and if the pores in the catalyst particles are completely filled with liquid, then similar methods can be used with appropriately modified diffusivities for trickle-bed reactors. Since diffusion coefficients in the liquid phase are considerably smaller than those in the gas phase, catalyst effectiveness can be low for trickle-bed reactors, even for relatively small particle sizes. Following the development in Chapter 7 we can still say that,

$$\eta = \frac{\tanh \phi}{\phi} \tag{8-236}$$

in the region of strong diffusion, with the Thiele modulus defined for arbitrarily shaped particles as

$$\begin{aligned} \phi &= \Lambda(k/D_{eff})^{1/2} \\ \Lambda &= \left(\frac{V_p}{S_p}\right) \end{aligned} \tag{8-237}$$

for our Academic Reaction #1. In Chapter 7 we discussed the nature of D_{eff} in some detail; here let us follow the simplest defining relationship,

$$D_{eff} = \left(\frac{\mathcal{D}\epsilon_p}{\tau}\right) \tag{8-238}$$

where ϵ_p is the particle void fraction, τ the tortuosity factor (normally about 3 to 5), and $\mathcal{D}$ the liquid-phase diffusion coefficient (normally of reactant).

If the catalyst particles are not completely wetted by the liquid phase and the pores consequently not completely filled with liquid phase (static holdup gives some indication of whether this is the case or not), the situation is considerably more complex. In addition to being a function of the Thiele modulus, the catalytic effectiveness will now depend on the fraction of external wetting, η_{CE}, and the fraction of pore volume filled with liquid, η_i. Dudokovic [M.P. Dudokovic, *Amer. Inst. Chem. Eng. Jl., 23*, 940 (1977)] proposed a reasonable approach that accounts for all three factors. If the reaction proceeds only on the catalyst surface effectively wetted by the liquid phase and components of the reaction mixture are nonvolatile, then one can in principle modify the definition of the Thiele modulus to

$$\phi_{TB} = \left(\frac{\eta_i}{\eta_{CE}}\right)\phi \tag{8-239}$$

The effectiveness factor in the trickle bed would then be defined as

$$\eta_{TB} = (\eta_{CE}/\phi) \tanh \left(\frac{\eta_i \phi}{\eta_{CE}}\right) \tag{8-240}$$

For small values of ϕ (slow reaction),

$$\eta_{TB} \rightarrow \eta_i \tag{8-241}$$

and for large ϕ,

$$\eta_{TB} = (\eta_{CE}/\phi) = (\eta_{CE})\eta \tag{8-242}$$

The general results accord with common sense. For example, for large diffusional resistances ($\phi \gg 1$) the reaction occurs in a narrow zone close to the external surface of the particle, and the utilization of the catalyst then becomes proportional to the fraction of external surface wetted, η_{CE}. Via similar reasoning, in the kinetically controlled regime ($\phi \ll 1$) the reaction rate is proportional to the internal volume wetted, η_i. Now, all of this sounds fine and the dedicated would undoubtedly scurry off immediately in search of appropriate correlations for the parameters η_{CE} and η_i. Unfortunately, they are doomed to return empty-handed, or nearly so, since there are essentially no correlations available for η_i, and those for η_{CE} are unreliable [J.G. Schwartz, E. Weger and M.P. Dudokovic, *Amer. Inst. Chem. Eng. Jl., 22*, 894 (1976)]. A rather detailed study of wetting efficiency was reported by Mills and Dudokovic [P.L. Mills and M.P. Dudokovic, *Amer. Inst. Chem. Jl. 22*, 894 (1981)] who gave a correlation in terms of nondimensional quantities. However, it is difficult to estimate the reliability of that correlation because of the few reliable experimental data available—then or now. One can always make an estimate, at risk, of η_i and η_{CE} from static holdup data.[20]

If the reaction is gas-reactant limited, Ramachandran and Smith [P.A. Ramachandran and J.M. Smith, *Amer. Inst. Chem. Eng. Jl., 25*, 538 (1978)] suggested that the overall effectiveness factor can be obtained as the weighted average of the wetted and unwetted parts of the catalysts. Hence,

$$\eta_0 = \frac{(\eta_{CE}/\phi)\tanh\phi}{1 + \dfrac{\phi\tanh\phi}{(N_{Sh})_L}} + \frac{(1-\eta_{CE})[(\tanh\phi)/\phi]}{1 + \dfrac{\phi\tanh\phi}{(N_{Sh})_G}} \tag{8-243}$$

but even this still leaves the dedicated in search of a correlation. If the catalyst is completely wetted by the liquid phase one can retreat to the basic definitions of equations (8-236) to (8-238). The rate constant k must, of course, be available from other sources, but Λ is directly measurable, as well as the particle porosity ϵ. The tortuosity τ may cause a bit more difficulty, but as discussed after equation (8-238) the general range of expected values is known, and values of this parameter have been measured for quite a number of typical porous materials including catalysts and catalyst supports (see Table 7.4, Chapter 7). Problems may come from an unexpected direction, which is the evaluation of a proper value for the effective diffusivity, D_{eff}. Many applications of trickle beds involve heavy molecular weight materials, in which the molecular size is significant compared to catalyst pore dimension. In such cases, the effective diffusivity decreases because of the proximity of the pore wall and estimates based on liquid-phase diffusivities will be too large. There is not a lot of fundamental information concerning this, but some approaches were suggested by Pitcher et al. [W.H. Pitcher, C.K. Colton and C.N. Satterfield, *Amer. Inst. Chem. Eng. Jl., 19*, 628 (1973)] and by Tamm et al. [P.W. Tamm, H.F. Harnsberger and A.G. Bridge, *Ind. Eng. Chem. Proc. Design Devel., 20*, 262 (1981)].

[20] "Any old port in a storm."—*Anonymous*

Illustration 8.6[21]

Satterfield defined an "ideal" trickle-bed reactor as one that obeys the following conditions.

1. Plug flow of liquid.
2. No mass- or heat-transfer limitations between gas and liquid, between liquid and solid, or intraparticle within the catalyst.
3. First-order, isothermal, irreversible reaction with respect to reactant in the liquid phase; gaseous reactant present in great excess.
4. Catalyst pellets completely wetted.
5. Reaction occurs only at the catalyst-liquid interface.
6. No vaporization or condensation.

Derive a workable set of equations, in accord with the restrictions above, to determine the reactant conversion in such in ideal trickle-bed reactor. What is the relationship of this to reality?

Solution

The answer to the question above is probably "very little" (see Section 8.3), however, let us take a closer look at the situation. From a mass balance across a differential volume element, $d\bar{V}$, of the reactor, we have

$$FC_0\,dx = (-r)\,d\bar{V} \tag{i}$$

where C_0 is the reactant concentration in the entering liquid phase in, say, mols/cm^3, x fractional conversion of reactant, and $d\bar{V}$ is the differential volume element under consideration. For first-order reaction,

$$(-r) = kC(1-\epsilon) \tag{ii}$$

where the rate constant is in units of (cm^3 liquid/cm^3 pellet-s). Combining (i) and (ii),

$$FC_0\,dx = k(1-\epsilon)C\,d\bar{V} \tag{iii}$$

$$C = C_0(1-x)$$

and

$$F\int\frac{dx}{x} = k(1-\epsilon)\int d\bar{V} \tag{iv}$$

Thence,

$$\ln\left(\frac{C_0}{C_{out}}\right) = \left(\frac{\bar{V}}{F}\right)k(1-\epsilon) = \frac{k(1-\epsilon)}{(L_v/h)} \tag{v}$$

or, in terms of the liquid hourly space velocity (LHSV),

$$\ln\left(\frac{C_0}{C_{out}}\right) = \frac{3600\,k(1-\epsilon)}{LHSV} \tag{vi}$$

[21] After C.N. Satterfield, *Amer. Inst. Chem. Eng. Jl., 21*, 209, with permission of the American Institute of Chemical Engineers, (1975).

where L_v is the liquid superficial flow rate in cm/s, and h is the depth of the packed bed.

Comparison with slurry reactor measurements
If the simplifying assumptions above also hold for a slurry reactor, one should be able to obtain values for the rate constant k in an autoclave experiment. One would measure changes in concentration with time (i.e., batch reactor procedure) rather than changes with position as in a trickle bed, but the two measures should be proportional to each other. For the slurry reactor,

$$\left(\frac{dC}{dt}\right) = \frac{(-r)(v_{cat} - v_L)}{v_L} \tag{vii}$$

where $(-r)$ is the rate in [mols/(cm^3 cat + cm^3 liquid)-s], v_{cat} is the volume of catalyst in the reactor in cm^3, and v_L is the volume of liquid in the reactor, also in cm^3. Now, using equation (ii) in equation (vii) we have

$$\left(\frac{dC}{dt}\right)\left(\frac{v_L}{v_{cat}}\right) = kC(1 - \epsilon) \tag{viii}$$

where $(1 - \epsilon)$ is the volume fraction of catalyst in the slurry. Integrating,

$$\ln\left(\frac{C_0}{C_t}\right) = \left(\frac{v_{cat}}{v_L}\right)kt(1 - \epsilon) \tag{ix}$$

where, for the slurry reactor, C_0 refers to the initial concentration. We may then evaluate k in the normal manner from C_t versus t data; the only thing to remember is that the slope of a plot of $\ln(C_0/C_t)$ versus t contains the factor (v_{cat}/v_L).

HORATIO SAYS

How much does all of this differ from the analysis of a typical plug-flow reactor? What are the corresponding terms between the two reactor models?

8.4.3 Axial Dispersion Considerations

We might wonder about the necessity of giving the illustration above, since the ideal trickle-bed reactor is nothing more than a glorified PFR with a couple of additional parameters. Such criticism is, in fact, hard to rebut. Possibly the best justification is that the ideal model gives us a place to start. The discussion of hydrodynamic factors in Section 8.1 suggests that nonidealities in the liquid flow are of potential importance, and indeed this is so. Here we can return to an old friend from Chapter 5, the axial dispersion coefficient D_L. In general Pellet numbers are significantly lower for trickle-flow conditions than for single-phase flow through conventional packed beds

under similar circumstances. There is no lack of proposed correlations. A simple and reasonably reliable one is that Mitchell and Furzer [R.W. Mitchell and I.A. Furzer, *Chem. Eng. Jl., 4*, 531 (1972)].

$$(N_{Pe})_L = (N_{Re})_L^{0.7}(N_{Ga})_L^{-0.32} \tag{8-244}$$

where

$$(N_{Pe})_L = \frac{u_L d_p}{D_L}; \qquad (N_{Re})_L = \frac{d_p \rho_L u_L}{\mu_L}; \qquad (N_{Ga})_L = \frac{d_p^3 g \rho_L^2}{\mu_L^2}$$

with u_L the interstitial velocity and D_L the axial dispersion coefficient. Early on Van Swaaij et al. [W.P.M. Van Swaaij, J. C. Charpentier and J. Villermaux, *Chem. Sci. Eng. Sci., 24*, 1083 (1969)] suggested that the Peclet number could be correlated with liquid holdup. Furzer and Mitchell [I.A. Furzer and R.W. Mitchell, *Amer. Inst. Chem. Eng. Jl., 2*, 380 (1970)] thus provided us with

$$(N'_{Pe})_L = 4.3[(N'_{Re})_L/\beta_f]^{1/2}(N_{Ga})_L \tag{8-245}$$

where the primed quantities are defined using the superficial liquid velocity instead of the interstitial value, and β_f is the dynamic holdup. The only difficulty found is that such correlations are for air-water systems. Some variety is provided by Hochman and Effron [J.M. Hochman and E. Effron, *Ind. Eng. Chem. Fundls., 8*, 63 (1969)], who studied the N_2-methanol system and proposed

$$(N_{Pe})_L = 0.042(N_{Re})_L^{0.5} \tag{8-246}$$

where $(N_{Re})_L$ was defined as

$$(N_{Re})_L = [u_{OL}\rho_L d_p/\mu_L(1-\epsilon)]$$

with u_{OL} the superficial velocity. The three correlations for Peclet number above are really quite similar; the role of the Galileo number is somewhat tenuous in these correlations and equation (8-246) is recommended for hydrocarbon systems in the book by Shah.

8.4.4 Some Combined Models

A long time ago,[22] in Chapter 5, we presented some combinations of PFR and CSTR as a means of modeling nonideal flow patterns—particularly when large deviations (short-circuiting, dead volume, etc.) were encountered. However, to this point we really have not done much to exploit such models. They do have a home, to some extent, in modeling flow patterns in trickle-bed reactors when the axial dispersion model is not up to the task. A number of those, classified as to the number of parameters involved (nothing in this life is completely free), were discussed in the text by Shah. It is not clear that any of these have ever been used as the basis for a design, but they are fun anyway. Table 8.3 gives an overview of some of these. The question as when to stop in Table 8.3 is arbitrary, since there are other four-parameter models around, and even some with five parameters. However, remember the little morality tale concerning the number of parameters involved in physico/chemical models that was set forth in Chapter 3.

[22] "... in a galaxy far, far away..."—*G. Lucas* (Star Wars).

Table 8.3 Some Combined Models Proposed for Trickle-Bed Flow

1. *Simple Bypass*
   Parameters: One: fraction of flow to perfect mixing.
   Reference: R.W. Mitchell and I.A. Furzer, *Trans. Inst. Chem. Eng., 50*, 334 (1972).
   Picture:

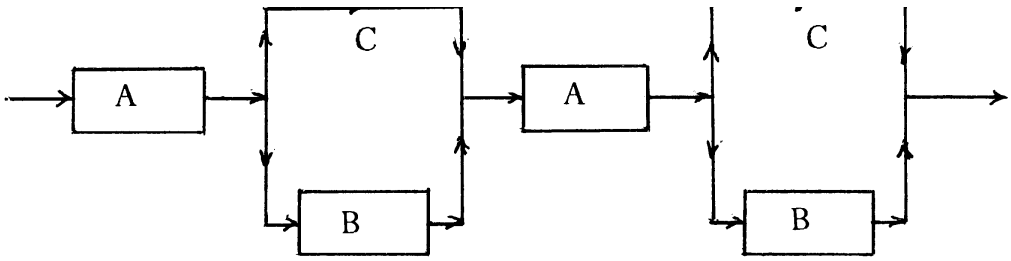

A: Laminar film region
B: Perfectly mixed static holdup region
C: Instantaneous bypass

2. *Deans and Lapidus Mixing Cells in Series*
   Parameters: Two: fraction of liquid that is stagnant and the mass-transfer coefficient between stagnant and flowing liquid.
   References: H.A. Deans and L. Lapidus, *Amer. Inst. Chem. Eng. Jl., 6,* 656 (196); H.A. Deans, *Soc. Pet. Eng. Jl., 3*, 49 (1963).
   Picture: See Chapter 6.
3. *Axial Dispersion*
   Parameters: Two: fractional liquid holdup and the axial dispersion coefficient.
   Reference: See Chapter 5.
   Picture:

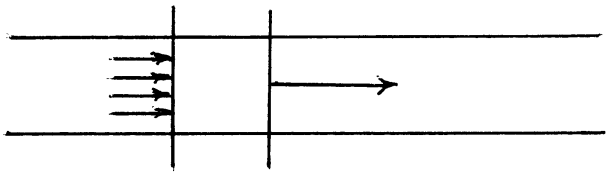

4. *Cross Flow*
   Parameters: Two: fraction of liquid in plug flow and the mass-transfer coefficient between stagnant and flowing liquid.
   References: J.M. Hochman and E. Effron, *Ind. Eng. Chem. Fundls., 8*, 63 (1969: C.J. Hoogendoorn and J. Lips, *Can. J. Chem. Eng., 43*, 125 (1965).
   Picture: Main plug flow channel flowing and stagnant liquid

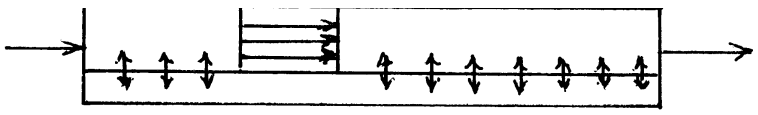

5. *Time delay*
   Parameters: Three: time for initial breakthrough of tracer in an $E(t)$ experiment, mean delay time, and total number of delays per element of fluid during its residence time. The delay times are exponentially distributed about a mean value.

Table 8.3 Continued.

5. *Time Delay*
   References: B.A. Buffham, *Chem. Eng. Jl., 1,* 31 (1971); B.A. Buffham and L.G. Gibilaro, *Chem. Eng. Jl., 1*, 31 (1970); B.A. Buffham, L.G. Gibilaro and M.N. Rathor, *Amer. Inst. Chem. Eng. Jl., 16*, 218 (1970).
   Picture: Main plug flow with lateral streams delayed at different points the bed (perfectly mixed).

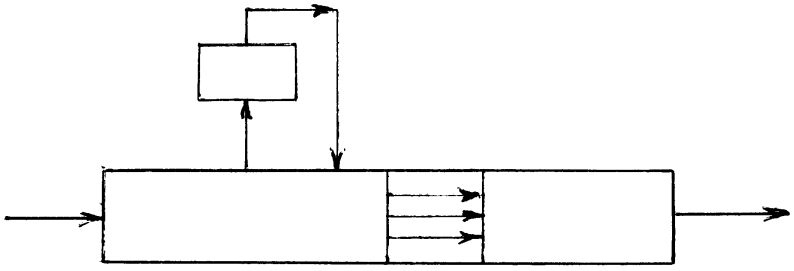

6. *Modified Cross Flow*
   Parameters; As for cross flow, plus axial dispersion in the flowing liquid.
   References: W.P.M. Van Swaaij, J.C. Charpentier and J. Villermaux, *Chem. Eng. Sci., 24*, 1083 (1969).
   Picture: See 4 above.
7. *Staged Backmixing*
   Parameters: Three: fraction of liquids in the mobile zone and relative volumes of mobile and stagnant zones, plus the number of stages.
   Reference: See 6 above; also J. Villermaux and W.P.M. Van Swaaij, *Chem. Eng. Sci., 24*, 1097 (1969).
   Picture: Split of feed into fractions α and $(1-\alpha)$ into stagnant, V_i, and mobile, V_s, zones. Figure is for the ith stage in the sequence.

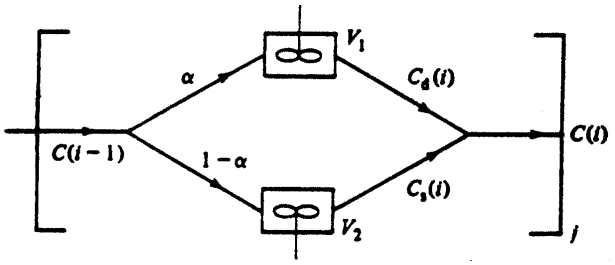

8. *Staged Mixing with Bypassing*
   Parameters: Four: fraction bypass flow, relative volumes of stagnant and mobile zones, and number of stages.
   Reference: J. Raghuraman and Y.B.G. Varma, *Amer. Inst. Chem. Eng. Jl., 22,* 612 (1976).
   Picture:

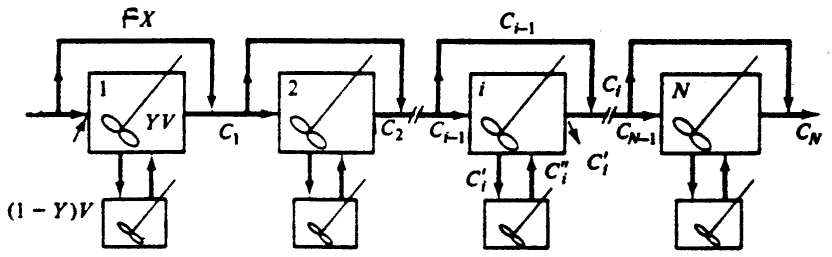

8.4.5 Trickle-Bed Reactor Models

It is very interesting, after all this discussion of hydrodynamics, mass transfer, and other properties of trickle beds, to see what people have actually done when they get down to the task of trickle-bed reactor design.[23] Things get fairly basic quite rapidly, and while we don't retreat all the way to the ideal trickle-bed reactor model, neither do we attempt the presumption of three or four parameters. Some have proposed simplified heterogeneous models, others consider only the degree of contact between the liquid and solid phases, and still others base the approach on the mass-transfer factors appearing in the three-phase reactor/reaction system. Finally, there are some approaches based on the directly-determined residence time distribution function. We will take a brief look at each.

Plug flow. This is a small modification of the ideal model, including the catalyst effectiveness factor. Then,

$$\frac{dC}{d\xi} = -\frac{k(1-\epsilon)\eta C^m}{(LHSV)} \tag{8-244}$$

where ϵ is the bed void fraction, m the order of reaction with rate constant k, and ξ a nondimensional distance (position within the reactor). In most applications m is either 1 or 2, with the result

$$\ln\left(\frac{C_0}{C_{out}}\right) = \frac{\eta k(1-\epsilon)}{(LHSV)}; \qquad m = 1 \tag{8-245}$$

$$\frac{1}{C_{out}} - \frac{1}{C_0} = \frac{\eta k(1-\epsilon)}{(LHSV)}; \qquad m = 2 \tag{8-246}$$

The effectiveness can be determined from the appropriate procedure in Section 8.4.2 for the case at issue. A consistent set of units would be $k(m=1)$ in cm^3 liquid/cm^3 solid-h or k $(m=2)$ in $(cm^3$ liquid$)^2$/g-cm^3 solid-h, LHSV in cm^3 liquid/cm^3 solid-h, and C in g/cm^3. Aside from Satterfield, this model has appeared in reports by Reiss [L.P. Reiss, *Ind. Eng. Chem. Proc. Design Devel., 6*, 486 (1967)] and Henry and Gilbert [G.H. Henry and J.B. Gilbert, *Ind. Eng. Chem. Proc. Design Devel., 12*, 328 (1973)].

Liquid holdup. This approach derives from the observation that at low flow rates (typical of many pilot-plant studies), the apparent rate of reaction is dependent upon liquid flow rate. This was investigated by Henry and Gilbert using a correlation proposed by Satterfield for the external holdup,

$$\beta_{te} = \beta_r + \beta_f = a(N_{Re})_L^{1/3}(N_{Ga})_L^{-1/3} \tag{8-247}$$

where

$$(N_{Re})_L = \frac{G_L d_p}{\mu_L}; \qquad (N_{Ga})_L = \frac{d_p^3 g \rho_L^2}{\mu_L^2}$$

where G_L is the mass flow rate of liquid per unit area, and a is a proportionality constant [C.N. Satterfield, A.A. Pelossof and T.K. Sherwood, *Amer. Inst. Chem.*

[23] As one might say, "... where the rubber meets the road ..."—Advertising copy, ca. 1970-1990).

Eng. Jl., 15, 226 (1969)]. Thus, for a first-order reaction,

$$\ln\left(\frac{C_{out}}{C_0}\right) \propto -\frac{k\beta_{te}}{(LHSV)^n} \tag{8-248}$$

Combining equations (8-247) and (8-248) gives

$$\ln\left(\frac{C_{out}}{C_0}\right) \propto -\frac{k\beta_{te}}{(LHSV)^{2/3}} \tag{8-249}$$

or, in more detail,

$$\ln\left(\frac{C_{out}}{C_0}\right) = (Z)^{1/3}(LHSV)^{-2/3}(d_p)^{-2/3}\nu^{1/3} \tag{8-250}$$

where $v = \mu/\rho$ for the liquid, and Z is bed length.

There is no *a priori* justification for assuming that the reaction rate is proportional to holdup, however, the experimental evidence is there (at least according to Henry and Gilbert). According to this view, a certain minimum amount of holdup is required for full catalyst utilization. The correlating parameter in terms of the hydrodynamics is the ratio $[(N_{Fr})_L/(N_{Re})_L]^{1/3}$, where $(N_{Fr})_L$ is given by $(G_L^2/\rho_L^2 d_p g)$ and $(N_{Re})_L$ is as defined above. The general situation is shown in Figure 8.22. The particular holdup correlation used by Henry and Gilbert has been criticized as lacking in generality. This is probably so, and more recent work has expanded the range of variables considered. However, one would like to use some of the more general approaches for holdup given previously in this chapter, but this apparently has not been done. There is disagreement about the critical value of $[(N_{Fr})_L/(N_{Re})_L]$ yielding 100% catalyst utilization, and the matter has not been resolved.

Catalyst wetting. As indicated by its name, this model is based on the assumption that the fraction of the outer surface of the catalyst wetted by the liquid phase is the critical factor in determining the overall reaction rate [D.E. Mears,

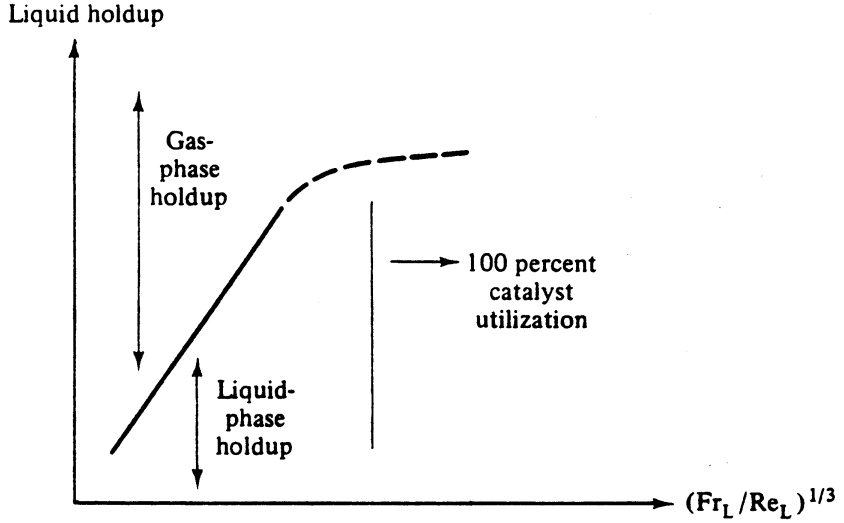

Figure 8.22 Liquid holdup regimes in downflow trickle-bed operation.

Advan. Chem., 133, 218 (1974)]. In this case we modify equation (8-244) to

$$\frac{dC}{d\xi} = -\frac{k(1-\epsilon)\eta a_W C}{(LHSV)} \tag{8-251}$$

where a_W is the ratio of wetted external area to total external area. It is thus an adjustable parameter, but the suggestion is to use the correlation of Purinak and Volelpohl [S.S. Purinak and A. Voqelpohl, *Chem. Eng. Sci., 29,* 501 (1974)]

$$a_W = 1.05(N_{Re})_L^{0.047}(N_{We})_L^{0.135}\left(\frac{\sigma_c}{\sigma_L}\right) \tag{8-252}$$

where $(N_{We})_L$, the Weber number for the liquid phase, is $(G_L^2 d_p/\sigma_L \rho_L)$, σ_L is the liquid surface tension, and σ_c is a critical surface tension for a contact angle between liquid and packing. Combining equations (8-251) and (8-252) and integrating gives

$$\ln\left(\frac{C_0}{C_{out}}\right) = \frac{(Z)^{0.32}(d_p)^{0.18}(\sigma_c/\sigma_L)^{0.21}\eta}{(LHSV)^{0.6}(\nu_L)^{0.05}} \tag{8-253}$$

Comparison of the a_W correlation with experiment, however, indicates that the results lie above the predictions of equation (8-252) at higher liquid rates ($\sim 500\,\mathrm{g/cm^2\text{-}h}$), and in this region the correlation of Onda et al. [K. Onda, H. Takeuchi and H. Koyama, *Kagaku, 31,* 121 (1976)] should be used.

$$a_W = 1 - \exp[-1.36 G_L^{0.05}(N_{We})_L^{0.2}(\sigma_c/\sigma_L)^{0.75}] \tag{8-254}$$

Combining this with equation (8-251) gives

$$\ln\left(\frac{C_0}{C_{out}}\right) = \frac{k(1-\epsilon)\eta}{(LHSV)}\{1 - \exp[-\gamma(Z)^{0.4}(LHSV)^{0.4}]\} \tag{8-255}$$

where dependencies on viscosity, surface tension, density, and particle size have been lumped into the factor γ. Since we are wandering away from the textbook to the handbook here, we will conclude this discussion of catalyst wetting now. Much more is available elsewhere.

External mass transfer. The method of moments applied to the pulse response of fixed-bed reactors [M. Suzuki and J.M. Smith, *Amer. Inst. Chem. Eng. Jl., 16,* 882 (1970); *Chem. Eng. Sci., 26*, 221, (1971)] was adapted to the consideration of reaction/mass-transfer effects in trickle beds [N.D. Sylvester and P. Pitayagulsarn, *Amer. Inst. Chem. Eng. Jl., 19*, 640 (1973); *Can. Jl. Chem. Eng., 52*, 539 (1974)]. In this latter work it was shown that the zeroth, first and second moments of the response to a pulse input can be divided rather neatly into several factors, each associated with a particular step in the overall reaction-transport process. The zeroth moment of the output is related to a series of parameters given by

$$1 - x = \exp(-\lambda_3 W) \tag{8-256}$$

where

$$W = (2Z/d_p); \qquad \lambda_1 = \left(\frac{3}{F}\right)[(\lambda_0 F)^{1/2}\coth(\lambda_0 F)^{1/2} - 1]$$

$$\lambda_2 = \frac{1}{(1/\lambda_1 + 1/S)}; \qquad \lambda_3 = \left(\frac{N_{Pe}}{2}\right)\{[1 + 4\lambda_2/(N_{Pe})]^{1/2} - 1\}$$

The significance of the factors above is as follows.

1. $F = u_{OL}d_p/2D_{eff}(1-\epsilon_p)$ considers the effect of intraparticle diffusion; u_{OL} is the superficial liquid velocity and ϵ_p is the particle void fraction.
2. $(N_{Pe}) = u_{OL}d_p/2D_L$ is the axial dispersion parameter.
3. $S = 3(1-\epsilon)K_T/u_{OL}$ is the external mass-transfer factor; K_T is the overall external mass-transfer coefficient.
4. $\lambda_0 = k(1-\epsilon)^2 d_p/2u_{OL}$ is the surface reaction factor. The overall mass-transfer coefficient, K_r, is defined as

$$\frac{1}{K_r} = \frac{1}{k_G H \beta_G} + \frac{1}{k_L} + \frac{1}{K_s} \tag{8-257}$$

where β_G is the gas holdup based on the total volume of the reactor and K_s is the liquid-solid mass-transfer coefficient. Overall, the term λ_3 can be considered as a reaction rate; when axial dispersion is negligible, $\lambda_3 = \lambda_2$, and when external diffusion is negligible, $\lambda_3 = \lambda_1$.

Note that this work of Sylvester and Pitayagulsarn does not present a design model per se; the moments analysis allows one to apply an experimental approach that is convenient for parameter evaluation in the reaction/reactor system when both transport and catalyst wetting are important in affecting overall conversion. We repeat a word of warning here. The evaluation of moments depends upon the numerical evaluation of a time-response versus time from 0 to ∞. Long tails on the response (often experimental artefact) can lead to very large $\pm$ estimates of parameters. Despite the theoretical appeal, moments analysis is hazardous [see W.E. Munro, S. Delgado-Diaz and J.B. Butt, *J. Catal., 37*, 158 (1975)].

General approach. It is interesting, as stated before, that when we get around to discussing the realities of reactor design we find simple models.[24] These are normally based on one particular factor, such as holdup, catalyst wetting, etc., and as a consequence have little value to more general design considerations. For this reason it is a good exercise to sit down and, at least, write out the mathematical relationships that are appropriate based on what we know about reactor analysis and design. So, here goes, considering the reaction to be

$$\mathrm{A}_{(g)} + \mathrm{B}_{(liq)} \rightarrow \mathrm{C}_{(liq)}$$

with intrinsic kinetics

$$(-r_A) = kA_S B_S \tag{8-258}$$

For isothermal reaction conditions, the mass balances are

<u>A – Gas</u>

$$D_G \frac{d^2 A_G}{dz^2} - u_{OG} \frac{dA_G}{dz} - K_L a_L (A_G - A_L) = 0 \tag{8-259}$$

[24] "The ugliest of trades have their moment of pleasure."—*D. Jerrold*

A – Liquid

$$D_L \frac{d^2 A_L}{dz^2} - u_{OL} \frac{dA_L}{dz} + K_L a_L (A_G - A_L) - K_{SA} a_S (A_L - A_S) = 0 \tag{8-260}$$

$$K_{SA} a_S (A_L - A_S) = k a_S \eta A_S B_S \tag{8-261}$$

B – Liquid

$$D_L \frac{d^2 B_L}{dz^2} - u_{OL} \frac{dB_L}{dz} - K_{SB} a_S S (B_L - B_S) = 0 \tag{8-262}$$

$$K_{SB} a_S (B_L - B_S) = k a_S \eta A_S B_S \tag{8-263}$$

C – Liquid

$$D_L \frac{d^2 C_L}{dz^2} - u_{OL} \frac{dC}{dz} + K_{SC} a_S (C_S - C_L) = 0 \tag{8-264}$$

$$K_{SC} a_S (C_S - C_L) = k a_S \eta A_S B_S \tag{8-265}$$

Also, with many boundary conditions

$$\begin{aligned} D_L \frac{dA_G}{dz} &= u_{OG}(A_G - A_{Gi}); \qquad z = 0^+ \\ D_L \frac{dA_L}{dz} &= u_{OL}(A_L - A_{Li}); \qquad z = 0^+ \end{aligned} \tag{8-266}$$

$$\begin{aligned} D_L \frac{dB_L}{dz} &= u_{OL}(B_L - B_{Li}); \qquad z = 0^+ \\ D_L \frac{dC_L}{dz} &= u_{OL}(C_L - C_{Li}); \qquad z = 0^+ \end{aligned} \tag{8-267}$$

and

$$\frac{dA_G}{dz} = \frac{dA_L}{dz} = \frac{dB_L}{dz} = \frac{dC_L}{dz} = 0; \qquad z = Z$$

Now one recognizes this instantly as an axial dispersion model, both gas and liquid phases, and by now we ought to be able to write it down from memory. Nonetheless, let us take one last look to make *sure* that we know what everything means. An important point, not explicit in the equations, is that the liquid holdup (or the catalyst wetting) does not vary through the bed. The individual terms are then [see Figure (8.23)],

D_G, D_L axial dispersion coefficients in gas and liquid phases; taken the same for A, B, C.

$k_L a_L$ overall gas-liquid volumetric mass-transfer coefficient (includes both gas- and liquid-side resistances for A).

$K_{Si} a_S$ liquid-solid mass-transfer coefficients ($i = A, B, C$), normally the same for all species.

z, Z axial coordinate and reactor length.

η effectiveness factor.

u_{OG}, u_{OL} superficial gas and liquid velocities.

G, L, S subscripts for gas, liquid, and solid surface.

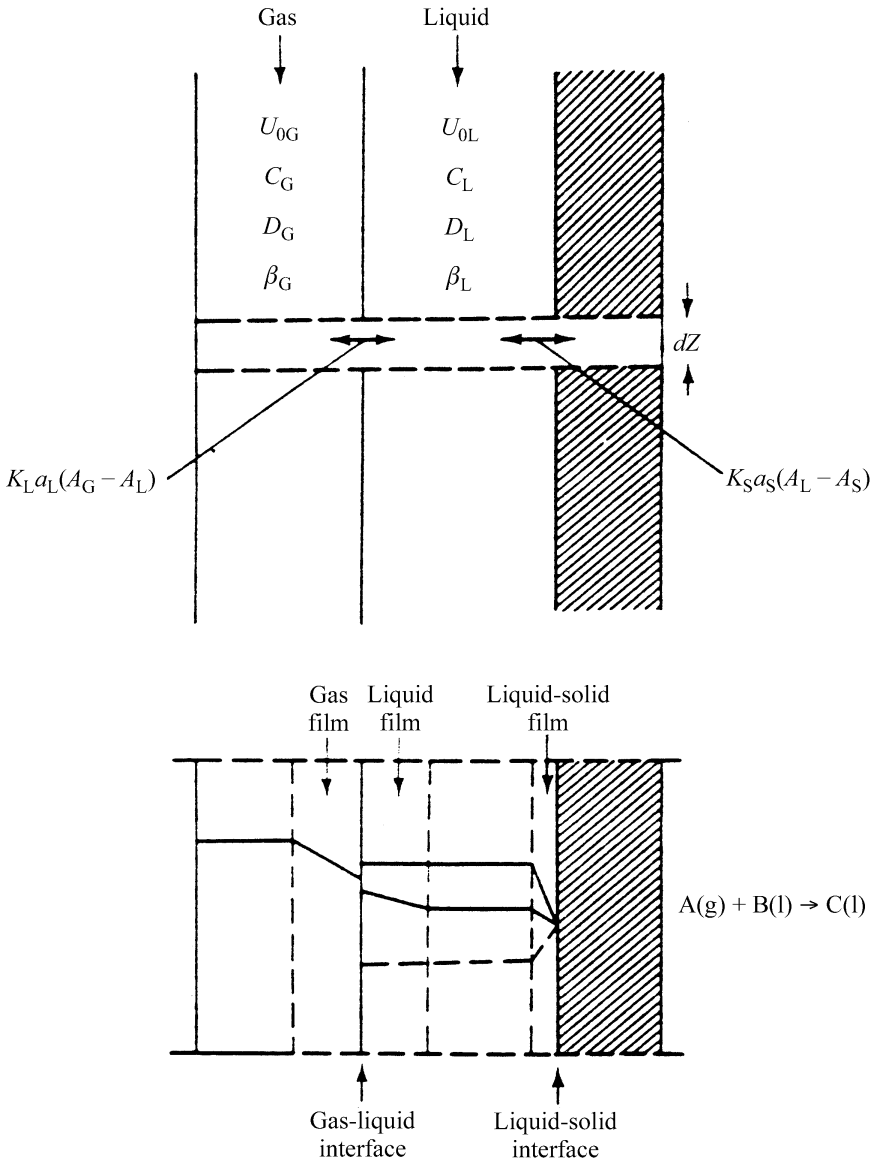

Figure 8.23 Schematic diagram of a trickle-bed system for a second-order reaction.[After Y-T. Shah, *Gas-Liquid-Solid Reactor Design,* with permission of McGraw-Hill Book Co., New York, NY, (1979).]

At this point we can also play the game of DOP ("drop the parameter"). Although this seems like something lighthearted, DOP is fairly serious. If the gas moves in plug flow, which is often the case, then the term with D_G in equation (8-259), disappears. If the concentration of B in the liquid phase is very large, which is often the case, then terms involving B_L are nearly constant and equations (8-262), (8-263) and the condition on (dB_L/dz) will disappear. If the liquid-solid mass-transfer resistances are small, then $A_L = A_S, B_L = B_S$, and $C_L = C_S$. If the feed gas is pure A, and B and C are nonvolatile, the $A_G = A_L$. Various limiting forms of the governing equations for this situation have been given in the literature [K. Ostergaard, *Advan. Chem., 26*, 1361 (1971); H. Hofmann, *Int. Chem. Eng., 17*, 19 (1977); S. Goto, S. Watabe and M. Matsubara, *Can. Jl., Chem. Eng., 54*, 531 (1976)].

We probably don't have to, at this point, say that the overall model here, or even considerable simplifications of it, are best left to numerical solution. The axial dispersion model seems to work pretty well, at least for cases where the holdup/wetting does not vary much with position in the reactor. For large changes in this factor, or for nonideal flows involving stagnant zones or liquid/gas bypassing, some version of one of the combined models will be required. It will be understood that these will be *very specific* to the particular design under consideration.

Illustration 8.7[25]

A new catalyst for the desulfurization of a heavy feedstock is to be evaluated. Some experimental results for operation at LHSV $= 1\,h^{-1}$, 136 atm, 400°C, and a hydrogen circulation rate of $1.4 \times 10^8\,cm^3$/bbl (STP), are available. The reactor was a 6.35 cm i.d. stainless steel tube provided with a 0.635 cm o.d thermowell mounted along the center-axis of the reactor. The catalyst size was 8-14 mesh.

The percentage desulfurization versus liquid flow rate data obtained with this catalyst are shown in Figure 8.24. As one explanation for the results shown in this figure it was proposed that axial dispersion in shorter beds caused their poor performance. Is this a viable explanation? Look at it. Based on the criterion of Mears, what is the maximum length required to eliminate axial dispersion as a factor important in reactor performance? Assume that the desulfurization reaction is pseudo-first-order, and that the reactor operation was isothermal. The relevant liquid properties are $\rho_L = 0.93\ g/cm^3$ and $\mu_L = 0.15\,cP$.

Additional notes:

1. The plot given, versus liquid flow rate, is equivalent to a plot versus length of reactor, since the LHSV was kept constant.
2. For analysis of dispersion effects see Montagna and Shah [A.A. Montagna and Y.T. Shah, *Ind. Eng. Chem. Proc. Design Devel., 14*, 479 (1975)].
3. According to the Mears criterion [D.E. Mears, *Chem. Eng. Sci., 26*, 1361 (1971)], the minimum (Z/d_p) required to hold the isothermal reactor length to within 5% of that of the plug-flow case is

$$\left(\frac{Z}{d_p}\right) \leq \frac{20m}{(N_{Pe})_L} \ln\left(\frac{C_0}{C_{out}}\right) \tag{i}$$

where m is the reaction order and N_{Pe} the Peclet number based on the particle diameter.

Solution

Montagna and Shah show that in cases where axial dispersion effects are important, a plot of ln $[C_{out}(\text{DISP})/C_{out}(\text{PFR})]$, outlet concentration with dispersion divided by outlet concentration for plug flow, values of the ln term versus Z should be a straight line with slope < -1. Values of this quantity as a function of Z obtained from Figure 8.24 are shown in Figure 8.25. Here the results from the longest bed, 80 cm, are taken to represent the plug-flow case. the results shown in the figure

[25] After Y-T. Shah, *Gas-Liquid-Solid Reactor Design*, with permission of McGraw-Hill Book Co., New York, NY, (1979).]

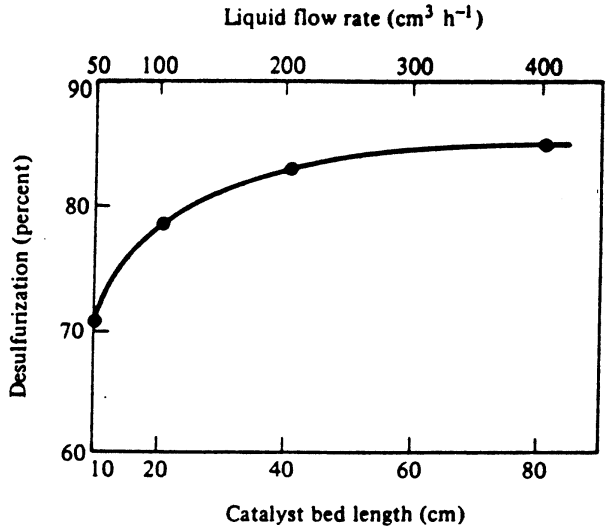

Figure 8.24 Percentage desulfurization as a function of bed length and flow rate.

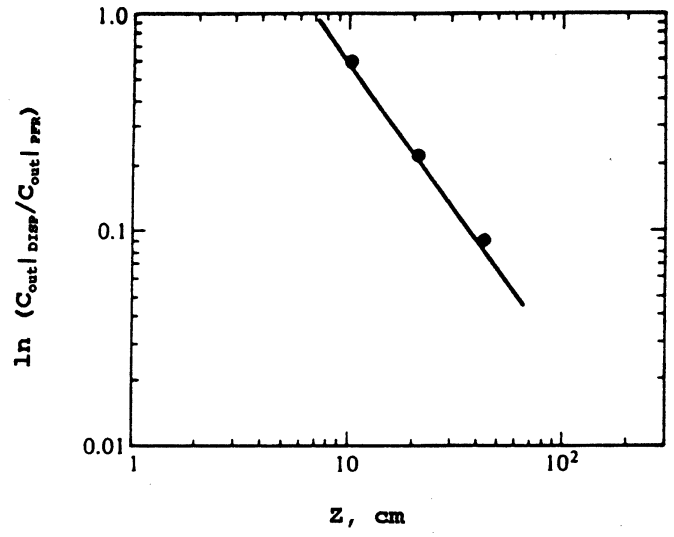

Figure 8.25 Test of trickle-bed HDS data for axial dispersion using the proposal of Montagna and Shah.

show a strong influence of axial dispersion, which we have not seen in homogeneous, tubular-flow reactors, or even in fixed-bed catalytic reactors with reactants and products in the gas phase.

If we set C_0 and C_{out} in the criterion of equation (i) as the inlet and outlet concentrations of sulfur, the effect of axial dispersion can be evaluated quantitatively. We will employ the correlation of Hochman and Effron [J.M. Hochman and E. Effron, *Ind. Eng. Chem. Fundls., 8,* 63 (1969)] for Peclet number

$$(N_{Pe})_L = 0.042(N_{Re})_L^{0.5} \tag{ii}$$

where N_{Re} is also based on particle diameter, and on the superficial liquid velocity. Now Z_{min} can be determined from equations (i) and (ii) for various bed lengths, with

Table 8.4 Minimum Bed Length to Eliminate Axial Dispersion Effects

Length, cm	$(N_{Pe})_L$	Z_{min}, cm
10	0.023	189
20	0.033	172
40	0.047	147
80	0.066	93

Note: L_{min} varies with bed length since at constant LHSV as the bed length is varied the liquid flow is also varied.

the results shown in Table 8.4. These show that the minimum bed length to eliminate axial dispersion effects is $\sim$80cm. Given uncertainties, let us call this ~ 100 cm.

HORATIO SAYS

Does the approach used above include pore diffusion effects, which seem to be of great possible import in the operation of trickle beds? if not, how can we modify the analysis?

Exercises

Section 8.1

1. Equation (8-11) expresses the behavior of the emulsion phase in the two-phase model when it is considered to be well-mixed. Derive this equation.
2. A decomposition reaction is carried out in a fluidized-bed reactor with the following parameters specified.

   $L = 38\,\text{cm}$ $\quad u_0 = 17\,\text{cm/s}$
   $\epsilon_m = 0.45$ $\quad \gamma_b = 0$
   $\epsilon_{mf} = 0.50$ $\quad \mathcal{D} = 0.19\,\text{m}^2/\text{s}$
   $k_r = 3\,\text{s}^{-1}$ $\quad d_p = 4\,\text{cm}$
   $u_{mf} = 2.1\,\text{cm/s}$ $\quad D_r = 25\,\text{cm}$
   $g = 980\,\text{cm/s}^2$

   Using the three-phase model, compute the conversion to be expected assuming operation in the Geldhart A′ region. Compare this with the equivalent PFR and CSTR results.
3. Given the extreme parametric sensitivity of some oxidation reactions carried out in PFRs, as shown in Chapters 4 and 6, it could be considered more desirable to utilize the closer control of temperature provided by a

fluidized bed. Again, naphthalene oxidation is a good example reaction, where the sequence is

$$A \rightarrow R \qquad (k_{r1})$$

$$R \rightarrow C \qquad (k_{r3})$$

where A is napththalene, R is phthalic anhydride, and C are the oxidation products. The following data are available:

$d_p(50\%) = 50\text{-}70\,\mu m; \qquad (25\text{-}35\%) < 44\,\mu m$

$u_{mf} = 0.005\,m/s; \qquad \gamma_b = 0.005$

$\epsilon_m = 0.52; \qquad \epsilon_{mf} = 0.57$

Feed composition = 2.27 mol% A in air

$\mathcal{D}_A = 8.1 \times 10^{-6}\,m^2/s; \qquad \mathcal{D}_R = 8.4 \times 10^{-6}\,m^2/s$

$T = 350^\circ C; \qquad P = 2.52\ bar; \qquad u_0 = 0.45\,m/s$

$L = 5\ m; \qquad D_R = 0.5\,m$

$k_{r1} = 1.5, \qquad k_{r3} = 0.01\,m^3(g)/m^3(cat)\text{-}s$

It is also estimated from correlation that d_b is 0.05 m and $u_b = 1.5\,m/s$. Calculate the conversion to desired product, and the selectivity, defined as $[R/(A_0 - A)]$.

Section 8.2

4. For the case of irreversible first-order kinetics, show how the result of equation (8-107) can be reduced to the form for rate of reaction given in Table 8.1b.
5. The hydrogenation of α-methylstyrene to cumene was studied in an agitated slurry reactor at 70–100°C using as a catalyst powdered 0.5 wt% Pd/Al_2O_3. The catalyst loading, W, was 4×10^{-3} g/cm^3 slurry, and the catalyst had a density, ρ_p, of 1.58 g/cm^3 and an average particle diameter, d_p of 0.005 cm. At 100°C the density of a α-methylstyrene is 0.84 g/cm^3, the viscosity is 0.47 cP, and the diffusivity of H_2 in the liquid is 3.6×10^{-6} cm^2/s. Determine if the rate of mass transfer is an important factor in the observed rate of reaction, which at 100°C was about 4.3×10^{-8} gmol/cm^3 slurry-s.
6.[26] Determine the liquid volume of a slurry reactor, which is well agitated, that will be required to convert 60% of the liquid reactant in an addition reaction at 525°K for

$$A(g) + 3B(1) \rightarrow P$$

The gaseous reactant is present in excess for saturation at 10^{-4} mol/cm^3, with a Henry's law constant of 3 $[(mol/cm^3)_g/(mol/cm^3)_1]$. The inlet concentration of B in aqueous solution is 10^{-5} mol/cm^3, and is introduced at

[26] After H.H. Lee, *Heterogeneous Reactor Design*, with the permission of Butterworth Publishers, Boston, MA, (1985).

a volumetric flow rate of $1\,cm^3/s$. The liquid-solid mass-transfer coefficient, $k_S S_p$, is $2\,s^{-1}$ for both A and B. The intrinsic rate of reaction has been determined separately and is given by

$$(-r_A) = 10^{10}[\exp(-20/RT)]C_B C_A^{1/2}$$

where the activation energy is in kcal/mol and the rate in mol/cm^3 catalyst-s. It may be assumed that the fraction of the liquid volume occupied by the catalyst is 0.02.

7. (a) Suppose oxygen is supplied from air into a well-dispersed suspension of bacteria in a mixed reactor. Oxygen transfer from the bubbles of air to the suspension liquor is usually the rate-limiting step in the overall aerobic process. Using the parameters below, find the apparent maximum rate of oxygen transfer from the suspension to the bacterial surface.

   $\mathcal{D}_0 =$ diffusivity of O_2 in the suspension $= 10^{-5}\ cm^2/s$

   $d_p =$ average cell diameter $= 2 \times 10^{-4}$ cm

   $C_0 =$ cell density $= 10^8\ cm^{-3}$

   $C_1 =$ bulk liquid O_2 concentration $= 6$ ppm

   $T = 25\,^\circ C$

   It may be assumed that the relative velocity between the bacteria and the suspension medium is very small.

   (b) The observed rate of O_2 uptake under the conditions stated above actually turns out to be some orders of magnitude less than that calculated in (a). Can you propose an explanation?

   (c) Do a little research and find out how the parameters described above are determined.

8. We are most accustomed to the generic problem of "given the parameters, how is something (often the conversion) determined?" However, it sometimes occurs that the conversion required is a specified design requirement, and we must determine a permissible feed concentration (or corresponding range). In this case let us consider a first-order irreversible reaction taking place in a given slurry reactor. All of the mass-transfer coefficients, the mass of the catalyst, the gas velocity, the Henry's law constant, etc., are known. The required exit concentration is specified. What should be the inlet concentration of the reactant?

   (a) To have fun with this problem, consider that the reaction is actually second-order in reactant.

   (b) For further fun assume that the catalyst (either case of kinetics) diminishes in activity in a linear fashion by 1/2 over one day (dependent only upon time-on-stream), and you must design for operation to final specifications over a three-day period.

9. Consider a slurry reactor with a well-mixed slurry phase in which the reaction of Problem 6 is taking place. The gas-phase concentration of A is $C_{A_0} = 10^{-4}\ mol/cm^3$, and the inlet liquid-phase concentration of B is $C_{B_0} = 10^{-5}\ mol/cm^3$. It is assumed that the products have no effect on

the system, and it is required that 60% of B is to be converted to products. Further details are

$\mathcal{D}_0 = 10^{-5}\ \text{cm}^2/\text{s}$

$\rho_p = 3.0\ \text{g/cm}^3$ (catalyst particles)

$d_p = 10^{-3}$ cm (catalyst particles)

$k_s S_p = 2\ \text{s}^{-1}$ (for B)

$k_m = k_0 \exp(\text{E}_\text{A}/\text{RT})\text{C}_\text{A}^{1/2}$

$k_0 = 10^{10}\ (\text{cm}^3/\text{mol})^{1/2}/\text{s}$

$E_A = 20$ kcal/mol

$H_A = 3[\text{cm}^3/\text{mol})_1/(\text{cm}^3/\text{mol})_\text{g}]$

$\rho_B = 0.5\ \text{g/cm}^3$

Additional information: All the parameters may be taken as independent of temperature. The liquid feed contains 2 vol% of catalyst, and it was determined that the rate of mass-transfer of A to the catalyst surface is much greater than that of B. The intrinsic rate of reaction of B is

$$(-r_B) = k_0 \exp(-E_A/RT)[C_B]^m[C_A]^{1/2}; \qquad m = 1$$

(a) Calculate the effectiveness factor for reaction temperatures of 350, 750 and 950°K (nonvolatile liquid phase). Determine from this whether the overall conversion is reaction limited, mass-transfer limited, or a mixture of the two, for each temperature level.
(b) Repeat part (a) for different kinetics: $m = 0.5$ and 2.0. Demonstrate the effect of apparent reaction order in B on the relative rate-controlling steps.

Section 8.3

10. As promised in the text, derive the expressions for the constants G_1, G_2, H_0, and H_1 appearing in the analysis of Section 8.3.2 for both batch and countercurrent cases.
11. Outline an experimental procedure and a method of data analysis that will enable one to determine the constants $K_D S$, K and k of Illustration 8.4 with a minimum of experimental effort. Assume that $D(t)$ measurements were taken at equal time increments (i.e., 0.1, 0.2, 0.3···h.)
12. Benzene is to be nitrated in a batch reactor with acid composed of 15 mol% HNO_3, 25 mol% H_2SO_4, and 60 mol% H_2O. The amount of this acid is to be 10% in excess of the theoretical amount required for 100% conversion, although only 96% conversion is required. The reaction temperature is 40°C, at which the densities are 0.87, 1.20 and 1.60 g/cm^3 for benzene, nitrobenzene, and the acid mixture, respectively.

    The changes in density with composition may be neglected, but volume changes upon reaction should be considered. The solubility of organics in the acid phase, and water and sulfuric acid in the organic phase, may be

neglected, but the distribution of nitric acid between the two phases is important and should be accounted for (the volume of nitric acid in the organic phase, however, can be neglected). The simplification of solubilities here is for material balance purposes, since the reaction actually occurs in both phases.

We must calculate the time required for 96% conversion. The rate information of Biggs and White [M. Biggs and R.R. White, *Amer. Inst. Chem. Eng. Jl., 2*, 321 91956)] can be used, and one may assume that the volume of benzene and nitrobenzene are additive. Note that the equation in the title of Figure 11 of that reference is in error. (Optional question: What does one do with the reaction mixture at the end—both to recover product and minimize environmental problems?)

13. Below are two sets of data on the hydrogenation of benzene and of phenol. Determine a means for the interpretation of the lowest and highest pressure data, and use your correlation to predict the middle-pressure results. Note that the original charge was apparently partially hydrogenated. Temperature in both cases was 120°C.

Percentage of Benzene Hydrogenated

Time, h	30 atm	169 atm	323 atm
0	17	29	34
0.5	40	68	75
1.0	61	90	93
1.5	76	98	100
2.0	87	100	—
2.5	96	—	—

Percentage of Phenol Hydrogenated

Time, h	40 atm	150 atm	330 atm
0	5	27	20
1	27	49	49
2	41	63	62
3	50	73	70
4	59	81	—
5	67	85	—
6	72	87	—
7	76	—	—

14. Let us now re-examine the data and your interpretation for the benzene hydrogenation data of Problem 13. We now need to design a suitable hydrogenation reactor system. It was proposed to charge an autoclave with 75 liters of pure benzene at operating temperature (120°C) under conditions such that at the end of the charging period there is negligible free space in the reactor. The pressure of the operation, though, must be maintained at 30 atm.

(a) Estimate the intake volume of the hydrogen compressor (liters/time at SC) required to duplicate the time cycle of the laboratory run.

(b) What is the time required to attain 99% conversion with a compressor with only half the capacity of (a).

Neglect any inerts in the hydrogen and the benzene vapor. The density of benzene at these conditions is 0.76 g/cm^3.

15. The heat of reaction for the nitration of benzene with the mixed acid of the composition considered in problem 12 is about 38 (kcal/gmol-benzene) at the start of the reaction. Calculate the rate of heat evolution under these conditions. This will be found to be a dangerously high value. What manner of reactor operation would you suggest to get around this difficulty?

Further, plan a process in which the reaction is to be carried out with a charge of 5000 pounds of benzene in a vessel equipped with internal heat-transfer coils and with sufficient surface area to satisfy an allowable temperature rise of 10°C. Cooling water is available at 20°C. In the reactor the heat-transfer area is 300 ft^2, and an overall heat-transfer coefficient of 200 Btu/ft^2-h-°F can be maintained. The reaction is to be carried out at 40°C, and under these conditions the nitric acid dissolved in the organic layer may be neglected. The acid is to be fed at a constant rate such that if it were all converted the limiting heat-removal rate would not be exceeded.

Now, calculate the rate and the conversion at the end of the feed period. Again, the total acid used should be 10% in excess of that theoretically required. Remember that after all the acid has been fed (after the feed period is over), the remaining time for the desired final conversion can be calculated in the usual way for a batch reaction.

Section 4.4

16. What system parameters are important in the scale-up of a trickle-bed reactor to be used for a gas-liquid-solid catalytic reaction if the reaction occurs in the liquid phase only and is controlled by
    (a) the gas-liquid mass transfer?
    (b) the liquid-solid mass transfer?
    (c) the intrinsic reaction kinetics.
17. Consider a fixed-bed column with downward cocurrent flow of liquid and gas phases. The column is packed with 0.3 cm diameter catalyst particles, with bed void fraction of 0.48, bed diameter of 5 cm, and bed length of 150 cm. Gas and liquid fluxes (both superficial) are 10^3 and 10^4 kg/m^2-h, respectively. Under reaction conditions the relevant gas properties are: average molecular weight = 10, density 0.06 g/cm^3, viscosity = 0.6 cP, surface tension = 10 dynes-cm, specific gravity = 0.9, and the molecular diffusivity of reactant = 10^{-3} ft^2/h. From these data estimate
    (a) Flow regime.
    (b) Pressure drop.
    (c) Gas and liquid holdups.
    (d) Axial dispersion coefficient (liquid).
    (e) Gas-liquid mass-transfer coefficient.
    (f) Liquid-solid mass-transfer coefficient.

18. Figure 8.21d presents some experimental data on liquid-solid mass-transfer coefficients. How well do these agree with values predicted by the correlations of equations (8-233), (8-234), and (8-235)?

Notation

A bed cross-sectional area, length^2; total surface area in reactor, length^2
A_c cross-sectional area, length^2
A_G concentration of A in gas phase, mols/volume
A_g concentration of A in gas phase, mols/volume
A_L concentration of A in liquid phase, mols/volume
A_1, B_1 bulk liquid concentrations of A and B, mols/volume
A_0 concentration of A at gas-liquid interface, mols/volume
A_{g1}, A_{1g} concentration of A (gas) or (liquid) at gas-liquid interface, mols/volume
A_{go}, A_{gi} outlet and inlet concentrations of A in slurry reactor, mols/volume
A_{g0}, A_{l0} inlet concentration of A in gas and liquid phases, mols/volume
A_{Li}, B_{Li}, C_{Li} inlet concentrations of A, B and C, mols/volume
A_S, B_S, C_S concentrations of A, B and C at external surface of catalyst particle, mols/volume
A_1, A_2 constants in equation (8-154); concentration of A in phases 1 and 2, mols/volume
$A_1, A_2, D_1, D_2, G_1, G_2, H_0, H_1$ constants in equations (8-160)-(8-163)
A^* modified concentration $= (A_{gi}/H_A)$; modified concentration $= (H_A A_g)$
A_2^* equilibrated concentration of A in phase 2, mols/volume
a surface area per unit volume of continuous phase; proportionality constant in equation (8-247)
a, b Constants in correlation of equation (8-206)
a_s nondimensional concentration of A, see equation (8-103); liquid-solid interfacial area per volume
a_v catalyst external surface area per volume of catalyst
a_w ratio of wetted external area to total external area
a' constant $= (a/V_L N)$; $(SV_b^{-1/3})$ in equation (8-173)
a_o' initial value of a'
$\bar{a}', \bar{V}_b, \bar{y}$ average values of a', V_b and y; see equation (8-169)
a_1, a_2 constants defined after equation (8-18)
B_1 concentration of B in liquid phase, mols/volume
B_{lo} initial concentration of B in liquid phase; see equation (8-111)
B_1, B_2 concentration of B in phases 1 and 2, mols/volume
C_b concentration of reactant in bubble phase; mols/volume
C_c concentration of reactant in cloud/wake phase, mols/volume
C_e concentration of reactant in emulsion phase, mols/volume
C_j concentration of component j in liquid phase, mols/volume
C_L $C_{eL} + C_{bL}$
C_0 inlet concentration of pure reactant, mols/volume
C_{Ai}, C_{Ao} inlet and outlet concentration of A in Denbigh sequence, mols/volume
C_{bL} bubble phase concentration at L, mols/volume
C_{ib}, C_{ic}, C_{ie} concentration of A in bubble, cloud and emulsion phases, mols/volume

C_{oj} inlet concentration of j in liquid phase, mols/volume
C_{ol} initial bulk concentration of liquid phase reactant, mols/volume
C_{ej} equilibrium concentration of j with reversible reaction, mols/volume
$C_{S_o}, C_{T_o}, C_{U_o}$ outlet concentrations of S, T and U, Denbigh sequence, mols/volume
C_{in}, C_{out} reactant concentration in and out of reactor, mols/volume
$C_R(max)$ maximum concentration of R, mols/volume
C_1 constant in equation (8-232)
D molecular diffusivity, length^2/time, typically cm^2/s
D_A, D_B diffusivities of A and B in liquid phase, cm^2/s
D_G, D_L axial dispersion coefficients for gas and liquid phases, cm^2/s
D_e effective diffusivity, cm^2/s
D_o orifice diameter, length
D_{AL} diffusivity of reactant A in liquid phase, length^2/time
D_{eff} effective diffusivity, cm^2/s
$Đ$ bulk diffusivity; diffusivity in liquid; see equation (8-238), cm^2/s
d_b bubble diameter, length
d_c diameter of cloud/wake phase, length
d_p particle diameter, length
d_{ob} initial bubble diameter, length
E efficiency at same conversion, (PFR/FBR); see equation (8-34)
E_G, E_L energy dissipation factor for gas and liquid phases, equations (8-231) and (8-232), W/m^3
F factor defined in equation (8-177)
F_1, F_2 flow rates of phases 1 and 2, volume/time
f nondimensional concentration of A = (A/A$_0$); frequency of bubble formation, time^{-1}; bed void fraction
f_c cloud volume factor; see equations (8-56) and (8-57)
f_w wake volume factor; see equations (8-56) and (8-57)
G gas phase flow rate, mols/time
G_L liquid mass flow rate, mass/area-time
G_0 inlet gas phase flow rate, mols/time
G_1, G_2 constants in equation (8-151); gas flow rate into and out of reactor, mols/time
g gravitational constant, length/time^2
H Henrys law constant, typically atm/(mol/volume)
H_A, H_B Henrys law constant for A and B, atm/(mol/volume)
H_0, H_1 constants in equation (8-154)
h gas phase holdup
I integral function defined in equation (8-112)
j_D mass transfer factor
K_A mass transfer coefficient, time^{-1}
K_A, K_B absorption equilibrium constants in Langmuir-Hinshelwood rate equation, volume/mol
K_s, K_{si} liquid-solid mass transfer coefficient for i, length/time
K_T overall external mass transfer coefficient, length/time
K_f composite rate constant; see equation (8-26), time^{-1}
K_o overall rate constant; see equation (8-117), time^{-1}

K_r rate constant, time^{-1}; see Figure 8.7
K_{bc}, K_{ce} overall mass transfer coefficients, bubble to cloud/wake phase and cloud/wake to emulsion phase, respectively, time^{-1}
K_{fA} rate constant defined in equation (8-75)
K_{fAR} rate constant defined in equation (8-74)
K_{f12}, K_{f34} overall rate constants in equations (8-72) and (8-73)
$K_{bc,i}K_{ce,i}$ mass transfer coefficients for i, bubble to cloud/wake phase and cloud/wake to emulsion phase, respectively, time^{-1}
K_Ga, K_Ga' overall gas phase mass transfer coefficients, mols/time-volume-atm
$(K_LS)_{\mathrm{A}}$ overall mass transfer coefficient for A, time^{-1}
K_2 rate constant in Langmuir-Hinshelwood scheme, typically (volume/mol)/time-wt; see equation (8-84)
k rate constant, time^{-1}
k_L, k_G individual liquid and gas phase mass transfer coefficients, length/time
k_d mass transfer coefficient, length/time; see equation (8-8)
k_e rate constant ratio $= (\mathrm{K_f/k_r})$
k_g gas phase mass transfer coefficient, length/time
k_1 liquid phase mass-transfer coefficient, length/time; mass-transfer coefficient in presence of reaction; see equation (8-138), length/time
k_m pseudo first-order rate constant, time^{-1}
$k_{(m+n)}$ rate constant, time^{-1}; see equation (8-83)
k_r rate constant, time^{-1}
k_s liquid-solid mass transfer coefficient, length/time
k_{bc}, k_{ce} mass-transfer coefficients, bubble to cloud/wake phase and cloud/wake to emulsion phase, respectively, (time-area)$^{-1}$
$k_{r1}, k_{r2}, k_{r3}, k_{r4}$ rate constants in Denbigh sequence, time^{-1}
k_{L_2} mass-transfer coefficient in liquid phase; see equation (8-233), length/time
$k_{lo}k_L^\circ$ liquid phase mass-transfer coefficient in absence of reaction, length/time
k_{r12}, k_{r34} combined constants $= (k_{r1} + k_{r2}), (k_{r3} + k_{r4})$
k_Ga_L, k_La_L gas and liquid phase mass-transfer coefficients in trickle bed, time^{-1}
(k_gS_b) gas phase mass-transfer coefficient, time^1
(k_1S_b) liquid phase mass-transfer coefficient, time^{-1}
(k_sS_b) liquid-catalyst surface mass-transfer coefficient, time^1
$(k_gS)_{\mathrm{A}}$ gas phase mass-transfer coefficient for A in slurry reactor, time^{-1}
$(k_1S_1)_{\mathrm{B}}$ liquid phase mass-transfer coefficient for B, time^{-1}
$(k_L^\circ)_{SB}, (k_L^\circ)_{BS}$ values of k_L° for single bubbles and bubble swarms
k_1, k_2 constants defined in equation (8-187b), time^{-1}
L bed length or height (expanded); liquid film thickness, length
L_0 height of unexpanded bed, length
l distance variable in liquid film, length
$LHSV$ liquid hourly space velocity, time^{-1}
M_{A} constant defined in equation (8-96)
m catalyst loading, wt catalyst/volume slurry; fitting constant in equation (8-221)
m, n reaction orders
N number of bubbles/volume of bed; number of bubbles/volumes of liquid
N_B number of bubbles/reactor volume
N_{Eo} Eötos number $= (\rho_L g d_p^2/\sigma_L)$

N_{Fr} Froude number = $(u^2 g/\delta)$
N_{Ga} Galileo number = $[d_p^3 \rho_L(\rho_L q + \Delta P_{LG})]/\mu_L^2$
N_{Sc} Schmidt number + (ν/D)
N_{Sh} Sherwood number = $(k_s d_p/D)$; $(k_{L2}/a_s D_{AL})$
N_{Re} Reynolds number = $(\rho_L L/A_c a_s \mu_L)$; see equation (8-233); $(g d_b/\mu)$
N_{We} Weber number = $(\delta \rho u^2/\sigma)$
$(N_{Da})_b$ gas phase Damköhler number = $(k_1/k_g H_A)$
$(N_{Da})_c$ Damköhler number for cloud/wake phase = (k_r/K_{bc})
$(N_{Da})_e$ Damköhler number for emulsion phase = (k_r/K_{ce})
$(N_{Da})_l$ liquid phase Damköhler number = $(\eta k/k_s)$
$(N_{Da})_o$ overall Damköhler number; see equation (8-124)
$(N_{Fr})_L$ Froude number = $(G_L^2/\rho_L^2 d_p G)$
$(N_{Pe})_L, (N_{Re})_L, (N_{Ga})_L$ Peclet, Reynolds and Galileo numbers defined on the basis of interstitial velocity; see equation (8-244)
$(N_{Re})_L$ Reynolds number = $(G_L d_p/\mu_W)$; see equation (8-247)
$(N_{Sh})_G, (N_{Sh})_L$ Sherwood numbers for gas and liquid phases
$(N_{We})_L$ Weber number = $(G_L^2 d_p/\sigma_L \rho_L)$
$(N_{Re'})_L$ modified Reynolds number = $(\rho_L u_L/a_s \mu_L \beta_t)$
n constant in equation (8-171); reaction order
P pressure, atm
$\Delta P_G, \Delta P_L$ pressure drop in gas and liquid phases, atm
ΔP_{LG} pressure drop of liquid-gas phase, atm
Q gas flow rate, volume/time; overall mass exchange coefficient
q cross flow mass transfer coefficient in fluid bed, volume/time; liquid phase flow rate, volume/time
R bed radius, length, catalyst particle radius, length; gas constant, kcal/mol-K
R_A rate of reactant consumption, mols/volume slurry-time; rate of reaction of A, mols/volume-time; flux of A, equation (8-137)
R_G gas holdup = $(1 - R_L)$
R_L liquid phase holdup
$(-r)$ rate of reaction, mols/wt-time; see equation (8-83)
$(-r_A)$ rate of reaction of A, mols/volume-time
r_j rate of reaction for component j, mols/volume-time
$[-r(A^*)]$ rate in terms of A*, mols/volume-time
r_1, r_2 constants defined after equation (8-200)
S interphase area; interphase area for mass transfer, typically area/volume; bubble shape factor; see equation (8-173); external mass-transfer factor; see after equation (8-256)
S_c interfacial area; see equations (8-156) and (8-157)
S_L interfacial area; see equation (8-133)
S_1 gas-liquid interfacial area; see equation (8-144), cm^2/cm^3
S_p particle external surface area, $length^2$
S_p, S_b interfacial areas for liquid-solid and gas-liquid in slurry reactor, area/volume
S_{bc}, S_{ce} interfacial area, bubble to cloud/wake phase and cloud/wake phase to emulsion phase
s, q correlation constants; see equation (8-235)
T temperature, °C, K

t time; exposure time for element of bubble surface in contact with emulsion phase
t_B batch time required for conversion x
t_D, t_R characteristic times for diffusion and extent of reaction; see equations (8-207) and(8-208)
t_L average liquid residence time $= (V_L/v)$
$(t_p)_L, (t_p)_G$ residence time for liquid and gas phases, respectively
t_p length of time that an element of fluid remains in reactor
U_{oG}, U_{oL} superficial gas and liquid velocities; see equation (8-256), length/time
u fluid velocity, length/time
u_b bubble phase velocity $= (u_o - u_{mf})$, length/time
u_o superficial velocity of gas through emulsion phase, length/time
u_g bubble velocity in slurry reactor, length/time
u_L interstitial liquid velocity, length/time
u_1, u_g liquid and gas velocity; see equations (8-130) and (8-131), m/s
u_0 inlet fluid velocity, length/time
u_t entrainment velocity, length/time
u_{br} bubble rise velocity, length/time
u_{mf} minimum fluidization velocity, length/time
u_{SL} superficial velocity of liquid phase, length/time
V average volume per bubble; liquid volume per volume of reactor; total reactor volume
V_b volume of bubble phase; volume of a single bubble
V_g gas phase volume
V_1 liquid phase volume
V_L slurry volume; volume of liquid phase
V_p particle volume
V_s volume of solids
V_{DG} volume of a bubble; see equation (8-203)
$V_{oG}, (V_{oG})_0$ average bubble volume; initial average bubble volume
V_{ob} initial bubble volume
V_1, V_2 volume of phases 1 and 2
v volumetric flow rate, volume/time
v_b bubble velocity, length/time
v_B average bubble rise velocity, length/time
v_L average velocity of liquid phase, length/time
W mass of catalyst/volume of slurry; constant $= 0.711 g^{1/2}(6/\pi)^{1/6}$
X reactant conversion $= [1 - C_{(outlet)}/C_{(inlet)}]$
x reactant conversion
y distance (reactor length) variable; nondimensional length $= (1/L)$
y_j mol fraction of component j in gas phase
y_{oj} inlet mol fraction of j
Z bed length
z length variable

Greek

α fraction of liquid phase occupied by liquid film; stoichiometric coefficient; constant in equation (8-221) $= (qP/HG)$
α, β constants in r_1, r_2, defined after equation (8-200)

α, β, γ constants in equations (8-21) and (8-13)
α_A constant $= (K_L S)_A / u_g H_A$
α_A, β_A constants in equilibrium relationship for A_2^*
β_L, β_G liquid and gas holdup based on total reactor volume
β_f, β_t dynamic holdup; total holdup
β_{te} external holdup
γ correlation factor in equation (8-255)
$\gamma_b, \gamma_c, \gamma_e$ volume solids/volume fluid in bubble cloud/wake, and emulsion phases, respectively
δ velocity ratio $= (u_0/u_b)$; volume fraction of bubbles in bed; see equation (8-59); stoichiometric coefficient; distributor orifice diameter, length
ϵ bed porosity; fraction of volume in phase 2
ϵ_f fluidized bed porosity
ϵ_{mf} bed porosity at u_{mf}
η overall effectiveness factor; see equation (8-101); effectiveness factor for catalyst
η_{CE} fraction of external catalyst particle surface wetted
η_{TB} effectiveness factor in trickle bed
η_b, η_l phase effectiveness factors; see equations (8-119) and (8-120)
η_o catalyst effectiveness factor; see equation (8-97)
η_i phase i effectiveness $= [\gamma_i/(1 + \gamma_i N_{Da_i})]$; fraction of catalyst pore volume filled with liquid
η_0 overall effectiveness; see equation (8-122)
θ catalyst porosity
λ enhancement factor; see equation (8-139); trickle bed scaling parameter; see equation (8-222)
Λ generalized dimension $= (V_p/S_p)$
$\Lambda_1, \Lambda_2, \Lambda_3$ parameters in equation (8-256)
μ gas viscosity, typically cP; viscosity, cP
μ_L liquid viscosity, cP
μ_{H_2O} viscosity of water, cP
ν stoichiometric coefficient; kinematic viscosity $= (\mu/\rho)$; bubble formation frequency, time^{-1}
ξ nondimensional distance $= (z/Z)$
ρ gas density, mass or mols/volume
ρ_L, ρ_G gas and liquid densities, mass or mols/volume
ρ_1 liquid density, mass or mols/volume
ρ_p catalyst particle density, mass/volume; solids density, mass/volume
ρ_s solids density, mass/volume
ρ_{air}, ρ_{H_2O} densities of air and water, mass/volume
ρ_1, ρ_2 constants in equations (8-154) and (8-160)
σ constant in equation (8-154); surface tension of gas-liquid interface, mass/time^2
σ_A constant in equation (8-103)
σ_L liquid surface tension; see equation (8-252), mass/time^2
σ_{H_2O} surface tension of water, mass/times^2
τ ratio $= (V_s/v)$
$\tau(max)$ τ corresponding to $C(max)$

ϕ generalized Thiele Modulus; see equations (8-100) and (8-135)
ϕ_0 Thiele Modulus $= L(k/D)^{1/2}$
ϕ_{TB} modified Thiele Modulus; see equation (8-239)
χ pressure drop ratio
Ψ trickle bed scaling parameter; see equation (8-223)

Note: Additional notation is given in Tables 8.1 and 8.3, in Figures 8.16 and 8.17, equations (8-191) and (8-192), and in Illustrations 8.4 and 8.6.